



University of
**Southern
Queensland**

**DEVELOPMENT OF BIOCHAR-HYDROGEL
COMPOSITES AND Fe₃O₄ NANOPARTICLES
FUNCTIONALISED POLYVINYL
ALCOHOL/CHITOSAN HYDROGEL COMPOSITES
AS EFFICIENT AND LOW-COST MATERIALS TO
REMOVE ARSENIC FROM AQUEOUS SOLUTIONS**

A Thesis submitted by

Lakshika Weerasundara, M.Phil.

For the award of

Doctor of Philosophy

2022

ABSTRACT

As one of the most dangerous contaminants, arsenic (As) is responsible for serious, negative impacts on human health. Therefore, As-contaminated water and wastewater must be treated with effective As removal processes before being used for human consumption or release into the environment. In the last few years, hydrogel composites have attracted significant interest for application in environmental remediation, including water treatment. However, synthetic hydrogels have some disadvantages such as high production cost and latent toxicity. This study focused on developing two different hydrogel composites with natural, low-cost, non-toxic and biodegradable materials. In the first phase of the study, modified poly(acrylamide) hydrogels were developed by incorporating rice hull biochar (RHBC) and sugar cane bagasse biochar (SUBC). In the second phase, a modified chitosan-polyvinyl alcohol hydrogel was developed by incorporating Fe₃O₄ nanoparticles. As an extension of this material, a further modification was achieved with the integration of copper (ChFe-Cu hydrogel). Batch sorption experiments, regeneration and re-usable capacities were conducted for As removal. The highest arsenic (V) (As(V)) adsorption (15% for both RHBC and SUBC) was at the pH range of 6-7. Within this range, the protonated -NH₂ and -CO groups in the hydrogels attracted As(V) oxyanions. The experimental kinetic and isotherm models predicted chemisorption and physisorption mechanisms. 0.1 M NaOH showed the best regeneration patterns and, because of this re-use capability, the As adsorption capacity was seen to be, not a single value from one adsorption cycle, but a cumulative value of several adsorption cycles. Considering arsenic (III) (As(III)), the optimum pH range was 6-7.5 for both the RHBC and SUBC hydrogels. The cumulative amount of As(III) adsorption was very low compared to the As(V) for both the RHBC and SUBC hydrogels. The limited functional group availability for As(III) adsorption was identified as the major reason for this result. The highest As(V) adsorption was achieved at pH range of 4-5 for both the ChFe (89%) and ChFe-Cu (99%) hydrogels. The kinetic and isotherm models predicted chemisorption mechanisms onto the ChFe and ChFe-Cu hydrogels. Electrostatic attractions with -NH₃⁺ and -OH₂⁺, ligand-exchange inner-sphere complexes formation and bidentate corner-sharing (²C), and bidentate edge-sharing (²E) trimetric surface complexes formation have been proposed as the adsorption mechanism of As(V). 0.1 M CH₃COOH showed the best regeneration pattern and the cumulative adsorption capacities were 15.1 mg/g and 12.4 mg/g for ChFe and ChFe-Cu hydrogels respectively, along with four adsorption cycles.

CERTIFICATION OF THESIS

I Weerasundara Mudiyansele Lakshika Sujeewani Weerasundara declare that the PhD Thesis entitled “Development of biochar-hydrogel composites and Fe₃O₄ nanoparticles functionalised polyvinyl alcohol/chitosan hydrogel composites as efficient and low-cost materials to remove arsenic in aqueous solutions” is not more than 100,000 words in length including quotes and exclusive of tables, figures, appendices, bibliography, references, and footnotes.

This Thesis is the work of Weerasundara Mudiyansele Lakshika Sujeewani Weerasundara except where otherwise acknowledged, with the majority of the contribution to the papers presented as a Thesis by Publication undertaken by the student. The work is original and has not previously been submitted for any other award, except where acknowledged.

Date: 14.11.2022

Endorsed by:

Prof. Jochen Bundschuh

Principal Supervisor

Prof. Yong Sik Ok

Associate Supervisor

Dr. Alla Marchuk

Associate Supervisor

Student and supervisors' signatures of endorsement are held at the University.

STATEMENT OF CONTRIBUTION

The following detail is the agreed share of contribution for candidate and co-authors in the presented publications in this thesis:

Paper 1:

Weerasundara, L., Gabriele, B., Figoli, A., Ok, Y.S. and Bundschuh, J., 2020. Hydrogels: Novel materials for contaminant removal in water—A review. *Critical Reviews in Environmental Science and Technology*, 1-45. <https://doi.org/10.1080/10643389.2020.1776055> (**Published; Q1 journal**; Impact Factor: 12.561 and SNIP: 2.55).

The overall contribution of **Lakshika Weerasundara** was 80% to the concept development, analysis, drafting, and revising the final submission; **Jochen Bundschuh, Bartolo Gabriele, Alberto Figoli, Yong-Sik Ok** assisted with the concept development, editing, and providing important technical inputs. Overall, their contribution to this manuscript is 20%.

Paper 2:

Weerasundara, L., Ok, Y.S. and Bundschuh, J., (2021). Selective removal of arsenic in water: A critical review. *Environmental Pollution*, 268, 115668. <https://doi.org/10.1016/j.envpol.2020.115668> (**Published; Q1 journal**; Impact Factor: 9.988 and SNIP: 1.79).

The overall contribution of **Lakshika Weerasundara** was 80% to the concept development, analysis, drafting, and revising the final submission; **Jochen Bundschuh, Yong-Sik Ok** assisted with the concept development, editing, and providing important technical inputs. Overall, their contribution to this manuscript is 20%.

Paper 3:

Weerasundara, L., Kumarathilaka, P., Marchuk, A. and Bundschuh, J., Development of regenerative, re-usable and easily water-adsorbent separable hydrogel composite with rice hull biochar for efficient removal of arsenic (V) from aqueous media.

The overall contribution of **Lakshika Weerasundara** was 80% to the concept development, analysis, drafting, and revising the final submission; **Jochen Bundschuh, Prasanna Kumarathilaka and Alla Marchuk** assisted with the concept development, editing, and providing important technical inputs. Overall, their contribution to this manuscript is 20%.

Paper 4:

Weerasundara, L., Kumarathilaka, P., Marchuk, A. and Bundschuh, J., Synthesis of reusable hydrogel composite integrating sugarcane bagasse biochar for large industrial to household scale arsenic (V) removal in aqueous media and comparison with rice-hull biochar hydrogel composite. (Submitted to a journal)

The overall contribution of **Lakshika Weerasundara** was 80% to the concept development, conducting research works, formal analysis, data curation, and drafting the manuscript; **Jochen Bundschuh, Prasanna Kumarathilaka and Alla Marchuk** assisted with the concept development, editing, and providing important technical inputs. Overall, their contribution to this manuscript is 20%.

Paper 5:

Weerasundara, L., Ok, Y.S., Kumarathilaka, P., Marchuk, A. and Bundschuh, J., (2023). Assessment and optimisation of As (V) adsorption on hydrogel composite integrating chitosan-polyvinyl alcohol and Fe₃O₄ nanoparticles and evaluation of their regeneration and reusable capabilities in aqueous media. *Science of the Total Environment*, 855, 158877. <https://doi.org/10.1016/j.scitotenv.2022.158877> (**Published; Q1 journal; Impact Factor: 10.753 and SNIP: 2.17**).

The overall contribution of **Lakshika Weerasundara** was 80% to the concept development, conducting research works, formal analysis, data curation, and drafting the manuscript; **Jochen Bundschuh, Yong Sik Ok, Prasanna Kumarathilaka and Alla Marchuk** assisted with the concept development, editing, and providing important technical inputs. Overall, their contribution to this manuscript is 20%.

Paper 6:

Weerasundara, L., Kumarathilaka, P., Marchuk, A. and Bundschuh, J., Cu(II)-loaded chitosan-polyvinyl alcohol and Fe₃O₄ nanoparticle integrated hydrogel composite for enhanced and efficient arsenic (V) adsorption. (Submitted to a journal)

The overall contribution of **Lakshika Weerasundara** was 80% to the concept development, conducting research works, formal analysis, data curation, and drafting the manuscript; **Jochen Bundschuh, Prasanna Kumarathilaka and Alla Marchuk** assisted with the concept development, editing, and providing important technical inputs. Overall, their contribution to this manuscript is 20%.

Paper 7:

Weerasundara, L., Kumarathilaka, P., Marchuk, A. and Bundschuh, J., Assessment of arsenic (III) removal from water with biochar hydrogel composites which were successful in arsenic (V) removal in water and overcame the classical drawbacks of adsorbent materials. (Submitted to a journal)

The overall contribution of **Lakshika Weerasundara** was 80% to the concept development, conducting research works, formal analysis, data curation, and drafting the manuscript; **Jochen Bundschuh, Prasanna Kumarathilaka and Alla Marchuk** assisted with the concept development, editing, and providing important technical inputs. Overall, their contribution to this manuscript is 20%.

ACKNOWLEDGEMENTS

The process of earning a PhD and writing a dissertation is long and arduous and it is certainly not done single-handedly. First and foremost, I acknowledge the traditional owners of the land on which I have lived and conducted my PhD research works. This research has been supported by the Australian Government Research Training Program Scholarship. I would like to express my sincere gratitude to University of Southern Queensland and Australian Commonwealth Government for granting me a scholarship to conduct my PhD study in Australia. My sincere gratitude goes to my principal supervisor, Prof. Jochen Bundschuh, for his continuous support of my PhD study, for his patience, motivation, enthusiasm, and immense knowledge. His guidance helped me during the whole period of my PhD research and the writing of this thesis. I could not have imagined having a better advisor and mentor for my PhD study. Also, I am deeply grateful to my co-supervisors, Prof. Yong Sik Ok, and Dr. Alla Marchuk for their insight, feedback, encouragement, and valuable guidance during this period.

Much of my experimental work would not have been completed without the technical assistance of Dr. Susette Eberhard, Mr. Brian Lenske, Mr. Mohan Trada, Mr. Adrin Blokland, Mrs. Piumika Ariyadasa and Ms. Katelynn Hadzi. Their assistance, cooperation and knowledge were essential for the completion of my PhD research work. I need to express my gratitude and deep appreciation to Ms. Belinda Clews, Laboratory Coordinator, Racecourse Mill, Mackay for providing sugarcane bagasse for the study. My sincere thanks go to Deceased, Dr. Babara Harmes for her kind and enormous support on English language. Dr. Barbara Harmes will be greatly missed but her kindness, warmth and gentle spirit will be remembered forever. I would like to thank Ms. Sandra Cochrane for spending her valuable time on language support and proof-reading journal articles and the thesis. I am grateful to many of my colleagues who shared their memories and experiences, Dr. Prasanna Kumarathilaka, Dr. Indika Herath, Mrs. Sara Al-Shaikhli, Mrs. Nuwanthi Senevirathna, Mrs. Jasmine Senevirathna and Mr. Meth Visula Gamage for their valuable time and help during various parts of my study. Last but not the least, I would like to thank my loving Husband, Dr. Prasanna Kumarathilaka, my son, my parents, my parents-in-law, my sister, and my brother-in-law for always being with me and inspiring me spiritually throughout my PhD journey.

DEDICATION

DEDICATED TO SRI LANKANS WHO CONTRIBUTED AND SACRIFICED
FOR FREE EDUCATION

TABLE OF CONTENTS

ABSTRACT.....	i
CERTIFICATION OF THESIS.....	ii
STATEMENT OF CONTRIBUTION.....	iii
ACKNOWLEDGEMENTS.....	vi
DEDICATION.....	vii
LIST OF FIGURES.....	x
ABBREVIATIONS.....	xi
CHAPTER 1: INTRODUCTION.....	1
1.1. Rationale of study.....	1
1.1.1. Background.....	1
1.1.2. Significance of study.....	3
1.2. Research gaps.....	4
1.3. Research questions.....	4
1.4. Research aims and objectives.....	5
1.5. Organisation of the thesis.....	5
CHAPTER 2: LITERATURE REVIEW.....	8
2.1. Paper 1: Hydrogels: Novel materials for contaminant removal from water— A review.....	8
2.1.1. Introduction.....	8
2.1.2. Manuscript.....	8
2.1.3. Concluding remarks.....	54
2.2. Paper 2: Selective removal of arsenic in water: A critical review.....	56
2.2.1. Introduction.....	56
2.2.2. Manuscript.....	57
2.2.3. Concluding remarks.....	76
CHAPTER 3: PAPER 3 – DEVELOPMENT OF REGENERATIVE, RE-USABLE AND EASILY WATER-ADSORBENT SEPARABLE HYDROGEL COMPOSITE WITH RICE HULL BIOCHAR FOR EFFICIENT REMOVAL OF As(V) FROM AQUEOUS MEDIA..	78
3.1. Introduction.....	78
3.2. Manuscript.....	79
3.3. Concluding Remarks.....	112

CHAPTER 4: PAPER 4 – SYNTHESIS OF RE-USABLE HYDROGEL COMPOSITE INTEGRATING SUGARCANE BAGASSE BIOCHAR FOR LARGE INDUSTRIAL TO HOUSEHOLD SCALE As(V) REMOVAL FROM AQUEOUS MEDIA AND COMPARISON WITH RICE-HULL BIOCHAR HYDROGEL COMPOSITE	114
4.1. Introduction	114
4.2. Manuscript	115
4.3. Concluding remarks	149
CHAPTER 5: PAPER 5 – ASSESSMENT AND OPTIMISATION OF As(V) ADSORPTION ON HYDROGEL COMPOSITE INTEGRATING CHITOSAN-POLYVINYL ALCOHOL AND Fe ₃ O ₄ NANOPARTICLES AND EVALUATION OF THEIR REGENERATION AND RE-USABLE CAPABILITIES IN AQUEOUS MEDIA	150
5.1. Introduction	150
5.2. Manuscript	151
5.3. Concluding remarks	164
CHAPTER 6: PAPER 6 – Cu(II)-LOADED CHITOSAN-POLYVINYL ALCOHOL AND Fe ₃ O ₄ NANOPARTICLE INTEGRATED HYDROGEL COMPOSITE FOR ENHANCED AND EFFICIENT As(V) ADSORPTION.....	165
6.1. Introduction	165
6.2. Manuscript	166
6.3. Concluding remarks	193
CHAPTER 7: PAPER 7 – ASSESSMENT OF As(III) REMOVAL FROM WATER WITH BIOCHAR HYDROGEL COMPOSITES WHICH WERE SUCCESSFUL IN As(V) REMOVAL FROM WATER AND OVERCAME THE CLASSIC DRAWBACKS OF ADSORBENT MATERIALS.....	194
7.1. Introduction	194
7.2. Manuscript	195
7.3. Concluding remarks	220
CHAPTER 8: DISCUSSION AND CONCLUSION	221
8.1. Discussion and Conclusions	221
8.2. Recommendations	224
REFERENCES	225
APPENDIX A.....	229
APPENDIX B	230

LIST OF FIGURES

CHAPTER 1: INTRODUCTION	1
Figure 1 Organisation of the thesis	7

ABBREVIATIONS

APS	Ammonium Persulfate
As	Arsenic
As(III)	Arsenite
As(V).....	Arsenate
BC	Biochar
ChFe.....	Chitosan-Fe ₃ O ₄
ChFe-Cu.....	Chitosan-Fe ₃ O ₄ -Cu
DNA	Deoxyribonucleic acid
FTIR.....	Fourier Transform Infrared Spectroscopy
ICP-MS	Inductively coupled plasma mass spectrometry
MBA	N, N'-methylene bisacrylamide
P(AAm).....	Poly(acrylamide)
PVA.....	Polyvinyl Alcohol
PZC	Point of Zero Charge
QA/QC	Quality Assurance/Quality Control
RHBC.....	Rice Hull Biochar
SEM	Scanning Electron Microscopy
SUBC	Sugarcane bagasse biochar
WHO.....	World Health Organisation
XPS	X-ray Photoelectron Spectrometer
XRD	Powder X-ray Diffraction

CHAPTER 1: INTRODUCTION

1.1. Rationale of study

1.1.1. Background

Environmental toxic compounds entering the life cycles of humans and animals is reported at an unprecedented scale and is an emerging worldwide concern. Amongst the most dangerous of contaminants, arsenic (As) plays a significant role as it creates several detrimental health impacts. Arsenic ranks 20th in natural abundance in the earth's crust, 14th in seawater and 12th in the human body (Baig et al., 2015; Ozturk et al., 2021; Tomiyasu et al., 2021). It is ubiquitous in the environment, and it possesses both metallic and non-metallic properties. Arsenic occurs in both solid and liquid phases, however, it rarely exists in nature in its native state. It is reported that there are 150 species of As-bearing minerals in nature, including arsenic sulphide (As_2S_2), arsenic trisulphide (As_2S_3) and arsenopyrite (FeAsS_2). More precisely, rocks, soils, water, air and biological tissues contain As in varying degrees (Kumarathilaka et al., 2018b; Marescotti et al., 2011; Zacharias et al., 2004).

Water contaminated with As is considered one of the well-known causes of cancer in humans in most parts of the world. The International Agency for Research on Cancer (IARC) classifies inorganic arsenic as a Group A carcinogen (IARC, 2004). Long-term chronic exposure to As causes a range of ailments including skin lesions, nervous system impairment, irritation of respiratory organs and the gastrointestinal tract, anaemia, liver disorders, vascular illnesses, cancers (i.e., skin, lung, liver, kidney and bladder) and even diabetes mellitus, and also can affect the intellectual development of children (Argos et al., 2012; Rahman et al., 2018; Yadav et al., 2021; Zhang et al., 2019). In addition, As can act as a catalyst in redox reactions, forming reactive oxygen species which damage DNA, proteins and lipids (Dutta et al., 2005; Lopez-Cueto and Ubide, 1990).

Arsenic is considered as a metalloid and there is no biodegradable mechanism for As in the natural environment as heavy metals and therefore, through As-contaminated water, the bioaccumulation can easily occur in human, animals and also in aquatic plant species. As well as direct contact from As-contaminated water, soil can be contaminated with irrigation water or wastewater coming from As rich sources. This creates serious, negative consequences for plants which become an As contaminated food source for human and animals. Environmental or water contamination by As can occur through either natural or anthropogenic sources. The natural sources for As contamination are mainly volcanic deposits, natural weathering activities, inputs from geothermal sources and mining waste. Moreover, anthropogenic

activities such as the smelting of metal ores, uncontrolled industrial discharge from mining, petroleum refining, use of arsenical pesticides, herbicides, use of As additives to livestock feed, wood preservative agents and different industrial activities can play a leading role in the release of As into water sources (He and Charlet, 2013; Kumarathilaka et al., 2018a; Villaescusa and Bollinger, 2008). Therefore, As-contaminated water and wastewater must be treated through effective removal processes before use for human consumption or release into the environment.

Arsenic removal is a significant challenge for scientists, engineers and policymakers as it is not naturally degradable, but can only be converted into other forms or insoluble compounds with metals such as iron and lead (Choong et al., 2007; Leist et al., 2000). As the impacts are dangerous and removal is of emerging importance, there is a number of research studies focused on the removal of As from both wastewater (Altowayti et al., 2021; Gupta et al., 2010; Singh and Sarma, 2010) and drinking water (Alburaih et al., 2022; Kobya et al., 2011; Qazi et al., 2022).

Several types of As remediation are currently available and, of these, adsorption has attracted significant interest as it requires minimal energy, involves easy setup, does not require additional chemicals, does not produce harmful by-products, requires minimal operator expertise and low operating and maintenance costs, and is environmentally-friendly. Therefore, the adsorption technique is an economical and efficient method.

A number of different materials have been investigated and shown to possess successful adsorption capabilities (Ahmad et al., 2022; Carneiro et al., 2022; Dutta et al., 2021). However, most of these materials lack the capability of easy separation of adsorbed materials from water after completion of the removal process, and face problems with reusability after use for one or two As removal cycles. These are vital characteristics for an effective and environmentally friendly removal method. Recently, hydrogels prepared from different materials have gained research interest due to their remarkable potential for removing metals and metalloids from wastewater (de Araujo et al., 2023; Hamza et al., 2022; Sanyang et al., 2016).

Hydrogels have become state-of-the-art applications in the past few decades as their unique properties make them advantageous for a number of applications such as agriculture (Das et al., 2021; Liu et al., 2022), drug delivery (Xiao et al., 2021; Zhao et al., 2021), coal dewatering (Ahmed, 2015), artificial snow (Ahmed, 2015), food additives (Li et al., 2021a), pharmaceuticals (Parhi, 2017), bio-medical applications such as tissue engineering, regenerative medicine, wound dressing, and as barrier material (Hoffman, 2012; Li et al., 2021b; Zhang et al., 2021). Although hydrogels have a long history in some of the above

applications (especially in the biomedical sector), their applications to water treatment have only been reported in the last decade.

Hydrogels are not strangers to nature as there are natural hydrogels. Examples of natural hydrogels are proteins and polysaccharides which are polymer forming natural hydrogels. However, due to their enhanced efficiency, synthetic hydrogels are the most considered hydrogels in all the abovementioned sectors. Hydrogel-composite preparation has gained significant interest in the last few years for applications in environmental remediation including water treatment. Synthetic hydrogels have some disadvantages such as high production cost and latent toxicity (Sanyang et al., 2016; Xiao, 2013).

To overcome these principal drawbacks related to cost and potential environmental problems, researchers have developed hydrogel composite materials with natural, low-cost, non-toxic and biodegradable materials. Combining a hydrogel with another material with a higher adsorption capacity may enhance the sorption capacity significantly. Further, since hydrogels can swell in water without dissociation or dissolving of their ingredients, adsorbent-water separation can be achieved without the need for high-tech methods and/or expertise.

1.1.2. Significance of study

Human consumption of As creates a number of acute and chronic health impacts including cancers and, ultimately, death. The major route for As in the human body is drinking water and agricultural crop products that have been contaminated with As through irrigation water. Therefore, removal of As in water before human consumption is essential. Many methods have been studied and/or implemented to recover water from As contamination. However, still there is no reliable As removal method for water that is both financially and environmentally sustainable. The major drawbacks of the available methods are the high cost and technical expertise required, lack of availability for regeneration and re-use, and the high-tech processes required to separate adsorbent from the water after the As removal process.

The major classic drawbacks addressed through this study are water-adsorbent separation and regeneration and reusability. To achieve an easy water-adsorbent separation that does not require high-tech procedures, the use of a hydrogel-based product is a significant approach. Hydrogel has a three-dimensional structure where polymer chains are connected through crosslinkers. Depending on the crosslinking density, hydrogel can undergo dissociation or remains intact when it swells in water. With the use of this feature, the correct amount of crosslinking density will help to create swelling in water without dissociation. Then the removal of the hydrogel from water is a simple method.

Taking these factors into account, this PhD study has assessed, developed and optimised cost-effective, novel, technically and practically employable adsorption materials for removal of As in aqueous media that can overcome the classic drawbacks of traditional adsorption processes. Modified hydrogels have been synthesised incorporating low-cost, good adsorbent materials to enhance the As adsorption capacity.

Regarding the incorporation material, we focused on waste materials from industries where we can recycle and re-use the waste in order to reduce the cost of waste disposal. Rice hull is one of the major waste products from rice production that can be accessed easily from any part of the world. Sugarcane bagasse is the major waste product generated in the sugarcane industry. It is a well-known fact that biochar is a low-cost material which can produce from many natural materials. Biochar can enhance the properties of material which can be used as an adsorbent material for many of environmental contaminants. Based on these facts, two different biochar have been used in this study to synthesis the modified hydrogels. Chitosan is another biomaterial that is readily available at a low cost. Further chitosan has been considered as a good adsorptive material for several environmental contaminants including As. The second modified hydrogel composite is based on chitosan.

1.2. Research gaps

Our literature review identified the following research gaps:

1. The reliable methods currently available for As removal are high-tech methods which are high cost and require expert knowledge. Such methods are not applicable at a household level, and even for large-scale industrial levels, they are not cost effective
2. The adsorption methods for As removal that have been studied so far require additional energy to separate the adsorbent from the water after the adsorption process. This makes the whole As removal process inefficient. Furthermore, these methods are not suitable for drinking water purification
3. Most of the identified As removal processes are not available for regeneration and re-use which creates lots of waste products and increases the cost of production and cost of waste disposal.

1.3. Research questions

There are three main research questions in this study:

1. How to develop an adsorbent that can be easily separated from water without additional energy or high-tech requirements?

2. How to incorporate hydrogels with low-cost biomaterials that can efficiently remove As from water?
3. How to regenerate the modified hydrogels that were used for As removal from water and re-use the same material for As removal from water?

1.4. Research aims and objectives

The overall aim of this PhD project is to develop an economically feasible and technically employable, easy to separate from water, environmentally friendly novel hydrogel material/s for effective removal of As in aqueous solutions. The specific objectives are listed below:

1. To synthesise and characterise two hydrogel composites using biochar (BC) which is prepared from waste materials and Fe₃O₄ nanoparticles functionalised polyvinyl alcohol/chitosan as an efficient and effective adsorbent for As removal from water and wastewater
2. To prepare and select the best BC-hydrogel material out of several BC types for the most efficient As removal from water and wastewater
3. To investigate the effect of various parameters (pH, adsorbent dosage, contact time, and initial As concentration) on the adsorption of As
4. To evaluate the adsorption capacities of two different hydrogel composites by using kinetic and isotherm models
5. To investigate the re-use capability of synthesised hydrogel composites to the removal of As in the aqueous solutions in order to maximise the efficiency of the materials and reduce the amount of waste material and the cost of the removal process.

1.5. Organisation of the thesis

This PhD thesis consists of eight chapters and the organisation of the thesis is shown in Figure 1.

Chapter 1 describes the background and significance of the study, research gaps, research questions, and research aims and objectives.

Chapter 2 presents the literature review for the study. This chapter comprises two Q1 ranked papers: **Paper 1** (Hydrogels: Novel materials for contaminant removal from water—A review) presents the current understanding of hydrogels and their use in the removal of contaminants from water. **Paper 2** (Selective removal of arsenic in water: A critical review) describes the methods currently available for As removal from water, and the pros and cons of

these methods. The new insights and research gaps highlighted in these articles were utilised for the development of the research studies in Chapters 3, 4 and 5.

Chapter 3 presents **Paper 3** (Development of regenerative, re-usable and easily water-adsorbent separable hydrogel composite with rice hull biochar for efficient removal of arsenic (V) from aqueous media) which investigates the adsorption capacities and mechanisms of As(V) adsorption into a rice-hull biochar hydrogel composite and its capacity for regeneration and re-use on As(V) adsorption.

Chapter 4 presents **Paper 4** (Synthesis of re-usable hydrogel composite integrating sugarcane bagasse biochar for large industrial to household scale arsenic (V) removal from aqueous media and comparison with rice-hull biochar hydrogel composite) which investigates adsorption capacities and mechanisms of As(V) adsorption into a sugarcane bagasse biochar hydrogel composite and its capacity for regeneration and re-use on As(V) adsorption. Further, its adsorption capacity will be compared with the adsorption capacity of the rice hull biochar hydrogel composite which is discussed in Chapter 1.

Chapter 5 presents **Paper 5** (Assessment and optimisation of As(V) adsorption on hydrogel composite integrating chitosan-polyvinyl alcohol and Fe₃O₄ nanoparticles and evaluation of their regeneration and re-use capabilities in aqueous media) which investigates the adsorption capacities and mechanisms of As(V) adsorption into a chitosan and Fe₃O₄ nanoparticles integrated hydrogel composite and its capacity for regeneration and re-use on As(V) adsorption.

Chapter 6 presents **Paper 6** (Cu(II)-loaded chitosan-polyvinyl alcohol and Fe₃O₄ nanoparticle integrated hydrogel composite for enhanced and efficient arsenic (V) adsorption) which investigates the adsorption capacities and mechanisms of As(V) adsorption into further modified chitosan and Fe₃O₄ nanoparticles integrated hydrogel composite with Cu and its capacity for regeneration and re-use on As(V) adsorption.

Chapter 7 presents **Paper 7** (Assessment of arsenic (III) removal from water with biochar hydrogel composites which were successful in arsenic (V) removal from water and overcame the classic drawbacks of adsorbent materials) which investigates the adsorption capacities and mechanisms of As(III) adsorption into a rice hull biochar hydrogel composite and sugarcane bagasse biochar hydrogel composite and their capacity for regeneration and re-use on As(III) adsorption.

Chapter 8 provides the conclusions and recommendations of this PhD research project whilst also highlighting future research directions.

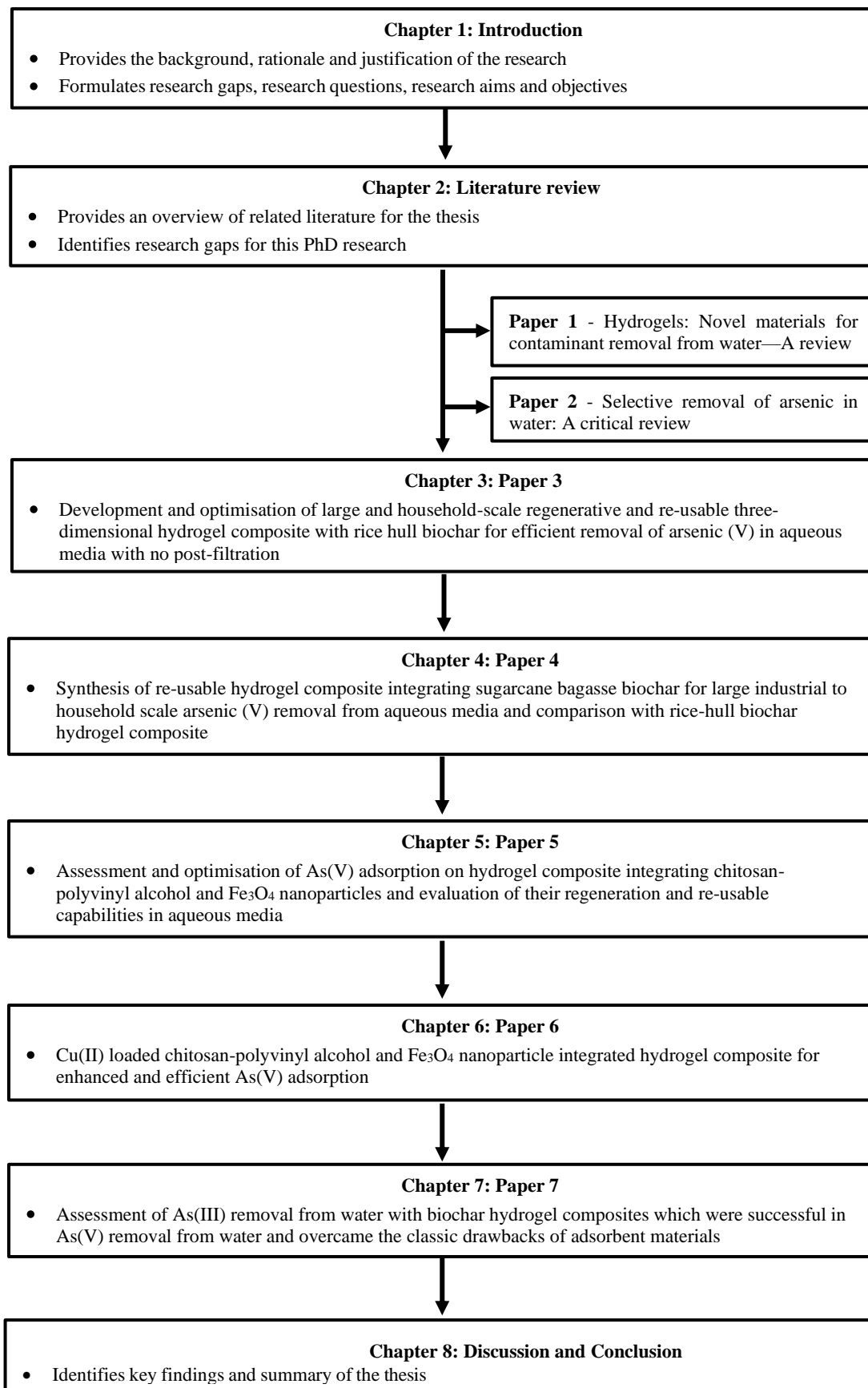


Figure 1 Organisation of the thesis

CHAPTER 2: LITERATURE REVIEW

This chapter is divided into two main sections based on the review articles published during the PhD research. The first subsection describes hydrogels; their preparation methods, classifications, characteristics and contaminant removal using hydrogels. The second section provides an overview of the selective removal of As from water. This part discusses the different As removal methods, removal mechanisms and the pros and cons of these As removal methods. Overall, this chapter provides a comprehensive discussion of hydrogels and As removal from water, and highlights future research directions.

2.1. Paper 1: Hydrogels: Novel materials for contaminant removal from water—A review

2.1.1. Introduction

This review describes the contaminant removal from water using hydrogel-based materials. It highlights the recent results achieved, unresolved problems and possible developments. Polymer and graphene hydrogels offer a very promising application for removing inorganic (i.e., metals and metalloids) and organic trace (i.e., dyes) contaminants from water. They can be prepared as composites with practically any conventional or innovative adsorbent and by incorporating more features (i.e., magnetic feature) for efficient contaminant removal. Obtaining a highly effective, three-dimensional network for adsorption (or other contaminant immobilisation mechanisms) is one of the significant features behind hydrogels, and this feature gives hydrogels specific characteristics including for selective removal, easy separation, and combination with conventional membranes creating a robust structure. There are a number of benefits of hydrogel use versus conventional adsorbents alone, such as easy separation and easy handling, large scale application, capability to regenerate and re-use, etc. However, at present the experiments on hydrogels for water purification are mostly limited to laboratory scale and further research is needed to move towards large-scale industrial applications. Moreover, present studies are narrow, focusing only on a few types of contaminants so that further experiments are needed for more contaminant types. Studies are also required for the removal of mixtures of contaminants as, in practice, there is often not a single type of contaminant.

This article cannot be displayed due to copyright restrictions. See the article link in the Related Outputs field on the item record for possible access.

2.1.3. Concluding remarks

Water contamination through inorganic and organic minor and trace elements is one of the most significant global issues as there is a very limited amount of water available for human and animal needs. Therefore, economically and technologically feasible and sustainable contaminant removal from aqueous media is a challenge for the global community; making water purification one of the most important sectors in research and development.

There have been thousands of attempts to remove contaminants from aqueous media, but still there are huge gaps in academic studies (mostly on a laboratory scale) and the practical onsite application following the broad goal of “Science for Society”. The invention of hydrogel was one of the turning points in the contaminant removal process. As an adsorbent, the modified hydrogel has shown remarkable advantages over most other adsorbents such as lower production cost, low operational cost, easy preparation, easy separation after the adsorption process, ability to recover and ability to re-use in a long-term manner. Moreover, some hydrogels which have pH independent characteristics can be used in natural waters to remove contaminants without pre- and post-treatments (i.e., pH adjustments). Further, hydrogels can be used at all scales with efficiency; ranging from single household to large industrial scale. Most importantly, hydrogel use in the water treatment sector is still developing with the preparation of novel hydrogel types incorporating many advantageous characteristics into conventional hydrogel types. However, we still cannot find any significant existing practical application of hydrogels in water purification processes.

Graphene based hydrogels, magnetic hydrogels and hydrogel composites are novel materials possessing enhanced properties. However, more research is required with field level applications and the optimisation of required conditions. Since water resources are contaminated with a great variety of contaminants or contaminant groups, interactions between the different contaminants and other chemical species present in the water together with variable physicochemical parameters must be studied to enable the design and development of optimal removal processes. Such processes must also adapt to the specific situations and tasks to which they will be applied. Future hydrogels could also be developed to integrate with micro-organisms (bacteria, fungi, microalgae, etc.) which degrade water contaminants.

The three-dimensional network structure may facilitate more spacious environments for such biological organisms, and if the attempt to develop such a structure is successful, it could enhance the reusability of hydrogels to a remarkable scale. All the features and capabilities of hydrogels prove that it is an excellent option for water purification, and with the

development of its capabilities to an industrial scale, it will create possibilities for changing and revolutionising the water treatment industry.

2.2. Paper 2: Selective removal of arsenic in water: A critical review

2.2.1. Introduction

This review identifies the importance of As removal from water and the currently studied selective As removal methods. More than 4000 freshwater systems requiring As mitigation measures to meet the guidelines of the World Health Organisation (WHO) for drinking water supply can be found globally. Most of these systems are groundwater reservoirs. More than 60% of anthropogenic As globally emitted originates from coal combustion and Cu smelting processes.

With such natural and anthropogenic factors in action, there are more than 105 countries and over 202 million people suffering from As contamination. Some of the most affected countries are Bangladesh, Vietnam, USA, West Bengal (India), Taiwan, Cambodia, Canada, Germany, Hungary, Japan, Laos, Nepal, Pakistan, Poland, Romania, Thailand, UK, Ghana, China, and Latin American countries including Mexico, Argentina, Chile and Nicaragua. Arsenic exposure has been linked to a number of cancerous and non-cancerous impacts in both acute and non-acute forms. In the carcinogenic grouping, As has been categorised into Group 1 elements. Hence, As is one of the major elements producing cancer. Therefore, the removal of As from water is needed urgently. Taking these facts into account, this study investigated, the methods that have been used for selective As removal from water.

This article cannot be displayed due to copyright restrictions. See the article link in the Related Outputs field on the item record for possible access.

2.2.3. *Concluding remarks*

The selective removal of As from aqueous solutions is a challenge for several reasons. In most cases, the common anions present in natural water and wastewater, which are generally present in much higher concentrations, are competing with As adsorption. Moreover, with the solution pH and the redox potential, the As changes into different oxidation forms, including arsenic (V) (As(V)) oxyanions and neutral arsenic (III) (As(III)) species. It has been identified that hydrated granular or amorphous Fe(III) has a significant capability to remove As(III) and As(V) in aqueous solutions in a selective manner.

To improve mechanical strength and adsorption capacities, there have been attempts to incorporate mechanically strong materials with hydrated granular or amorphous Fe(III). Chitosan and ion-exchange resins are examples of this. The firm deposition of hydrated granular or amorphous Fe(III) in the used matrix is an important step in the preparation procedure to improve the selective As removal. Instead of Fe(III), metal ions such as Cu(II), La(III), and Al(III) have been used for selective As removal, and they also show significant As removal capabilities.

There is no single material that can be used for selective As removal which is pH-independent. Therefore, the pH of the solution is a limiting factor for As removal by any of the selective As removal materials. However, most of the selective As removal materials are suitable within a pH 6-8 range which is the range of most natural water. Moreover, there is evidence to show that microbial methods for selective As removal from aqueous media can be effective. Most of the co-existing anions such as sulfate, nitrate, bicarbonate, chloride and fluoride do not interfere with As removal through most of the selective As removal materials. However, phosphate adversely impacts As removal via many of the methods. This is because phosphate ions have the same chemical structure as As and it is chemically compatible with As.

Chitosan and Cu(II) integration can form two types of bonds which remove As and phosphate separately. Both bonds present as a mix and to enhance the As removal over phosphate the formation of As removal bond should be optimised. Even though phosphate is also removed with most of the selective As removal measures, the selective As removal in natural water is an important achievement. In most of the cases, the phosphate concentrations are much lower than those of the main ions. Therefore, the abovementioned selective As removal methods are well suited to addressing the global As contamination issue. As a consequence, more studies are needed to overcome the interference of phosphate with As removal, especially for water resources that have high phosphate concentrations.

Thiol based removal methods have the ability to target specific As species when both As(III) and As(V) are present in water. Moreover, the high affinity of thiol groups towards As species offers greater future potential to minimise competition from phosphate in selective As removal. If such an affinity could be combined with the Cu(II) and chitosan, it may even prevent phosphate competition.

Even though there are microbial methods to remove As in a selective manner, the studies have not extended to testing the interference of phosphate with As removal. Therefore, more studies into an extended scope in microbial methods as a selective As removal strategy are needed. If the microbial methods are strong enough to compete with phosphate, the incorporation of both chemical and microbiological methods may overcome the interactivity issues associated with common ions. Further studies are needed to assess the possibility of a combination of chemical and microbiological methods.

CHAPTER 3: PAPER 3 – DEVELOPMENT OF REGENERATIVE, RE-USABLE AND EASILY WATER- ADSORBENT SEPARABLE HYDROGEL COMPOSITE WITH RICE HULL BIOCHAR FOR EFFICIENT REMOVAL OF As(V) FROM AQUEOUS MEDIA

3.1. Introduction

Natural contamination through As mobilisation from geogenic sources is the major reason for the presence of As (up to >1000 µg/L) in most groundwater resources. Human activities such as mining and related processes can accelerate this release of As by several orders of magnitude. With the increasing global population, the agricultural demand and excessive groundwater withdrawal have resulted in the dissolution of As within the aquifers. More than 60% of anthropogenic As globally emitted originates from coal combustion and Cu smelting processes.

Arsenic exposure has been linked to a number of cancerous and non-cancerous impacts in both acute non-acute forms. Therefore, As contaminated water must be treated for As before use for any purpose. Among many different As removal methods the adsorption technique has gained interest due to several advantages such as easy and simple setup, not requiring expertise knowledge, sustainability, environmental friendliness and low cost. However, the adsorption methods still show several classic drawbacks such as difficulty in water-adsorbent separation, lack of availability for regeneration and re-use. Considering these facts this study focused on the development of a novel material for As(V) removal in water that supports easy water-adsorbent separation, regeneration and reusability.

Development of regenerative, re-usable and easily water-adsorbent separable hydrogel composite with rice hull biochar for efficient removal of As(V) from aqueous media

Lakshika Weerasundara^a, Prasanna Kumarathilaka^a, Alla Marchuk^b Jochen Bundschuh^{*a,c}

^a*School of Civil Engineering and Surveying, Faculty of Health, Engineering and Sciences, University of Southern Queensland, West Street, Toowoomba, Queensland, 4350, Australia*

^b*Institute for Life Sciences and the Environment, University of Southern Queensland, West Street, Toowoomba, Queensland, 4350, Australia*

^c*Doctoral Program in Science, Technology, Environment, and Mathematics, Department of Earth and Environmental Sciences, National Chung Cheng University, 168 University Rd., Min-Hsiung, Chiayi County, 62102, Taiwan*

*Corresponding author

E-mail address: jochen.bundschuh@usq.edu.au (Jochen Bundschuh), School of Civil Engineering and Surveying, Faculty of Health, Engineering and Sciences, University of Southern Queensland, Toowoomba, Queensland 4350, Australia. Doctoral Program in Science, Technology, Environment, and Mathematics, Department of Earth and Environmental Sciences, National Chung Cheng University, 168 University Rd., Min-Hsiung, Chiayi County, 62102, Taiwan

Abstract

A modified poly(acrylamide) hydrogel was developed by incorporating rice hull biochar (RHBC); characterisations were conducted and assessed the capability on Arsenic (V) (As(V)) removal in water. Three RHBC types were developed with slow pyrolysis using three different temperatures: 500, 600 and 700 °C, and separated into three size fractions: 1.18, 0.60 and 0.06 mm. In total, nine hydrogel types were obtained. Batch sorption experiments and regeneration and re-use studies were conducted. The highest As(V) adsorption (15%) was at the pH range of 6-7. Within the pH 6-7 range, the protonation of the -NH₂ and -COOH groups in the polymer chain created a positively charged hydrogel surface that attracted H₂AsO₄⁻ and HAsO₄²⁻ oxyanions. The adsorption showed 6 h equilibrium time and 0.074 mg/g of equilibrium capacity. The experimental kinetic and isotherm models best fitted with pseudo-first order (R² 0.96) and Langmuir (R² 0.99) respectively, predicting chemisorption and physisorption mechanisms. 0.1 M NaOH showed the best regeneration pattern with 26%, 81%, 23% and 26% of 1st, 2nd, 3rd and 4th adsorption, respectively.

Keywords: Arsenic(V), hydrogel composite, biochar, water treatment

1. Introduction

The screening of drinking water for arsenic is considered a high priority (WHO, 2006). Worldwide, more than 105 countries are potentially contacted to toxic levels of arsenic in drinking water (Kumarathilaka et al., 2020; Shahab et al., 2019; Weerasundara et al., 2021). Arsenic is readily soluble in water, therefore both groundwater and surface water can be contaminated efficiently and agricultural crop harvests can be contaminated easily (Kumarathilaka et al., 2018a; b). Ingestion of inorganic arsenic leads to both acute and chronic detrimental health impacts (Kumarathilaka et al., 2021c). Once ingested, inorganic arsenic has the ability to be distributed quickly to various organs in the human body and rapid absorption into those organs (Steinmaus et al., 2000; Weerasundara et al., 2021).

The World Health Organisation has recommended the guideline value for arsenic in drinking water as <10 µg/L to minimise the adverse health impacts (WHO, 2006). Achieving the guideline value is a challenging task for arsenic contaminated water. In the last few decades, various arsenic decontamination methods have been developed (Weerasundara et al., 2021). All these methods have both comparative advantages and disadvantages. Adsorption is one of the most employed methods because it requires simple setup and many adsorptive material

options are available. Biochar (Amen et al., 2020), coal fly ash (Ochedi et al., 2020), metal-organic framework-based materials (Ploychompoo et al., 2020), natural materials (Elizalde-González et al., 2001; Maji et al., 2011), agricultural components (Shabbir et al., 2020; Tabassum et al., 2019), industrial by-products (Jovanović et al., 2011; Lekić et al., 2013) and graphene oxide (Xikhongelo et al., 2021) are the most common types of adsorptive materials used for arsenic removal from water (Uddin and Jeong, 2020). However, due to the importance of removing arsenic from water, researchers are working on novel materials which have potential adsorption capacities and elevated efficiency.

Although adsorption is an economical method for removing arsenic from water, if the adsorbent tends to disperse in water and change its colour, it requires additional energy or high-tech to separate the adsorbent from the water. Therefore, most adsorbent materials are not reliable and economical for both small- and large-scale applications. Hydrogels are materials with a three dimensional structure and, when maintaining correct gel strength, they can swell in water without dispersal or dissociation of structure (Weerasundara et al., 2020). Therefore, hydrogel can be identified as an excellent option for overcoming the most significant disadvantage of other adsorbent materials: water-adsorbent separation.

Hydrogel is a widely used concept in various sectors (Asadi et al., 2021; Liang et al., 2021; Mandal et al., 2020; Weerasundara et al., 2020). However, the use of hydrogel as an adsorptive material is gaining research interests due to its high adsorption and swelling capacity, low production cost, possibility for modification, and availability for regeneration and re-use (Weerasundara et al., 2020; Weerasundara et al., 2022). Different types of hydrogels and modified hydrogels have been used to remove many pollutants from water such as metal ions, pharmaceuticals, dyes and organic contaminants (Karakoyun et al., 2011; Pereira et al., 2021; Weerasundara et al., 2020). Different hydrogels have been used to remove arsenic from water. Some of these are: polyvinyl alcohol based hydrogels, chitosan based hydrogels, cationic hydrogels and montmorillonite based hydrogels (Baigorria et al., 2020; Barakat and Sahiner, 2008; Weerasundara et al., 2022; Yan et al., 2020). The availability for modification open the way to incorporation of another material to improve its performances.

Biochar, metal ions such as ferric oxide, cupric oxide and lanthanum are some of the materials that can be used for the synthesis of modified hydrogels for arsenic removal (Weerasundara et al., 2022; Yan et al., 2020). Biochar, it is a low-cost material which can be produced with different feedstocks. As the negative environmental and human health impacts of biochar are minimal, it is a material suitable for any water treatment scale and place. Modified biochar has significant adsorption capacity for arsenic in water (Kumarathilaka et al.,

2021b), but it requires aftercare operations to separate the water from the biochar. Nevertheless, the incorporation of biochar into hydrogel avoids the release of biochar into water (Sanyang et al., 2016). Therefore, the incorporation of biochar into hydrogel enhances its advantages while reducing its disadvantages. However, there are very few studies that focus on hydrogel-biochar composites for the removal of arsenic from water.

The incorporation of biochar into the hydrogel matrix adds a number of advantages to the adsorption process. Firstly, biochar helps to enhance the hydrogel's gel strength, giving it stability in aqueous environments. Secondly, biochar enhances its adsorption capacity through favourable functional groups (Sanyang et al., 2016).

This study focused on the development of a novel composite material based on poly(acrylamide) hydrogel with the incorporation of rice hull biochar (RHBC); determining and comparing the efficiency of the composite on As(V) adsorption. The hydrogels were synthesised by incorporating biochar produced under different pyrolysis temperatures and into different particle sizes. The resulting materials were then compared on the basis of the hydrogel's As(V) adsorption performance. To the best of our knowledge, this is the first time such a comparison has been conducted. Material regeneration and reusability were also assessed.

2. Experimental

2.1. biochar preparation

To produce RHBC, dried rice hulls purchased from Grain and Grape, Victoria, Australia. The RHBC produced using a slow pyrolysis and continuous nitrogen flow (to facilitate O₂ free environment) (2 L/min) in a muffle furnace (CS₂, RIO GRANDE) at three different temperatures (500, 600 and 700 °C) for 2 h holding time. The heating rate was 7 °C/min. The RHBCs were de-mineralised and oven dried (STERIDIUM) at 50 °C for 72 h. The obtained RHBCs were ground and sieved to create three different sized fractions: 1.18, 0.6 and 0.06 mm. In total, nine different RHBC types were obtained for hydrogel preparation.

2.2. Synthesis of RHBC hydrogel composite

To prepare the hydrogel-rice hull biochar composite (RHBC hydrogel composite), acrylamide (monomer), N, N'-methylene bisacrylamide (crosslinker), and ammonium persulfate (initiator) were used. The preparation of RHBC hydrogel was conducted following the method described in Sanyang et al. (2016). In brief, 1.0 g of acrylamide dissolved in 1.0

mL distilled water. 0.6 g and 0.001 g of biochar and N, N'-methylene bisacrylamide respectively were added to the acrylamide solution. After thorough

mixing of the solution with a vortex mixer, 0.2 mL of (0.5 g/mL) ammonium persulfate was added to initiate the polymerisation. The RHBC hydrogel precursor solution was immediately placed into 5 mm clear vinyl tubes and, after 24 h the RHBC hydrogel was removed from the tubes and washed. Nine different hydrogels were resulted (Table 1). The preparation of pure acrylamide hydrogel followed the abovementioned procedure except for the addition of biochar step.

Table 1 *Nine different hydrogels based on pyrolysis temperature and particle size of biochar*

		BC particle size		
		1.18 mm	0.60 mm	0.06 mm
Pyrolysis temperature	500 °C	5R 1.18 hydrogel	5R 0.6 hydrogel	5R 0.06 hydrogel
	600 °C	6R 1.18 hydrogel	6R 0.6 hydrogel	6R 0.06 hydrogel
	700 °C	7R 1.18 hydrogel	7R 0.6 hydrogel	7R 0.06 hydrogel

2.3. RHBC hydrogel characterisation

2.3.1. Swelling and point of zero charge

Swelling behaviour was measured by placing the selected RHBC hydrogel composite in distilled water. The swelling percentage was measured with four different NaCl concentrations (3, 1, 0.1 and 0.01 M) to determine the swelling behaviour with different ionic strengths. Periodically, the mass increase was measured at room temperature until it becomes nearly constant and equation 1 was used to calculate the swelling percentage.

$$\text{Swelling \%} = \frac{W_{\text{swollen}} - W_{\text{dry}}}{W_{\text{dry}}} \times 100 \quad (1)$$

W_{swollen} is mass of swollen hydrogel, W_{dry} is mass of dry The point of zero charge (PZC) of the selected RHBC hydrogel composite was measured by The salt addition method described by Bakatula et al. (2018) used to measure the point of zero charge (PZC).

2.3.2. Physical and chemical characterisation

Scanning Electron Microscopy (SEM) analysis (JCM-6000, JEOL, 1 min gold coating), Fourier Transform Infrared (FTIR) analysis (IRAffinity-1S, Shimadzu, within the spectral range of 400-4000 cm^{-1}) X-ray Photoelectron Spectrometer (XPS) analysis (Kratos Axis Ultra XPS) and powder X-ray diffraction (XRD) analysis (Bruker Advance D8 X-ray Diffractometer) were conducted.

2.4. Batch sorption experiments for RHBC hydrogel composite

Sodium arsenate dibasic heptahydrate ($\text{Na}_2\text{HAsO}_4 \cdot \text{H}_2\text{O}$) used to prepare 1000 mg/L of As(V) solution. This stock solution was used for the preparation of As(V) solutions with required concentrations, and the solutions were freshly prepared for each study. As(V) were measured using Inductively Coupled Plasma Mass Spectrometry (ICP-MS) (PerkinElmer NexION™ 300X). To ensure the Quality Assurance/Quality Control (QA/QC) measures, all the samples were measured as triplicates. The laboratory blanks and standard blanks were measured. Further, the standards and blank samples were tested per every twelve samples. The complete standard curve testing was conducted per every 60 samples. To assess the best solution pH for optimum As(V) adsorption for the nine different hydrogels (Table 1), an adsorption edge experiment was conducted at 5 mg/L As(V) at different pHs from 4-10 for a biochar dosage of 1 g/L. Control experiments was conducted as a quality control/quality assurance measure.. To determine the optimum hydrogel dosage on As(V) adsorption, the selected RHBC hydrogel composite was shaken at 5 mg/L of As(V) at different dosages from 1 to 100 g/L. In this experiment, RHBC hydrogels were used in two different ways: swollen and dry. A 5 mg/L As(V) was used for the kinetic experiments. The As(V) concentrations of the solution were measured at time intervals from 0.5 - 72 h. For Batch isotherm studies the As(V) concentration range of 0.025 - 7 mg/L was used. An equilibrium time of 6 h was chosen based on the kinetic experiment. The equation 2 calculates the amount of As(V) retained in the adsorbent phase (Mayakaduwa et al., 2016).

$$q_e = [C_0 - C_e]VM^{-1} \quad (2)$$

q_e - adsorbed As(V) amount (mg/g), C_0 - initial As(V) concentration (mg/L), C_e - the equilibrium As(V) concentrations (mg/L), V solution volume (L), M - hydrogel mass (g).

2.5. Experimental data modeling

Five non-linear kinetic models, and four non-linear isotherm models were used to determine the adsorption mechanisms (Ho et al., 2002) Microcal Origin software (Version 6) was used for modelling and statistical graphing of the data.

2.6. Desorption and re-sorption experiment

Desorption experiments were utilised to evaluate and verify the reusability of RHBC hydrogel. The desorption study was performed with H_2SO_4 , CH_3COOH , $NaOH$ and $NaHCO_3$ with concentrations of 1, 0.1, 0.01 and 0.001 M for each acid/base. for the shaking times were 6, 24 and 48 h. Four desorption and re-sorption cycles were conducted to determine the recycling capacity of the RHBC hydrogel composite.

3. Results and discussion

3.1. RHBC hydrogel composite synthesis

The RHBC hydrogel composites were synthesised by grafting copolymerisation The Figure 1 shows the steps and mechanism of the synthesis process. As the first step, ammonium persulfate generates sulfate anion radicals with an elevated temperature. More macro-radicals are generated by extraction of hydrogen from hydroxyl groups with reactions of sulfate anion radicals. Then, the macro-radicals reacted with acrylamide monomers to generate acrylamide monomer radicals, where these monomer radicals act as free radical donors and generate the polymeric. Simultaneously, the growing polymeric chain reacted with N, N'-methylene bisacrylamide and, as a result, the crosslinked three-dimensional structure formed (Ren et al., 2014; Tanan et al., 2019).

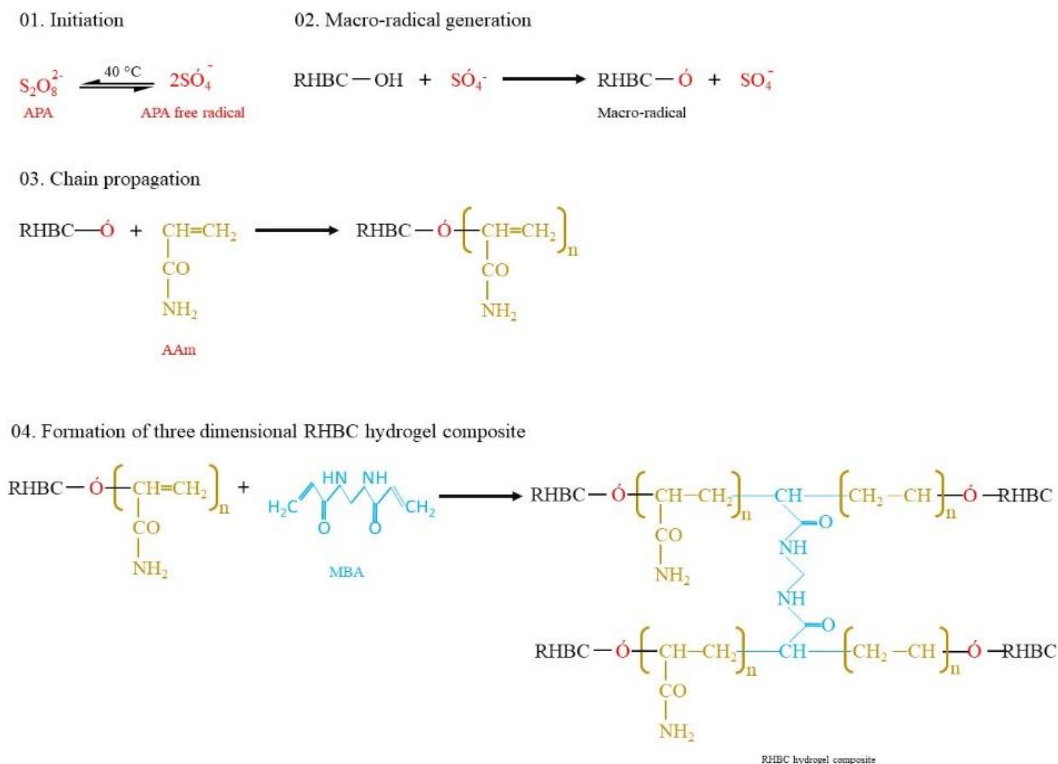


Figure 1 Mechanism of RHBC hydrogel preparation

3.2. Characterisation of RHBC hydrogel composite

3.2.1. RHBC hydrogel composite swelling behaviour

The selected hydrogel was a 700 °C 0.06 RHBC hydrogel composite (hydrogel biochar composite synthesised using RHBC produced at 700 °C and sieved through a 0.06 mm sieve). The selection procedure will be discussed with the sorption experiments. hydrogels can hold liquids with help of structure swelling. Therefore, the dissolved metal/metalloid can also uptake by the hydrogel structure. The crosslinking degree directly affect on the swelling behaviour (Sanyang et al., 2016). Figure S1(a) illustrates the swelling of an RHBC hydrogel in distilled water. A rapid swelling can be seen during first 7 h, and then swelling equilibrium is reached without any further significant increase. At equilibrium level, the RHBC hydrogel can adsorb water, increasing its mass by about 900%. This is one of the most significant characteristics of the RHBC hydrogel composite compared to most other traditional and developed adsorbents including different types of hydrogels (Qi et al., 2021; Tang et al., 2021; Wang et al., 2021).

One of the reasons for such high swelling capacity is that the RHBC hydrogel composite's polymeric chain is made on acrylamide which is considered a highly hydrophilic polymer (Zhao et al., 2010). This water absorption occurs due to repulsion between the hydrophilic groups of the polymer hydrogel and osmotic pressure alteration (Nakhjiri et al., 2021). As depicted in Figure 1, the hydrogel network consisted of a large amount of $-NH_2$ functional groups which were hydrophilic. Since the group came with the crosslinking agent, (N, N'-methylene bisacrylamide) each junction of the three-dimensional structure consisted of the $-NH_2$ group and, therefore, high water adsorption capacity was achieved (Sanyang et al., 2016). Figure S1(b) shows the swelling behaviour of RHBC hydrogel composite with different ionic strengths. Compared to the swelling behaviour in distilled water, the NaCl solutions reduced the swelling capacity of RHBC hydrogel. This can be explained by changes in electrostatic repulsions. The water absorbance in the RHBC hydrogel occurred through electrostatic repulsion between hydrophilic groups within the hydrogel. However, the presence of Na^+ ions in the media could reduce the electrostatic repulsions. This decreased electrostatic repulsion leads to decreased osmotic pressure between the hydrogel network and the salt solution (Huang et al., 2012). Figure S1(b) clearly indicates that the increase in salt concentration is the reason to decrease the hydrogel's swelling capacity. Therefore, the ion concentrations in the water affected target contaminant removal with the RHBC hydrogel.

3.2.2 Point of zero charge for RHBC hydrogel composite

Figure S2 illustrates the PZC of the RHBC hydrogel composite. When the hydrogel PZC is lower than the solution pH, the surface of the material was negatively charged and vice versa (Herath et al., 2016). Figure S2 shows how the ΔpH changes with the pH_i . Within the researched range of pH (2-10), all the plotted values are negative. However, at pH 2 the plot value is almost zero. Therefore, when the solution pH was higher than 2, the surface charge of the RHBC hydrogel was negative. In real life, all applications will be at pH levels higher than 2 and, therefore, it can be assumed that the surface charge of the RHBC hydrogel was negative at all times.

3.2.3. Characterisation of RHBC hydrogel

Figure 2 shows the SEM micrographs of the RHBC hydrogel composite. Figures 2(a) and 2(b) illustrate the surface of RHBC hydrogel composite was rough and covered by macroporous of various sizes. This macro-porous structure provided easy access for the

solution entering the hydrogel. Furthermore, Figure 2(c) shows that the hydrogels consisted of multiple layers which were interconnected to make the three-dimensional structure. Figure 2(d) shows the inside of a pore, and proves that even within the pores, microporous can be found which can help to increase the unit surface area that leads to efficient adsorption capacity.

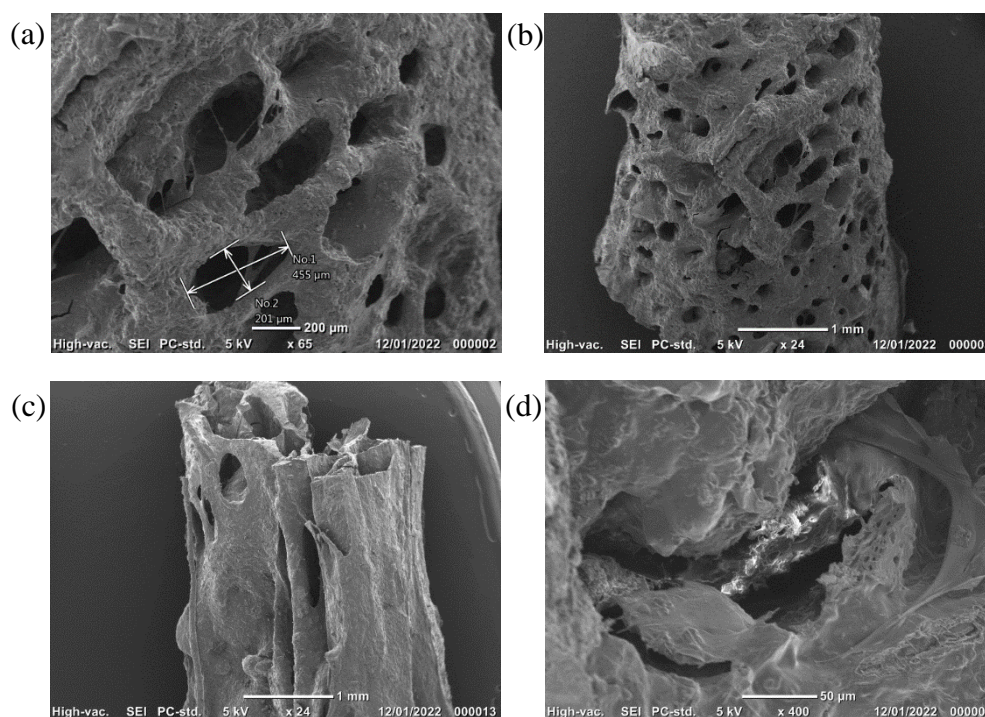


Figure 2 SEM images of RHBC hydrogel composite (a), (b), (c) - Surface (d) - Inside a pore

The FTIR spectra of the RHBC hydrogel composite, acrylamide hydrogel without RHBC, and RHBC are shown in Figure 3. RHBC hydrogel composite and acrylamide hydrogel show vibration stretching of the -NH_2 group from acrylamide at 3178 and 3170 cm^{-1} respectively. This functional group is the key advantage for the RHBC hydrogel composite over RHBC for As(V) removal in the pH range of 4-7 and will be further discussed in Section 3.3. The peaks at 1419 and 1411 cm^{-1} of the RHBC hydrogel composite and acrylamide hydrogel respectively, represent COO^- stretching of the polymeric chain. At 1604 cm^{-1} of the RHBC hydrogel composite, the peak represents the $\text{C}=\text{C}$ functional group of the hydrogel structure. RHBC shows a peak at 1064 cm^{-1} which represents the presence of oxygenated

functional groups and in the RHBC hydrogel composite, it can be the alcohol -OH group. This peak shifted to 1080 cm^{-1} .

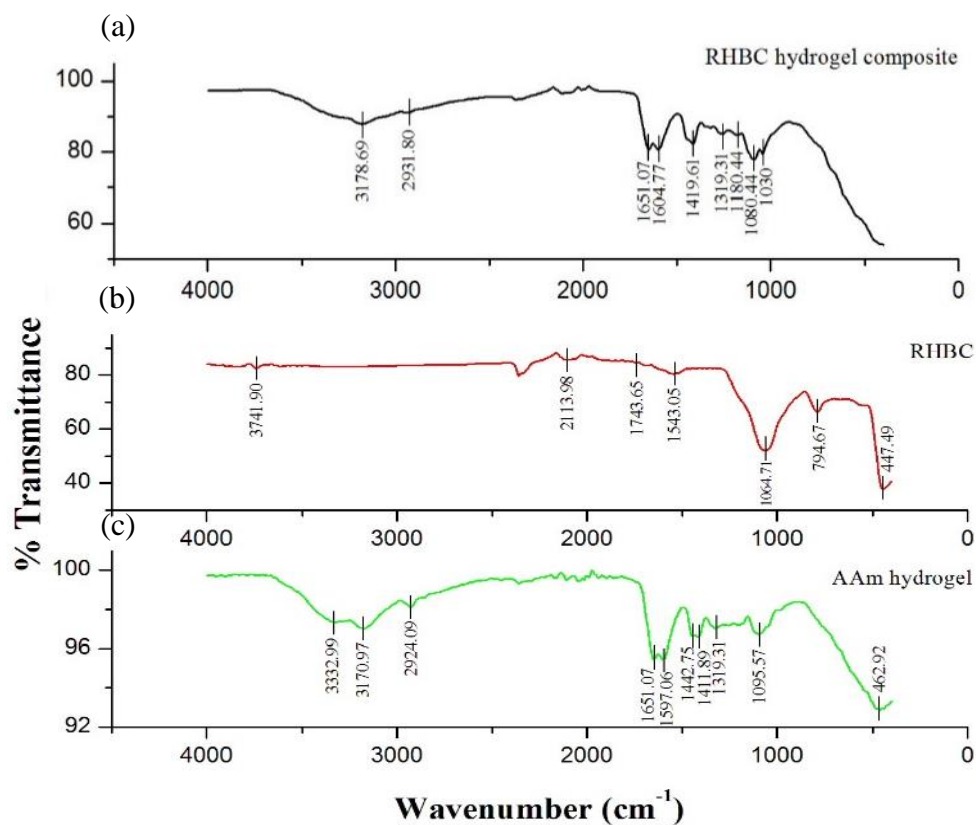


Figure 3 FTIR spectra for (a) RHBC hydrogel composite, (b) RHBC and (c) Acrylamide hydrogel without RHBC

Figure S3 shows the XRD analysis of the hydrogel. The RHBC hydrogel composite had mostly an amorphous structure from the area of the XRD pattern at $35\text{--}80^\circ$ of 2θ angles since there are no identified peaks. Besides, the peak in the 2θ angles of $19\text{--}20^\circ$ area, is related to the polymeric chain of the hydrogel ($\text{C}_{10}\text{H}_{12}\text{O}_9$). Moreover, in the 2θ angles of $22\text{--}23^\circ$ area, a peak was found related to the silica which could be from the RHBC. Karam et al. (2021) show a similar peak in their study with rice husk biochar. These silica-related peaks can be identified as silicate, silicon oxide or silicate hexane. In the process of hydrogel synthesis, the RHBC is bound to the polymeric chain through a free-radical reaction (Figure 1) and, therefore, the silica content can be bound to the polymeric chain and form RHBC which was identified with XRD pattern analysis.

The XPS analysis for RHBC hydrogel composite are depict in Figure 4. The peaks are related to Si2p, S2p, C1s, N1s and O1s. The binding energy for Si (2p) is between 102.9 and 103.9 eV (Figure 4(f)). The literature shows that SiO₂ has 103.5 eV of XPS binding energy therefore, here it can be assumed that the form of Si in the RHBC hydrogel composite is SiO₂ (Wagner et al., 2003). This fact was confirmed with XRD analysis with Si related peaks (Figure S3). In the XRD analysis, the Si content was identified as silicate, silicon oxide or silicate hexane, and with XPS analysis it was confirmed to be SiO₂. The rice hull was 5% silica by its mass and therefore, in RHBC, Si is a major compound (Karam et al., 2021). Figure 4(e) shows a peak in the range of 165.9 and 171.9 eV which is related to S. It should come from the ammonium persulfate which was the initiator of the process of hydrogel preparation. According to the hydrogel structure (Figure 1), few C types can be proposed above the C binding energy range. C-C and C-H bonds were at 285.0 eV and C=O at 287.8-288.3 eV (Beamson, 1992). A sharp N peak is found in the range of 369.9 - 402.9 eV (Figure 4(c)). Considering the hydrogel structure, these N peaks are N-(C=O)- and C-NH₂. The literature proves that N-(C=O)- can be found at 399.7 eV and C-NH₂ at 399.4 eV (Beamson, 1992; Mohtasebi et al., 2016; Wagner et al., 2003). The C-NH₂ and N-(C=O)- were the major contributors of the hydrogel structure, which transforms the hydrogel surface into a positively charged surface within the pH range of 4-7. Therefore, one of the significant functions of the hydrogel composite came with the C-NH₂ group. This fact is discussed further in Section 3.3. The O peak refers to several O bonds types that all the O bonds in the proposed hydrogel structure could explain. Moreover, O bonding in the SiO₂ appears at the binding energy of 532.9 eV which can be explained by the XPS O peak.

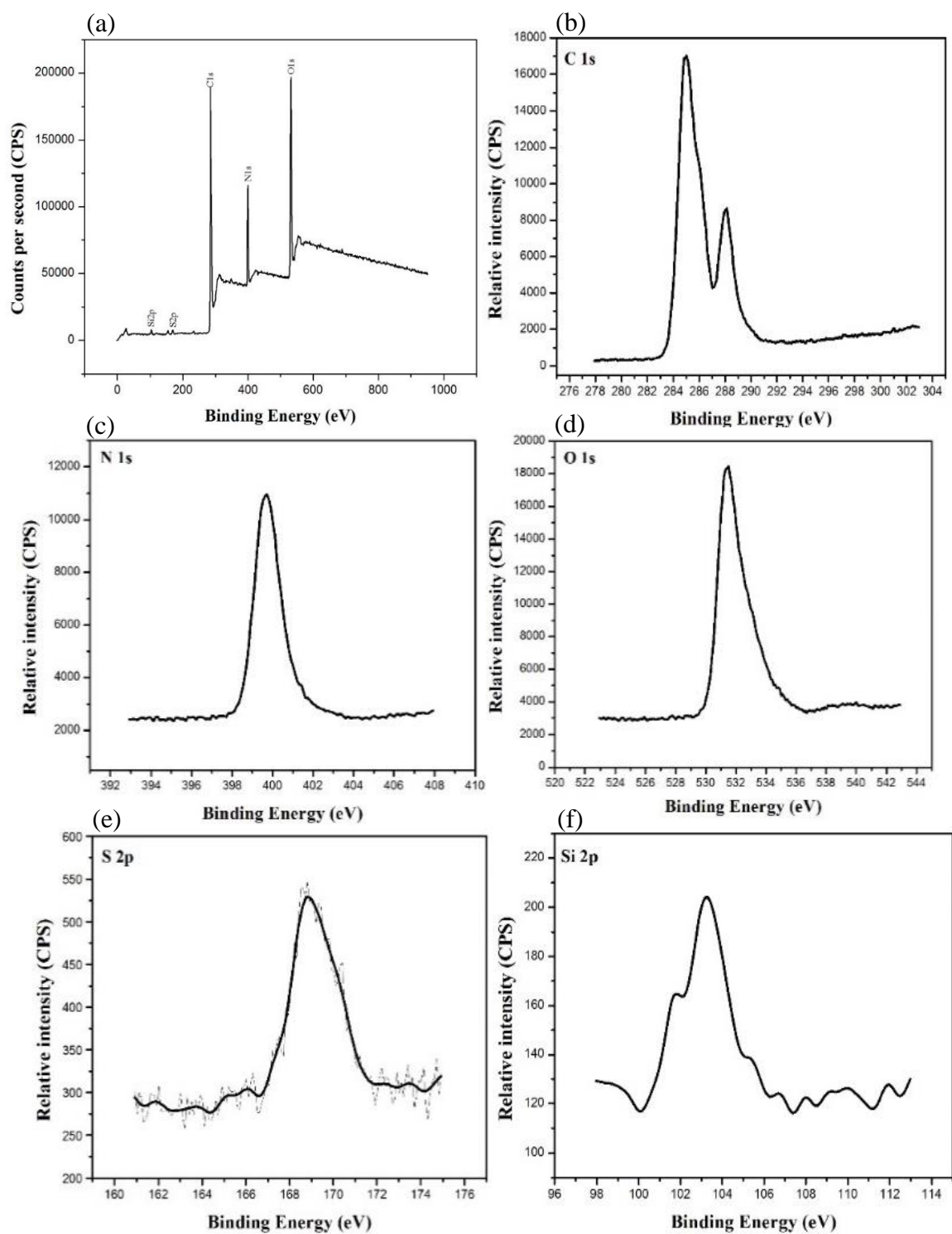


Figure 4 XPS spectra of RHBC hydrogel composite (a) The wide-scan XPS spectra, refined XPS spectra of (b) C 1s, (c) N 1s, (d) O 1s, (e) S 2p, (f) Si 2p

3.3. Effect of pH on As(V) adsorption and selection of the best hydrogel type

The effect of pH on the As(V) adsorption of nine different RHBC hydrogel types was investigated at various pH values ranging from 4-10, as depicted in Figure 5. Of the nine different hydrogel types, the highest adsorption rate is shown by 7R 0.06 hydrogel (Figure 5(i)) which was chosen for continuing the experiment as the best hydrogel type. It shows that with the increase in biochar pyrolysis temperature, the adsorption capacity increased. With the increased pyrolysis temperature, a high amount of volatile matter discharged from the rice hull. This created additional new microporous inside the RHBC which increased the surface area of the RHBC (Leng et al., 2021). Considering the size of the RHBC within the hydrogel, the smaller particles can easily disperse into the hydrogel structure while the hydrogel synthesis takes place.

During the hydrogel synthesis, the residual content of the hydrogel was high with 1.18 mm RHBC, and the residual content was at a minimum with 0.06 mm RHBC. Therefore, when the particle size is 0.06 mm, the maximum RHBC content can be expected within the hydrogel structure and the adsorption is more efficient. Further, with the 0.06 mm RHBC particles, the unit surface area was higher than those of the 1.18 mm RHBC particles, and the adsorption capacity was high with 0.06 mm RHBC hydrogel composite compared to the 1.18 mm RHBC hydrogel composite.

Almost all the hydrogels showed the highest adsorption at the pH range of 6-7 which is the As(V) solution without any pH alterations. At the pH range of < 7 the H^+ ions in the solution made the surface protonated through ionizable functional groups (Wu et al., 2018). This protonation is crucial to creating a positively charged surface at the pH range of < 7 despite its negative PZC. The $-NH_2$ and $-COOH$ were the available ionizable functional groups within the RHBC hydrogel composite that tended to be protonated. At the pH range of < 7 the O atom in the C=O of $-COOH$ functional group showed base characteristics and attracted H^+ ions to form $-COH^+$ groups. After protonation, the $-NH_3^+$ and $-COH^+$ groups converted the hydrogel surface into a positively charged surface. At the pH levels higher than 2, $H_2AsO_4^-$ (pH 2-7) and $HAsO_4^{2-}$ (pH 6-12) dominate in the solution and those oxyanions could easily be adsorbed by a positively charged surface. Considering the pH ranges of $H_2AsO_4^-$ and $HAsO_4^{2-}$ oxyanions and the pH range for positive charged surface, pH range of 6-7 was the range common for both of abovementioned oxyanions and the positive surface charge range (Figure S4). This explains the maximum adsorption at pH range of 6-7.

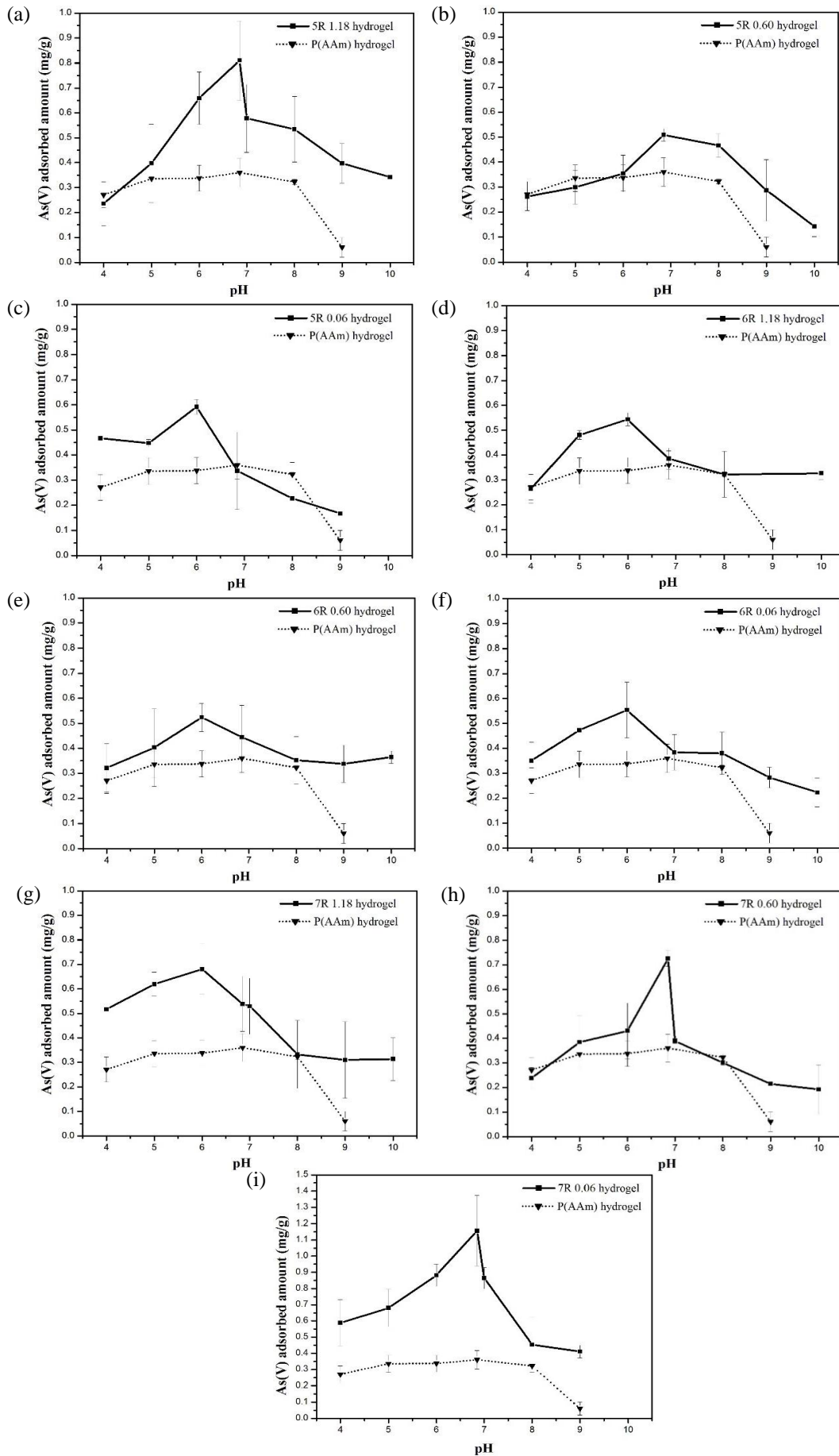


Figure 5 Arsenic adsorption pattern of nine different RHBC hydrogel types with different initial pH (a) 5R 1.18 hydrogel, (b) 5R 0.6 hydrogel, (c) 5R 0.06 hydrogel, (d) 6R 1.18 hydrogel, (e) 6R 0.6 hydrogel, (f) 6R 0.06 hydrogel, (g) 7R 1.18 hydrogel, (h) 7R 0.6 hydrogel, (i) 7R 0.06 hydrogel

Within the fully swollen hydrogel, H_2AsO_4^- and HAsO_4^{2-} ions can diffuse through electrostatic interactions. This was proved by allowing As(V) to adsorb into dry and fully swelled RHBC hydrogel in parallel with the dosage experiment which will be discussed in Section 3.4. At the lower pH values (<2), the dominant As(V) species was H_3AsO_4 which is not an oxyanion and was not attracted by a negatively charged surface (at pH <4, the surface is negatively charged). Therefore, the As(V) adsorption at the lower pH was low. At the pH higher than 7, the hydroxyl ions (OH^-) dominated in the solution over As(V) oxyanions, and therefore, As(V) adsorption decreased after exceeding pH 7. This pattern of adsorption is supported by several other studies in the literature (Chakraborty et al., 2007; Sanyang et al., 2016). 7R 0.06 hydrogel is now indicated as the RHBC hydrogel composite.

3.4. Pre-swelling and As(V) adsorption

There was approximately 20-30% of increment in As(V) adsorption with the fully swollen hydrogel over dry hydrogel (Figure S5). As discussed in Section 3.3, the fully swollen hydrogel provide sufficient active sites for H_2AsO_4^- and HAsO_4^{2-} ions through electrostatic interactions. Therefore, pre-swelling can consider as a vital step on effective As(V) adsorption.

3.5. Adsorption kinetics

During first 7 h, the adsorption achieved its equilibrium with 39.6% (0.04 mg/g) of adsorption. At the beginning all the positively charged active sites are available and adsorption is fast. With continuing the adsorption, adsorption process reached the equilibrium stage with decreasing of available active sites. Table 2 shows the kinetic model parameters for each model. According to the R^2 values the best fitted model is the pseudo-first-order suggesting non-dissociating molecular adsorption into the adsorbent (Figure 6). It can be suggested that the adsorption of As(V) into the RHBC hydrogel composite would be more inclined towards the physisorption mechanism, and that the adsorption process depended on the initial concentration of As(V). The goodness of fitting of experimental data to the pseudo-first-order non-linear model was further proven by the value of adsorption capacity evaluated by the pseudo-first-order model (0.04 mg/g), as it was similar to the experimental value (0.04 mg/g).

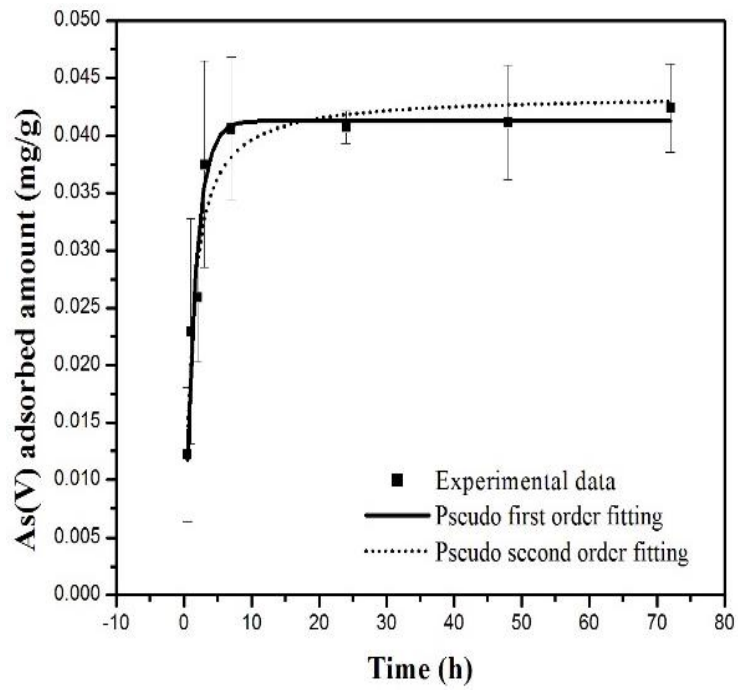


Figure 6 *Pseudo-first order and pseudo-second order models on kinetic data*

Table 2 *Non-linear kinetic parameters of As(V) adsorption into RHBC hydrogel composite*

Model	Non-linear equation	Description	Isotherm parameters	Value	R ²
Pseudo-first order	$q_t = q_e[1 - e^{-K_1 t}]$	K_1 – the rate constant (min ⁻¹) q_e, q_t – sorption capacity at equilibrium and at time t , respectively (mg/g)	K_1 q_e	0.66765 0.04126	0.96161
Pseudo-second order	$q_t = \frac{q_e^2 K_2 t}{1 + K_2 t q_e}$	K_2 – the rate constant (g/mg/min) q_e, q_t – sorption capacity at equilibrium and at time t , respectively (mg/g)	K_2 q_e	23.4751 0.04352	0.9432
Elovich	$q_t = b \ln(ab) + \ln(t)$	q_t – sorption capacity at time t (mg/g) a – initial sorption rate (mg/g/min) b – desorption constant (g/mg)	a b	0.40696 185.9421	0.77694
Power function	$q_t = b(t^{k_f})$	q_t – sorption capacity at time t (mg/g) b – power function constant k_f – power function rate constant	b k_f	0.02462 0.14629	0.70125
Parabolic	$q_t = a + k_p \sqrt{t}$	q_t – sorption capacity at time t (mg/g) a – parabolic constant k_p – parabolic rate constant	a k_p	0.02327 0.00278	0.53663

3.6. Adsorption isotherm

Work on adsorption isotherm models with experimental data gives details on evaluating and designing the adsorption mechanism of a particular sorbent and sorbate interface. Table 3 shows the isotherm parameters for each model.

The best fitted models are Langmuir and Freundlich isotherm models with high R² values of 0.992 and 0.987, respectively (Figure 7). The Langmuir model describes a monolayer coverage, and quantitative interpretation of the solute phase distribution between the solution and the solid (Duman et al., 2019; Duman et al., 2020; Duman et al., 2022). With the RL values

of less than 1 describe the adsorption of As(V) into the RHBC hydrogel composite is a favourable and feasible process.

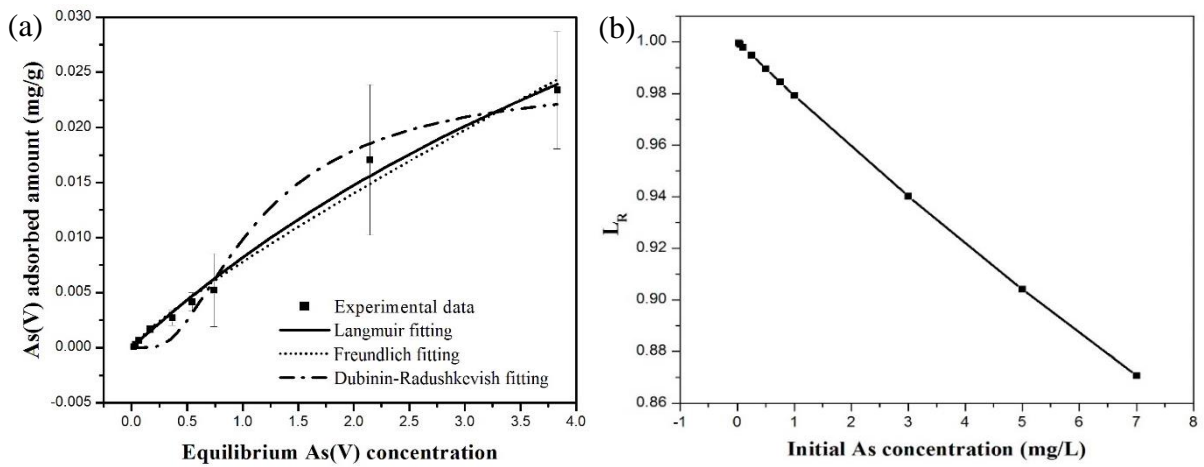


Figure 7 (a) Langmuir, Freundlich and Dubinin-Radushkevich adsorption isotherms of As(V) by RHBC hydrogel composite, (b) Separation factor (R_L) obtained from the Langmuir isotherm model

Table 3 *Non-linear isotherm parameters for As(V) adsorption into RHBC hydrogel composite*

Model	Non-linear equation	Description	Isotherm parameters	Value	R ²
Langmuir	$q_{\text{ads}} = \frac{q_{\text{max}}K_L C_e}{1+K_L C_e}$	q_{ads} – the amount of adsorbate adsorbed per unit mass of adsorbent (mg/g) q_{max} – the maximum adsorption capacity (mg/g) K_L – the Langmuir affinity parameter (L/mg) C_e – the equilibrium adsorbate aqueous phase concentration (mg/L)	q_{max} K_L	0.07471 0.12296	0.99283
Freundlich	$q_{\text{ads}} = K_F C_e^n$	K_F – the Freundlich affinity – capacity parameter ((mg/g)/(mg/L) ⁿ) n – the Freundlich exponent	K_F n	0.00788 0.84857	0.9875
Dubinin-Radushkevich	$q_{\text{ads}} = q_D \exp(-B_D [RT \ln(1 + 1/C_e)]^2)$	q_D – Monolayer adsorption capacity (mg/g) B_D – mean free energy sorption (mol ² /kJ)	q_D B_D	0.02449 1.8971	0.97797

3.7. Mechanisms for adsorption of As(V) into RHBC hydrogel

The modeling data suggest As(V) adsorption is a physisorption mechanisms. Physical adsorption occurs by the forces of molar interactions including Π +- Π electron donor-acceptor interactions, porous diffusion and H-bonding via H-donor-acceptor interactions. Porous diffusion can be identified as the major mechanism as the hydrogel surface contained a porous structure as shown in Figure 2 and the hydrogel made a three-dimensional structure as it swelled in the aqueous media. The molecules that diffused through porous diffusion underwent further chemisorption and physisorption mechanisms since the swelled hydrogel opened more functional groups and more porous structures within the RHBC particles. The possible mechanisms for As(V) adsorption into RHBC hydrogel is illustrated in Figure 8.

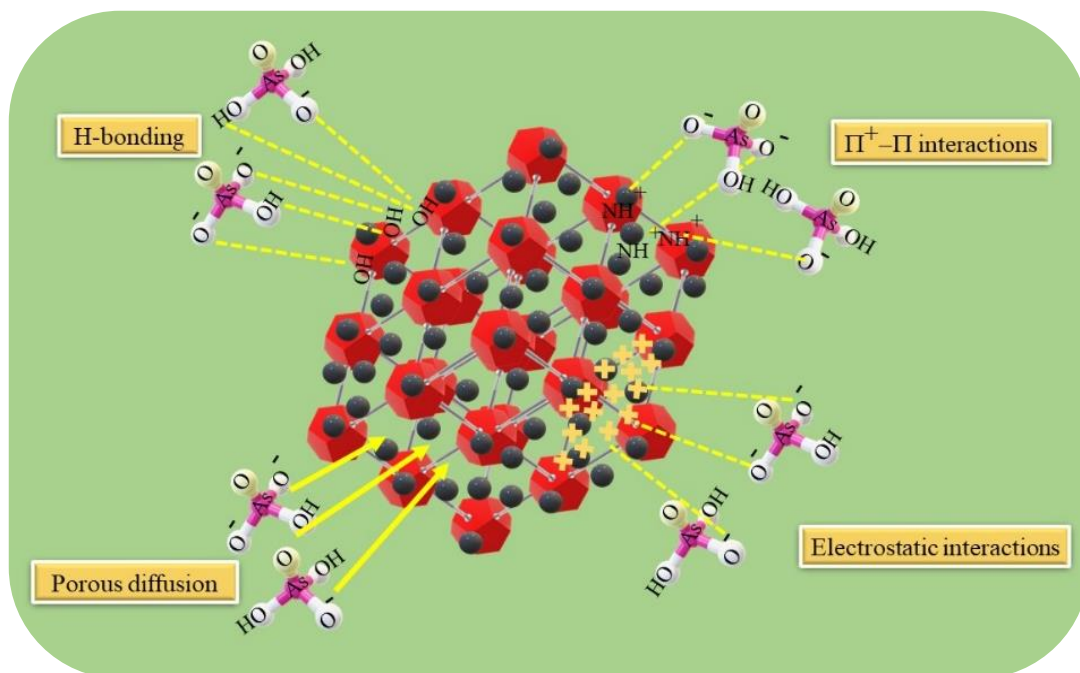


Figure 8 Graphical representation of possible mechanisms for As(V) adsorption into RHBC hydrogel composite

3.8. Desorption and re-adsorption of As(V) on RHBC hydrogel

The capability of regeneration of an adsorption material is significant in decreasing the cost of production and enhancing sustainability. Recognition of a reliable method for desorption is one of the most important aspects of this phenomenon.

Figure 9 (a) to (e) explains the desorption-resorption patterns of the RHBC hydrogel composite for one cycle. H_2SO_4 showed around 20-30% of desorption and resorption capacity with concentrations of 0.1 and 0.01 M. The 1 M H_2SO_4 shows 100% of desorption and zero resorption. Therefore, 1 M of H_2SO_4 could be a reason for the degradation of the RHBC hydrogel structure and all the adsorbed As(V) being released into the solution. CH_3COOH showed around 20-31% desorption percentage while showing 0-21% of resorption capacity. The same as it is valid for H_2SO_4 , and the best concentration range of CH_3COOH was 0.1-0.01 M.

On the other hand, NaOH showed 20-31% of desorption capacity and 0-81% of resorption over various concentrations. Remarkably, 0.1 M NaOH showed 81% of resorption capacity for a shaking duration of 6 h and it was the highest resorption recorded over all other treatments. As a weak base, NaHCO_3 showed 9-54% of desorption capacity but there was no significant resorption recorded and, therefore, NaHCO_3 is not a suitable regeneration agent for the RHBC hydrogel composite. It should be noted that the pattern of desorption and resorption

of NaHCO_3 is almost the same as in the control study where distilled water was used as the desorption agent.

The literature reveals that the desorption of metal ions requires acidic conditions (Weerasundara et al., 2020). However, in the present study, the most suitable was the alkaline condition. With the high pH levels of 0.1 M NaOH (12.19), the surface of the RHBC hydrogel became negatively charged and the adsorbed As(V) was released into the solution. Interestingly, after the desorption with 0.1 M NaOH, the adsorption capacity increased more than the initial adsorption capacity. Under the alkaline condition with the 0.1 M NaOH, the RHBC hydrogel composite went through a hydrolysis reaction. Hydrolysed hydrogels tend to change their swelling percentage significantly.

For the polyacrylic acid the ionisation equilibrium constant (pKa) is around 4.2. Therefore, the hydrolysed acrylamide hydrogels swelled further at a pH value higher than 4.2 (pKa). This increased swelling was achieved due to the electrostatic repulsion of the anionic carbonyl groups (Zhao et al., 2010). Therefore, 0.1 M NaOH further increased its adsorption capacity while showing significant desorption capacity on As(V) with the RHBC hydrogel composite.

Figure S6 shows the images of the RHBC hydrogel composite, (a) dry hydrogel, (b) hydrogel swelled in distilled water for 12 h, and (c) after desorption treatment with 0.1 M NaOH. These figures illustrate the size difference of the same RHBC hydrogel composite and how it swelled after desorption treatment. Figure 9(f) shows reusability of hydrogel with 0.1 M NaOH. Even after three desorption cycles, the RHBC hydrogel composite showed a similar As(V) adsorption capacity as it did in the initial adsorption step. This fact demonstrates that the adsorption capacity is not limited to the values reported with the above experimental data, but was four or five times higher than the experimental maximum/equilibrium adsorption capacity. Therefore, the RHBC hydrogel composite can be re-used and recycled, enhancing the effectiveness of the process and, therefore, economic and environmental sustainability.

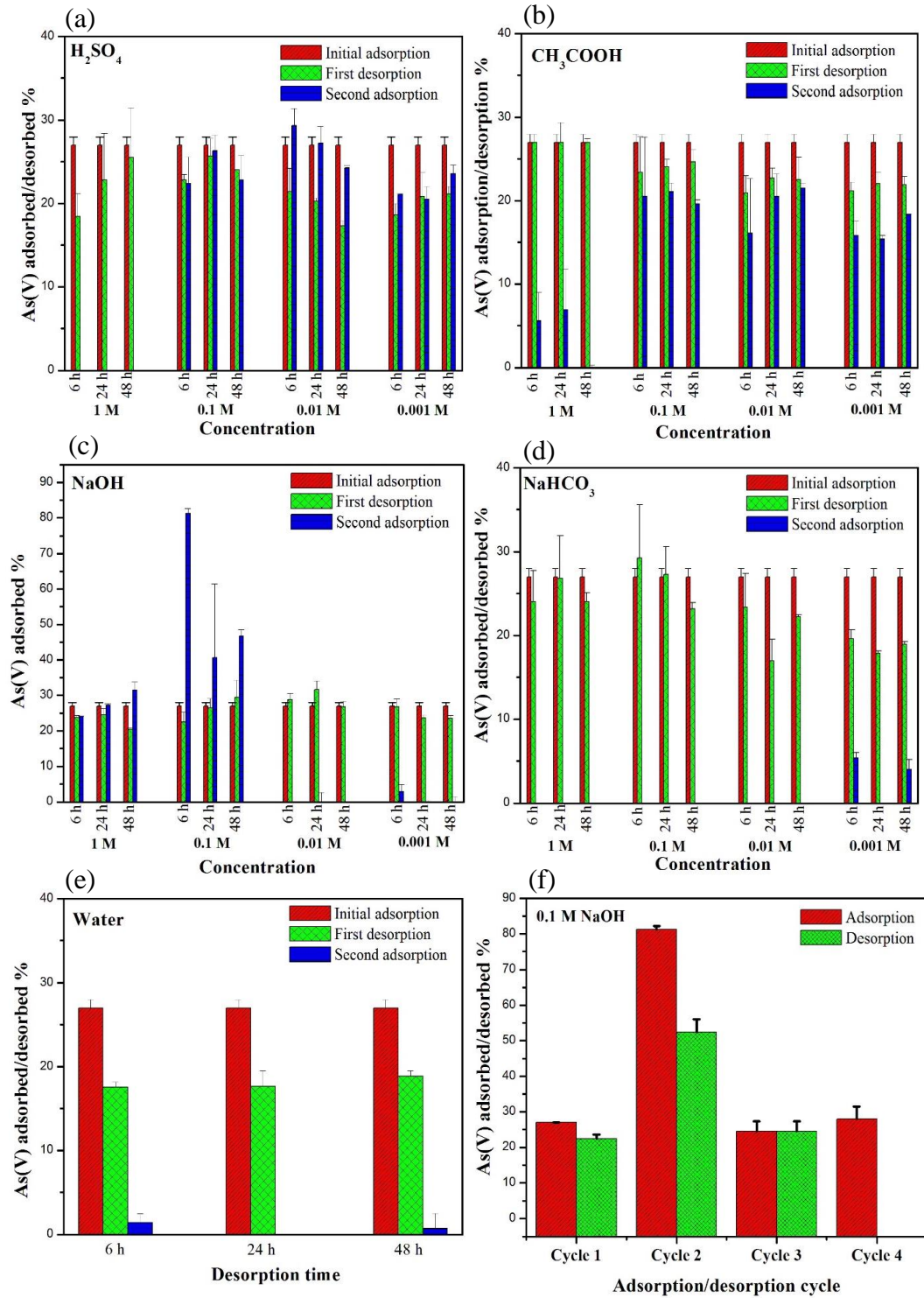


Figure 9 Desorption and resorption capacity for (a) H_2SO_4 , (b) CH_3COOH , (c) $NaOH$, (d) $NaHCO_3$, (e) Distilled water, (f) Selected desorption method with four cycles

4. Conclusion

Arsenic contaminated ground water systems may not be suitable to consume directly for purposes such as drinking water and irrigation water since those directly involve with environmental and human health. It is safe to check the arsenic levels of such water before using and apply remediation measures if required. Further, industrial wastewater released from mining and any arsenic related activities must undergo an arsenic removal process before being released into the environment. Considering this critical need, a RHBC hydrogel composite was synthesised with acrylamide hydrogel and RHBC to adsorb As(V) from aqueous solutions. The solution pH altered its adsorption. The range of pH 6-7 was favorable for As(V) adsorption with RHBC hydrogel. This is an advantageous factor of RHBC hydrogel because it is the pH range for most natural water and, as a result, RHBC can be used directly in As(V) contaminated natural water. Physisorption adsorption mechanisms involved for the adsorption of As(V) into RHBC hydrogel composite based on kinetic and isotherm data. The experimental data showed 0.04 mg/g of adsorption capacity at a single adsorption cycle.

The RHBC hydrogel composite is a sustainable solution for the treatment of As(V) in water. The reusability further enhances its capabilities and 0.1 M NaOH can use as a solution for the desorption of As(V) from the RHBC hydrogel composite and it brings the adsorption capacity towards 55%. Use of RHBC hydrogels shows further advantages such as easy water-adsorbent separation.

The innovative aspects of the proposed hydrogel such as regeneration, re-use and easy separation from water make the material suitable for large-scale use. Further, since the adsorbed As(V) is not being released when treated with water, it allows the use of the RHBC hydrogel composite as a storage material for As(V) without harming the environment including ground and surface water resources. This emphasises the global importance of the RHBC hydrogel composite because it significantly reduces the amount of waste produced with the water purification process.

The integration of acrylamide hydrogel with RHBC further expands the application range on contaminant removal since RHBC is a material that can be used for several other contaminants as well. This fact opens the way for further research for using of RHBC hydrogel composites as a removal agent for other contaminants simultaneously.

Acknowledgements

The authors acknowledge the support from Anya J. E. Yago, Dr Craig Stoppiello and Dr Lachlan Casey at the Centre for Microscopy and Microanalysis (CMM) at the University of Queensland.

The authors thank Dr. Barbara Harmes and Sandra Cochrane from University of Southern Queensland, Australia for providing help on proofreading.

This work was supported by the University of Southern Queensland, QLD, Australia (RTP Stipend Scholarship programme).

Conflict of interest disclosure: The authors declare that they have no conflict of interest.

References

- Amen, R., Bashir, H., Bibi, I., Shaheen, S.M., Niazi, N.K., Shahid, M., Hussain, M.M., Antoniadis, V., Shakoor, M.B. and Al-Solaimani, S.G., 2020. A critical review on arsenic removal from water using biochar-based sorbents: the significance of modification and redox reactions. *Chemical Engineering Journal* 396, 125195.
- Asadi, N., Pazoki-Toroudi, H., Del Bakhshayesh, A.R., Akbarzadeh, A., Davaran, S. and Annabi, N., 2021. Multifunctional hydrogels for wound healing: Special focus on biomacromolecular based hydrogels. *International Journal of Biological Macromolecules* 170, 728-750.
- Baigorria, E., Cano, L.A., Sanchez, L.M., Alvarez, V.A. and Ollier, R.P., 2020. Bentonite-composite polyvinyl alcohol/alginate hydrogel beads: Preparation, characterisation and their use as arsenic removal devices. *Environmental Nanotechnology, Monitoring & Management* 14, 100364.
- Bakatula, E.N., Richard, D., Neculita, C.M. and Zagury, G.J., 2018. Determination of point of zero charge of natural organic materials. *Environmental Science and Pollution Research* 25(8), 7823-7833.
- Barakat, M. and Sahiner, N., 2008. Cationic hydrogels for toxic arsenate removal from aqueous environment. *Journal of Environmental Management* 88(4), 955-961.
- Beamson, G., 1992. High resolution XPS of organic polymers. The Scienta ESCA 300 Database.
- Chakraborty, S., Wolthers, M., Chatterjee, D. and Charlet, L., 2007. Adsorption of arsenite and arsenate onto muscovite and biotite mica. *Journal of Colloid and Interface Science* 309(2), 392-401.

- Duman, O., Özcan, C., Polat, T.G. and Tunc, S., 2019. Carbon nanotube-based magnetic and non-magnetic adsorbents for the high-efficiency removal of diquat dibromide herbicide from water: OMWCNT, OMWCNT-Fe₃O₄ and OMWCNT-κ-carrageenan-Fe₃O₄ nanocomposites. *Environmental Pollution* 244, 723-732.
- Duman, O., Polat, T.G., Diker, C.Ö. and Tunç, S., 2020. Agar/κ-carrageenan composite hydrogel adsorbent for the removal of Methylene Blue from water. *International Journal of Biological Macromolecules* 160, 823-835.
- Duman, O., Polat, T.G. and Tunç, S., 2022. Development of poly (vinyl alcohol)/β-cyclodextrin/P (MVE-MA) composite nanofibers as effective and selective adsorbent and filtration material for the removal and separation of cationic dyes from water. *Journal of Environmental Management* 322, 116130.
- Elizalde-González, M., Mattusch, J., Einicke, W.-D. and Wennrich, R., 2001. Sorption on natural solids for arsenic removal. *Chemical Engineering Journal* 81(1-3), 187-195.
- Herath, I., Kumarathilaka, P., Al-Wabel, M.I., Abduljabbar, A., Ahmad, M., Usman, A.R. and Vithanage, M., 2016. Mechanistic modeling of glyphosate interaction with rice husk derived engineered biochar. *Microporous and mesoporous materials* 225, 280-288.
- Ho, Y., Porter, J. and McKay, G., 2002. Equilibrium isotherm studies for the sorption of divalent metal ions onto peat: copper, nickel and lead single component systems. *Water, air, and soil pollution* 141(1), 1-33.
- Huang, Y., Zeng, M., Ren, J., Wang, J., Fan, L. and Xu, Q., 2012. Preparation and swelling properties of graphene oxide/poly (acrylic acid-co-acrylamide) super-absorbent hydrogel nanocomposites. *Colloids and Surfaces A: Physicochemical and Engineering Aspects* 401, 97-106.
- Jovanović, B.M., Vukašinović-Pešić, V.L., Veljović, Đ.N. and Rajaković, L.V., 2011. Arsenic removal from water using low-cost adsorbents: A comparative study. *Journal of the Serbian Chemical Society* 76(10), 1437-1452.
- Karakoyun, N., Kubilay, S., Aktas, N., Turhan, O., Kasimoglu, M., Yilmaz, S. and Sahiner, N., 2011. Hydrogel–Biochar composites for effective organic contaminant removal from aqueous media. *Desalination* 280(1-3), 319-325.
- Karam, D.S., Nagabovanalli, P., Rajoo, K.S., Ishak, C.F., Abdu, A., Rosli, Z., Muharam, F.M. and Zulperi, D., 2021. An overview on the preparation of rice husk biochar, factors affecting its properties, and its agriculture application. *Journal of the Saudi Society of Agricultural Sciences*.

- Kumarathilaka, P., Bundschuh, J., Seneweera, S., Marchuk, A. and Ok, Y.S., 2021a. Iron modification to silicon-rich biochar and alternative water management to decrease arsenic accumulation in rice (*Oryza sativa* L.). *Environmental Pollution* 286, 117661.
- Kumarathilaka, P., Bundschuh, J., Seneweera, S. and Ok, Y.S., 2021b. An integrated approach of rice hull biochar-alternative water management as a promising tool to decrease inorganic arsenic levels and to sustain essential element contents in rice. *Journal of Hazardous Materials* 405, 124188.
- Kumarathilaka, P., Seneweera, S., Meharg, A. and Bundschuh, J., 2018a. Arsenic accumulation in rice (*Oryza sativa* L.) is influenced by environment and genetic factors. *Science of the Total Environment* 642, 485-496.
- Kumarathilaka, P., Seneweera, S., Meharg, A. and Bundschuh, J., 2018b. Arsenic speciation dynamics in paddy rice soil-water environment: sources, physico-chemical, and biological factors-a review. *Water Research* 140, 403-414.
- Kumarathilaka, P., Seneweera, S., Ok, Y.S., Meharg, A.A. and Bundschuh, J., 2020. Mitigation of arsenic accumulation in rice: An agronomical, physico-chemical, and biological approach—A critical review. *Critical Reviews in Environmental Science and Technology* 50(1), 31-71.
- Lekić, B.M., Marković, D.D., Rajaković-Ognjanović, V.N., Đukić, A.R. and Rajaković, L.V., 2013. Arsenic removal from water using industrial by-products. *Journal of Chemistry* 2013.
- Leng, L., Xiong, Q., Yang, L., Li, H., Zhou, Y., Zhang, W., Jiang, S., Li, H. and Huang, H., 2021. An overview on engineering the surface area and porosity of biochar. *Science of the Total Environment* 763, 144204.
- Liang, Y., He, J. and Guo, B., 2021. Functional hydrogels as wound dressing to enhance wound healing. *ACS nano* 15(8), 12687-12722.
- Maji, S., Kao, Y.-H. and Liu, C.-W., 2011. Arsenic removal from real arsenic-bearing groundwater by adsorption on iron-oxide-coated natural rock (IOCNR). *Desalination* 280(1-3), 72-79.
- Mandal, A., Clegg, J.R., Anselmo, A.C. and Mitragotri, S., 2020. Hydrogels in the clinic. *Bioengineering & Translational Medicine* 5(2), e10158.
- Mayakaduwa, S., Kumarathilaka, P., Herath, I., Ahmad, M., Al-Wabel, M., Ok, Y.S., Usman, A., Abduljabbar, A. and Vithanage, M., 2016. Equilibrium and kinetic mechanisms of woody biochar on aqueous glyphosate removal. *Chemosphere* 144, 2516-2521.

- Mohtasebi, A., Chowdhury, T., Hsu, L.H., Biesinger, M.C. and Kruse, P., 2016. Interfacial charge transfer between phenyl-capped aniline tetramer films and iron oxide surfaces. *The Journal of Physical Chemistry C* 120(51), 29248-29263.
- Nakhjiri, M.T., Marandi, G.B. and Kurdtabar, M., 2021. Preparation of magnetic double network nanocomposite hydrogel for adsorption of phenol and p-nitrophenol from aqueous solution. *Journal of Environmental Chemical Engineering* 9(2), 105039.
- Ochedi, F.O., Liu, Y. and Hussain, A., 2020. A review on coal fly ash-based adsorbents for mercury and arsenic removal. *Journal of Cleaner Production* 267, 122143.
- Pereira, A.G., Rodrigues, F.H., Paulino, A.T., Martins, A.F. and Fajardo, A.R., 2021. Recent advances on composite hydrogels designed for the remediation of dye-contaminated water and wastewater: A review. *Journal of Cleaner Production* 284, 124703.
- Ploychompoo, S., Chen, J., Luo, H. and Liang, Q., 2020. Fast and efficient aqueous arsenic removal by functionalized MIL-100 (Fe)/rGO/ δ -MnO₂ ternary composites: Adsorption performance and mechanism. *Journal of Environmental Sciences* 91, 22-34.
- Qi, X., Zeng, Q., Tong, X., Su, T., Xie, L., Yuan, K., Xu, J. and Shen, J., 2021. Polydopamine/montmorillonite-embedded pullulan hydrogels as efficient adsorbents for removing crystal violet. *Journal of Hazardous Materials* 402, 123359.
- Ren, J., Kong, W. and Sun, R., 2014. Preparation of sugarcane bagasse/poly (acrylic acid-co-acrylamide) hydrogels and their application. *BioResources* 9(2), 3290-3303.
- Sanyang, M., Ghani, W.A.W.A.K., Idris, A. and Ahmad, M.B., 2016. Hydrogel biochar composite for arsenic removal from wastewater. *Desalination and Water Treatment* 57(8), 3674-3688.
- Shabbir, Z., Shahid, M., Khalid, S., Khalid, S., Imran, M., Qureshi, M.I. and Niazi, N.K., 2020. Use of agricultural bio-wastes to remove arsenic from contaminated water. *Environmental Geochemistry and Health*, 1-10.
- Shahab, A., Qi, S. and Zaheer, M., 2019. Arsenic contamination, subsequent water toxicity, and associated public health risks in the lower Indus plain, Sindh province, Pakistan. *Environmental Science and Pollution Research* 26(30), 30642-30662.
- Steinmaus, C., Moore, L., Hopenhayn-Rich, C., Biggs, M.L. and Smith, A.H., 2000. Arsenic in drinking water and bladder cancer: environmental carcinogenesis. *Cancer Investigation* 18(2), 174-182.
- Tabassum, R.A., Shahid, M., Niazi, N.K., Dumat, C., Zhang, Y., Imran, M., Bakhat, H.F., Hussain, I. and Khalid, S., 2019. Arsenic removal from aqueous solutions and

- groundwater using agricultural biowastes-derived biosorbents and biochar: a column-scale investigation. *International Journal of Phytoremediation* 21(6), 509-518.
- Tanan, W., Panichpakdee, J. and Saengsuwan, S., 2019. Novel biodegradable hydrogel based on natural polymers: Synthesis, characterization, swelling/reswelling and biodegradability. *European Polymer Journal* 112, 678-687.
- Tang, X., Luo, Y., Zhang, Z., Ding, W., Liu, D., Wang, J., Guo, L. and Wen, M., 2021. Effects of functional groups of $-NH_2$ and $-NO_2$ on water adsorption ability of Zr-based MOFs (UiO-66). *Chemical Physics* 543, 111093.
- Uddin, M.J. and Jeong, Y.-K., 2020. Efficiently performing periodic elements with modern adsorption technologies for arsenic removal. *Environmental Science and Pollution Research*, 1-25.
- Wagner, C., Naumkin, A., Kraut-Vass, A., Allison, J., Powell, C. and Rumble Jr, J., 2003. NIST standard reference database 20, Version 3.4 (Web version). National Institute of Standards and Technology: Gaithersburg, MD 20899.
- Wang, Z., Li, T.-T., Peng, H.-K., Ren, H.-T., Lou, C.-W. and Lin, J.-H., 2021. Low-cost hydrogel adsorbent enhanced by trihydroxy melamine and β -cyclodextrin for the removal of Pb (II) and Ni (II) in water. *Journal of Hazardous Materials* 411, 125029.
- Weerasundara, L., Gabriele, B., Figoli, A., Ok, Y.-S. and Bundschuh, J., 2020. Hydrogels: Novel materials for contaminant removal in water—A review. *Critical Reviews in Environmental Science and Technology*, 1-45.
- Weerasundara, L., Ok, Y.-S. and Bundschuh, J., 2021. Selective removal of arsenic in water: A critical review. *Environmental Pollution* 268, 115668.
- Weerasundara, L., Ok, Y.S., Kumarathilaka, P., Marchuk, A. and Bundschuh, J., 2022. Assessment and optimization of As (V) adsorption on hydrogel composite integrating chitosan-polyvinyl alcohol and Fe_3O_4 nanoparticles and evaluation of their regeneration and reusable capabilities in aqueous media. *Science of the Total Environment* 158877.
- WHO, W.H.O., 2006. Guidelines for Drinking-water Quality. First addendum to third edition. Geneva 1.
- Wu, J., Huang, D., Liu, X., Meng, J., Tang, C. and Xu, J., 2018. Remediation of As (III) and Cd (II) co-contamination and its mechanism in aqueous systems by a novel calcium-based magnetic biochar. *Journal of Hazardous Materials* 348, 10-19.
- Xikhongelo, R.V., Mtunzi, F.M., Diagboya, P.N., Olu-Owolabi, B.I. and Düring, R.-A., 2021. Polyamidoamine-functionalized graphene oxide–SBA-15 mesoporous composite:

adsorbent for aqueous arsenite, cadmium, ciprofloxacin, ivermectin, and tetracycline. *Industrial & Engineering Chemistry Research* 60(10), 3957-3968.

Yan, S., An, Q., Xia, L., Liu, S., Song, S. and Rangel-Méndez, J.R., 2020. As (V) removal from water using the La (III)-Montmorillonite hydrogel beads. *Reactive and Functional Polymers* 147, 104456.

Zhao, Q., Sun, J., Lin, Y. and Zhou, Q., 2010. Study of the properties of hydrolyzed polyacrylamide hydrogels with various pore structures and rapid pH-sensitivities. *Reactive and Functional polymers* 70(9), 602-609.

Supplementary materials

Development of regenerative, re-usable and easily water-adsorbent separable hydrogel composite with rice hull biochar for efficient removal of arsenic (V) from aqueous media

Lakshika Weerasundara^a, Prasanna Kumarathilaka^a, Alla Marchuk^c Jochen

Bundschuh^{*a,d}

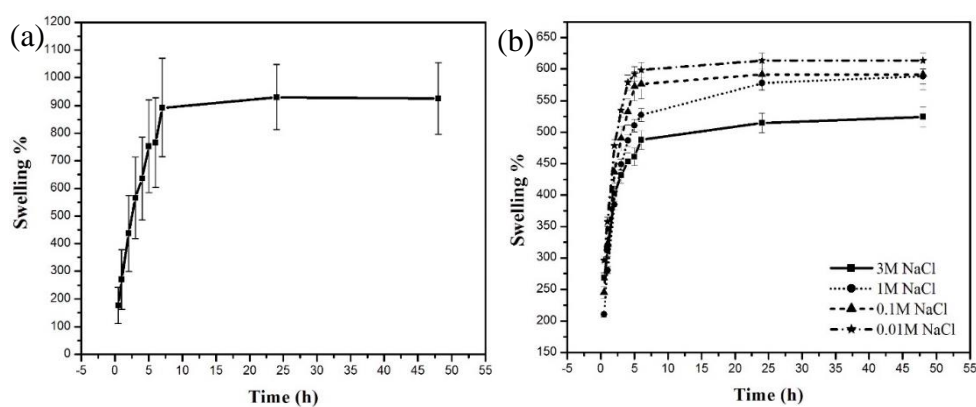


Figure S1 Percentage of swelling capacity for RHBC hydrogel (a) In distilled water (b) In NaCl solutions over the time

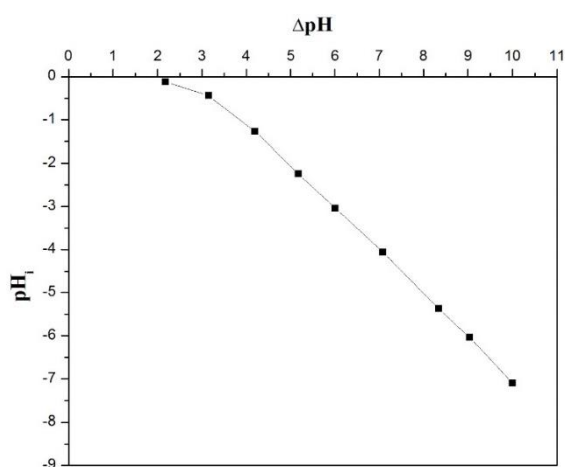


Figure S2 Plot of ΔpH vs pH_i for salt addition method to determine the PZC of RHBC hydrogel composite

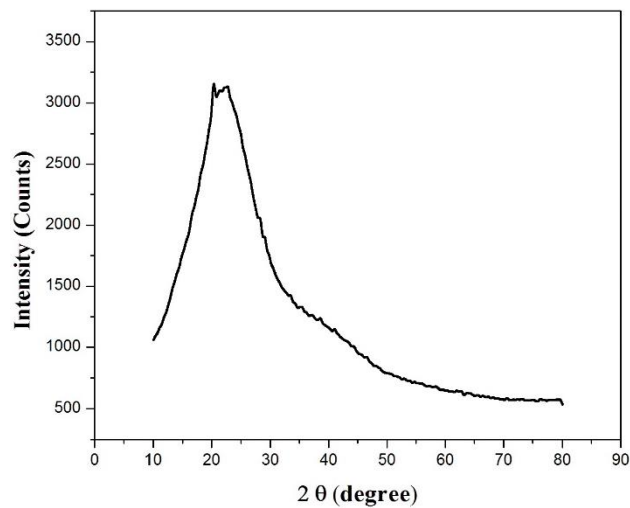


Figure S3 XRD pattern for RHBC hydrogel composite

pH	Positive surface charge range	H ₂ AsO ₄ ⁻ active range	HAsO ₄ ²⁻ active range
2			
3			
4	Dark Green		
5	Dark Green	Medium Green	
6	Dark Green	Medium Green	Light Green
7	Dark Green	Medium Green	Light Green
8			Light Green
9			Light Green
10			Light Green
11			Light Green
12			Light Green

Figure S4 The best pH range (outlined with redline, pH 6-7) for As(V) adsorption with RHBC hydrogel composite

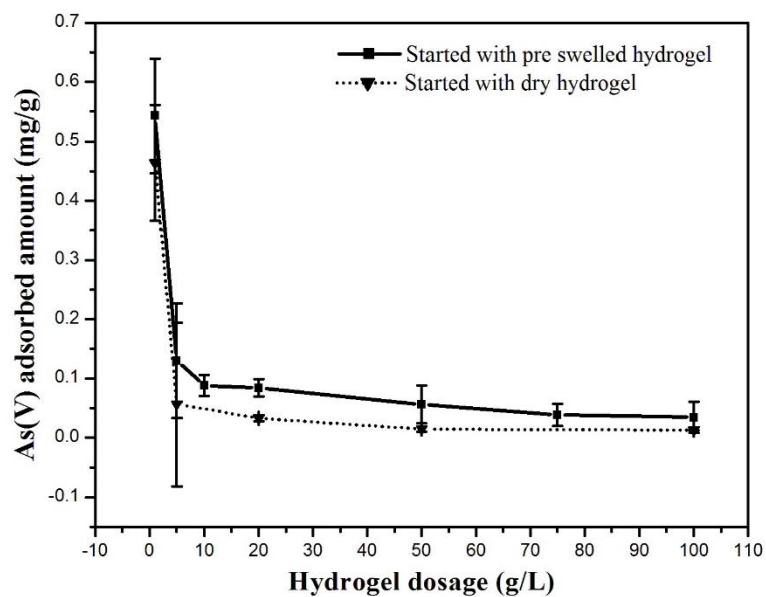


Figure S5 As(V) adsorption capacity with the different RHBC hydrogel composite and the effect of pre-swelling on adsorption capacity

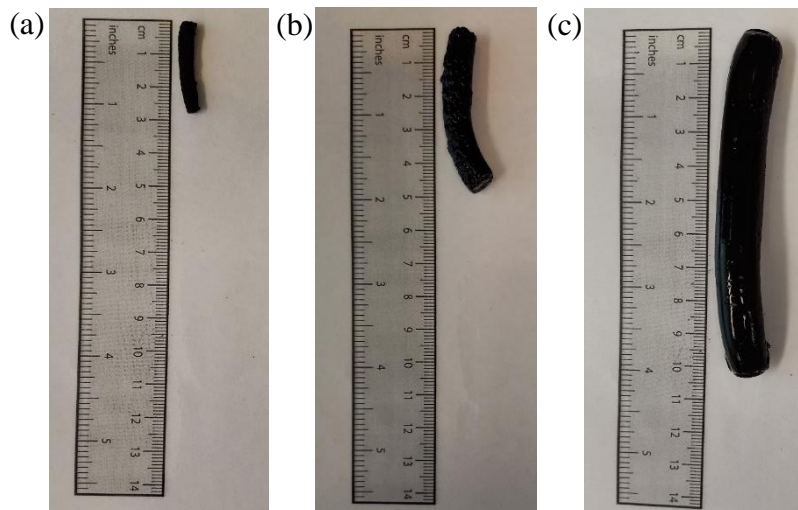


Figure S6 Images of RHBC hydrogel composite (a) Dry hydrogel, (b) Swelled in distilled water for 12 hours, (c) After desorption treatment with 0.1 M NaOH

3.3. Concluding Remarks

A RHBC hydrogel was successfully developed as a composite of acrylamide hydrogel and RHBC to remove As(V) from water. The change in the solution pH affected the adsorption capacity. The highest adsorption was recorded in the range of pH 6-7. Within the pH 6-7 range, the hydrogel surface became positively charged due to the protonation of the $-NH_2$ and $-CO$ groups in the polymer chain, and the positive surface attracted $H_2AsO_4^-$ and $HAsO_4^{2-}$ oxyanions. This is an advantageous factor of RHBC hydrogel because it is the pH range of most natural water and, as a result, the RHBC can be used directly in As(V) contaminated natural waters. At higher pH values the increased OH^- ions in the solution results a competition for positive adsorption sites and decrease the As(V) adsorption. The use of swollen RHBC hydrogel for As(V) removal was more efficient than the direct use of dry hydrogel. The hydrogels are 3D structured which tends to increase pore volumes and the unit surface area in aqueous environments. Once the RHBC hydrogel composite is full swollen, it acts at its maximum capacity to adsorb As(V). The chemisorption and physisorption adsorption mechanisms have been proposed for the adsorption of As(V) into the RHBC hydrogel composite based on kinetic and isotherm data.

The RHBC hydrogel composite can be considered a revolutionary solution for removing As(V) from water because of its availability for regeneration and re-use. 0.1 M NaOH is a solution suitable for the desorption of As(V) from the RHBC hydrogel composite and it further increases the adsorption capacity of RHBC hydrogel for As(V). Further, the RHBC hydrogel composite can be considered as a solution that overcomes the classic drawbacks of adsorbents such as adsorbent-water separation which hinders upscaling to large industrial scale. Furthermore, the RHBC hydrogel composite does not require additional energy (i.e., post filtration) to separate the adsorbent from water and, therefore, allows upscaling to large scale industrial applications.

Considering the large-scale application, the RHBC hydrogel composite shows several advantageous characteristics. The material can be developed in any shape and any size. Therefore, according to the water purification system, the material can be synthesised. Further, the adsorption equilibrium time is 6-7 h, and this time period is reliable for most large-scale water purification systems. The innovative aspects of the proposed hydrogel such as regeneration, re-use and easy separation from water make it well suited to large-scale use. Further, since the adsorbed As(V) is not released when treated with water, the RHBC hydrogel composite can be used as a storage material for As(V) without harming the environment,

including ground and surface water resources. This makes the RHBC hydrogel composite important globally as it significantly reduces the amount of waste produced during the water purification process. When the hydrogel is dry, it can shrink to its original size which is about 900% smaller than its swollen condition. Therefore, the disposal of hydrogel waste will not require large dumping facilities.

CHAPTER 4: PAPER 4 – SYNTHESIS OF RE-USABLE HYDROGEL COMPOSITE INTEGRATING SUGARCANE BAGASSE BIOCHAR FOR LARGE INDUSTRIAL TO HOUSEHOLD SCALE As(V) REMOVAL FROM AQUEOUS MEDIA AND COMPARISON WITH RICE-HULL BIOCHAR HYDROGEL COMPOSITE

4.1. Introduction

As safe drinking water is an increasingly scarce source, removal of contaminants from water is a challenging necessity. Water may contain many contaminants due to different anthropogenic and natural sources such as heavy metals, metalloids, phosphates, pharmaceuticals, chlorination disinfection by-products, pathogens etc. Arsenic (As) is one of the alarming contaminants which has both anthropogenic and natural sources of origin. Since the impacts of As consumption are critical to human health, the guideline value set by the WHO has been established as $<10 \mu\text{g/L}$. In different parts of the world drinking water sources contain As contents higher than to WHO guideline. Therefore, removal techniques are necessary to ensure safe drinking water through the achievement this guideline.

A modified polyacrylamide hydrogel was developed by incorporating sugarcane bagasse biochar (SUBC). Nine SUBC hydrogel composites were prepared based on pyrolysis temperatures and size fractions of the SUBC. The exhausted SUBC hydrogels were tested for their regeneration and re-use capability using different acids and bases. The best hydrogel for As(V) adsorption was 0.06 mm sized and pyrolysed under $700 \text{ }^\circ\text{C}$ SUBC containing hydrogel. The highest As(V) adsorption (15%) was at the pH range of 6-7. The swollen hydrogel showed higher As(V) adsorption than the dry hydrogel. The kinetic and isotherm models predicted physisorption and chemisorption mechanisms on the SUBC hydrogel composites. 0.1 M NaOH showed the best regeneration pattern with 43%, 81%, 14% and 30% of 1st, 2nd, 3rd and 4th adsorption, respectively. The material requires no post-treatment for adsorbent-water separation. The modification with the SUBC further expands the application capacity since the SUBC can remove other contaminants as well.

Synthesis of re-usable hydrogel composite integrating sugarcane bagasse biochar for large industrial to household scale arsenic (V) removal from aqueous media and comparison with rice-hull biochar hydrogel composite

Lakshika Weerasundara^a, Prasanna Kumarathilaka^a, Alla Marchuk^b, Jochen Bundschuh^{*a,c}

^a*School of Civil Engineering and Surveying, Faculty of Health, Engineering and Sciences, University of Southern Queensland, West Street, Toowoomba, Queensland, 4350, Australia*

^b*Institute for Life Sciences and the Environment, University of Southern Queensland, West Street, Toowoomba, Queensland, 4350, Australia*

^c*Doctoral Program in Science, Technology, Environment, and Mathematics, Department of Earth and Environmental Sciences, National Chung Cheng University, 168 University Rd., Min-Hsiung, Chiayi County, 62102, Taiwan*

*Corresponding author

E-mail address: jochen.bundschuh@usq.edu.au (Jochen Bundschuh), School of Civil Engineering and Surveying, Faculty of Health, Engineering and Sciences, University of Southern Queensland, Toowoomba, Queensland 4350, Australia. Doctoral Program in Science, Technology, Environment, and Mathematics, Department of Earth and Environmental Sciences, National Chung Cheng University, 168 University Rd., Min-Hsiung, Chiayi County, 62102, Taiwan.

Abstract

Adsorption is the most sustainable method of arsenic (V) (As(V)) removal from water. However, the adsorbents currently in use have common drawbacks: additional energy for adsorbent-water separation and no reusability. To remove As(V) from water while resolving these deficiencies, a modified material was developed by incorporating sugarcane bagasse biochar (SUBC) with a hydrogel. Nine different SUBC hydrogel composites were prepared based on different pyrolysis temperatures and size fractions of the SUBC. Equilibrium isotherms and kinetics data were obtained by adsorption experiments. The exhausted SUBC hydrogels were tested for regeneration and re-use capability using different acids and bases. The best hydrogel for As(V) adsorption was 0.06 mm sized and pyrolysed under 700 °C SUBC holding the hydrogel. The highest As(V) adsorption (15%) was at the pH range of 6-7. Within the pH 6-7 range, the hydrogel surface became positively charged due to protonation of the -NH₂ and -CO groups in the polymer chain where the positive surface attracted H₂AsO₄⁻ and HAsO₄²⁻ oxyanions. The experimental kinetic data was well-fitted to the pseudo-second order (R^2 0.97) and pseudo-first order (R^2 0.91) models, while the Langmuir (R^2 0.98), Dubinin-Radushkevich (R^2 0.97) and Freundlich (R^2 0.96) isotherm models best described the isotherm data. The models predicted physisorption and chemisorption mechanisms on the SUBC hydrogel composites. 0.1 M NaOH showed the best regeneration pattern with 43%, 81%, 14% and 30% of 1st, 2nd, 3rd and 4th adsorption, respectively. Therefore, the SUBC hydrogel was efficient at As(V) removal with easy adsorbent-water separation and re-usable capabilities.

Keywords: Arsenic(V), hydrogel, biochar, composite, adsorption

1. Introduction

Water plays the most crucial role for every single lifeform on Earth. For the human population, the availability of safe water is critical. The increasing influence of anthropogenic activities has raised the need to remove harmful contaminants from water to make it safe for human consumption and the environment. A number of methods to remove different contaminants from water have been studied, however their sustainability remains an issue in terms of economic and environmental sustainability. The adsorption method has shown preferable characteristics over most of the contaminant removal methods in terms of economic and environmental sustainability. However, most adsorbent materials show significant drawbacks such as additional energy demand on adsorbent-water separation after the

adsorption process. This additional energy demand makes the whole process less economically efficient. Therefore, it is important to consider easy water-adsorbent separation ability when developing adsorbent materials to remove the water contaminants. Hydrogel has been identified as an excellent solution.

Hydrogels are crosslinked polymeric three-dimensional networks that can swell heavily in aqueous environments. Hydrogels can be formed from various natural polymers such as collagen, gelatine, fibrin, hyaluronic acid, heparin, alginates, pectin and chitosan (Peppas and Hoffman, 2020). Hydrogels can be classified in different ways such as those based on the method of preparation, ionic charges on the backbone polymers, and physicochemical structural features. Knowledge of the classification of hydrogels is important as it helps with the selection of monomer and crosslinker according to the proposed application. The use of hydrogels has been reported since 1940, and since then various sectors have utilised different types of hydrogels for a variety purposes. Some of these sectors are agriculture (as water retention granules), drug delivery, coal dewatering, artificial snow, food additives, pharmaceuticals, bio-medical applications, regenerative medicine and barrier materials (Asadi et al., 2021b; Liang et al., 2021; Mandal et al., 2020; Weerasundara et al., 2021a). The mechanical strength of the hydrogels is determined mainly by the amount of crosslinking within the polymeric chain. Hydrogels with less crosslinking density are prone to breakage and rich crosslinking limits the swelling/water retention capacity. These basic features are major factors in deciding the type of hydrogel for any particular purpose.

The removal of contaminants from water using a hydrogel as an adsorbent has not been studied widely but has gained research interest in the last few years. The three-dimensional structure of hydrogels facilitates significant water retention capabilities leading to the use of hydrogels as a potential adsorbent for various contaminants. Metals, metalloids, organic and inorganic dyes and antibiotics have been studied with hydrogels for their removal for water. The functional groups of hydrogels are determined by the type of polymeric chain of hydrogels (Weerasundara et al., 2021a). When using hydrogels as adsorbents, the types of available functional groups are crucial factors to be considered.

As they are open to modification such as magnetisation, the creation of hydrogel composites is another advantage of hydrogels that can make the hydrogel superior to most adsorbents. Hydrogel composites allow the integration of other adsorbents into the hydrogel structures to gain maximum adsorption capacity and enhance effectiveness at the same time. The use of low-cost biomaterials that can enhance the adsorption capacity of hydrogel, creating financial efficiencies whilst also making a pathway for the recycling of agricultural and/or

industrial waste products. Starch, cellulose, lignin and biochar are some of the materials that have a potential application with hydrogel.

Biochar has been identified as a low-cost biomaterial that shows significant adsorption capacity for numerous contaminants (Bandara et al., 2017; Herath et al., 2016; Mayakaduwa et al., 2016). The literature provides evidence that biochar can be made from different types of biomaterials such as sugar cane bagasse, rice hull, woody biomass, organic waste, sewage sludge, etc (Ji et al., 2022). The incorporation of biochar into hydrogels could, therefore, be an advantage for application range. A limited number of studies of hydrogel-biochar composites were found in the literature considering applications such as organic contaminant removal from water (Karakoyun et al., 2011), controlled release fertilisers (Das and Ghosh, 2022), metal ion adsorption (Akl et al., 2021; Sanyang et al., 2016; Simeng and Chen, 2018) and soil amendment (Zhang and Guan, 2022).

There are many water contaminants due the variety of anthropogenic and natural sources such as heavy metals, metalloids, phosphates, pharmaceuticals, chlorination disinfection by-products and pathogens. Arsenic (As) is one of the serious contaminants which has both anthropogenic and natural sources of origin (Kumarathilaka et al., 2021a; Weerasundara et al., 2021c). Since the impacts of As consumption are critical to human health, the guideline value set by the World Health Organisation (WHO) has been established as <10 µg/L. In different parts of the world, the drinking water sources contain higher As contents (Bibi et al., 2017). Therefore, to achieve this guideline limit and ensure safe drinking water, As removal techniques are necessary.

This study focused on the development of a novel composite hydrogel material based on poly(acrylamide) hydrogel with the incorporation of sugarcane bagasse biochar (SUBC), and determining and comparing the efficiency of this composite on As(V) adsorption. The hydrogels were synthesised by incorporating biochar produced under different pyrolysis temperatures and different particle sizes. Regeneration of the material with different methods and resorption capacity were also assessed.

2. Experimental

2.1. Preparation of biochar

Dried sugarcane bagasse was obtained from Mackay Sugar Limited (Mackay, Queensland, Australia) to produce SUBC. The sugarcane bagasse was subjected to a slow pyrolysis process under continuous nitrogen flow (2 L/min) in a muffle furnace (CS2, RIO

GRANDE) at three different temperatures (500, 600 and 700 °C) for 2 h holding time to produce SUBC. The heating rate of the pyrolysis process was set at 7 °C/min. The produced SUBC was washed with 0.1 mol/L HCl for 6 h for de-mineralisation, and washed again with distilled water until a neutral pH was obtained. The filtered SUBC was dried in an oven (STERIDIUM) at 50 °C for 72 h. The obtained SUBC was grounded and sieved to make three different size fractions 1.18, 0.60 and 0.06 mm. In total, nine different SUBC types were obtained for the hydrogel composite preparation.

2.2. Synthesis of hydrogel-SUBC composite

For the preparation of hydrogel-SUBC composite (SUBC hydrogel), acrylamide was used as the monomer, N, N'-methylene bisacrylamide as the crosslinker, and ammonium persulfate as the initiator. The preparation of SUBC hydrogel was conducted following the method described in Sanyang et al. (2016). In brief, 1.0 g of acrylamide was dissolved in 1.0 mL of distilled water. 0.6 g of SUBC and 0.001 g of N, N'-methylene bisacrylamide were added to the acrylamide solution. After the thorough mixing of the solution, 0.2 mL of 0.1 g aqueous solution of ammonium persulfate was added to initiate the polymerisation. The SUBC hydrogel precursor solution was immediately placed into 5 mm clear vinyl tubes and placed in an oven at 40 °C. The SUBC hydrogel was kept in the oven to speed up the polymerisation and crosslinking process, thus avoiding biochar settling at the bottom of the vinyl tubes. After 30 min, the straws were removed from the oven and kept at room temperature (25-30 °C) for 24 h to complete the polymerisation.

After 24 h, the prepared SUBC hydrogel was removed from the tubes and cut into 1 cm pieces. These cuttings were washed with distilled water several times to remove all un-reacted monomers and low molecular weight polymeric matter. Then, the washed SUBC hydrogel composites were dried in the air. The air-dried hydrogels were placed in a vacuum oven at 40 °C for another 24 h and then placed into a desiccator until use. Nine different hydrogels were prepared based on pyrolysis temperature and particle size of the biochar. These samples were used to compare and optimise the adsorption capacity of the resulting hydrogel composites. Table 1 illustrates nine different SUBC.

Table 4 *Different SUBC prepared based on pyrolysis temperature and particle size*

		Biochar particle size		
		1.18 mm	0.60 mm	0.06 mm
Pyrolysis temperature	500 °C	5R 1.18 SUBC	5R 0.60 SUBC	5R 0.06 SUBC
	600 °C	6R 1.18 SUBC	6R 0.60 SUBC	6R 0.06 SUBC
	700 °C	7R 1.18 SUBC	7R 0.60 SUBC	7R 0.06 SUBC

2.3. Characterisation of sugarcane bagasse hydrogel biochar composite

2.3.1. Swelling ratio

The swelling behaviour was measured by placing the selected SUBC hydrogel composite in distilled water. The weight increase was measured periodically at room temperature until it became constant. Equation 1 was used to calculate the swelling ratio.

$$\text{Swelling \%} = \frac{W_{\text{swollen}} - W_{\text{dry}}}{W_{\text{dry}}} \times 100 \quad (1)$$

where W_{swollen} and W_{dry} are the weight of the swollen and dry samples, respectively.

2.3.2. Point of zero charge

The point of zero charge of the selected SUBC hydrogel composite was measured with the salt addition method described by Bakatula et al. (2018). In brief, this method entailed a series of 15 mL centrifuge tubes 0.05 g of SUBC sample added to 10 mL of 0.1 M NaNO_3 solution. The pH was adjusted with 0.1 M HNO_3 and 0.1 M NaOH as needed to obtain pH values of 2, 3, 4, 5, 6, 7, 8, 9 and 10 (± 0.1). The initial pH of each sample was denoted as pH_i . The samples were shaken for 24 h in a shaker at room temperature at 200 rpm (Orbital shaker OM15, RATEK). After 24 h of shaking, the final pH (pH_f) of each sample was measured. The point of zero charge was obtained from the plot of ΔpH ($\text{pH}_f - \text{pH}_i$) against pH_i .

2.3.3. Physical and chemical characterisation

All physical and chemical characterisations were conducted for the SUBC hydrogel composite selected for further experiments. The selection procedure and criteria will be discussed in Section 3.3. Fourier Transform Infrared Spectroscopy (FTIR) analysis was used to investigate the functional groups that existed in the SUBC hydrogel, SUBC and

poly(acrylamide) hydrogel. The morphology of the SUBC hydrogel was characterised by scanning electron microscopy (JCM-6000, JEOL). The selected SUBC hydrogel was analysed by X-ray photoelectron spectrometer (Kratos Axis Ultra XPS, Centre for Microscopy and Microanalysis, The University of Queensland) to determine the chemical status of the surface functional groups. The powder X-ray diffraction patterns of the hydrogel were obtained by a Bruker Advance D8 X-ray Diffractometer equipped with a LynxEye detector, Cu tube and operated at 40 kV and 40 mA (Centre for Microscopy and Microanalysis, The University of Queensland). The conditions of the analysis were 15 rpm rotation, 10-80 degrees 2-theta (start and end angles), 0.02° increment, 1.13 s/step and 1 h 10 min scan time. The traces were processed using the *Diffraction*^{plus} Evaluation Package Release V5.1 and PDF-4 Release 2022.

2.4. Batch sorption experiments for SUBC hydrogel composite

A stock solution (1000 mg/L) of As(V) was prepared by dissolving sodium arsenate dibasic heptahydrate ($\text{Na}_2\text{HAsO}_4 \cdot \text{H}_2\text{O}$) in distilled water. This stock solution was used for the preparation of As(V) solutions at the required concentrations and the solutions were freshly prepared for each study. After every experiment, the samples were separated from hydrogels and the solutions were filtered through a glass fibre filtration technique (0.6 μm), and the remaining As(V) concentrations were measured using inductively coupled plasma mass spectrometry (PerkinElmer NexION™ 300X). Every analysis was conducted as triplicate and control experiments were conducted. The laboratory blank samples were prepared and tested. The standard and blank samples were tested in between every 12 samples to comply with Quality Assurance/Quality Control (QA/QC) measures. To assess the best pH of the solution, for optimum As(V) adsorption for nine different hydrogels, an adsorption edge experiment was conducted at 5 mg/L As(V) at different pHs from 4-10 for a biochar dosage of 1 g/L. The solutions with SUBC hydrogels were shaken at 100 rpm for 24 h at room temperature (25 °C). At the same time, a control experiment was conducted with hydrogel but without biochar.

To determine the optimum dosage for As(V) adsorption, the selected SUBC hydrogel from the edge experiment was shaken for 24 h in 5 mg/L of As(V) at different dosages from 1 - 100 g/L. In this dosage experiment, SUBC hydrogels were used in two different ways: swelled and dry. For swelled SUBC hydrogels, the hydrogels were allowed to swell in distilled water for 24 h before As(V) adsorption. A 5 mg/L As(V) was used for kinetic experiments. Samples of the swollen hydrogels were taken at predetermined time intervals from 0.5 - 72 h. Batch isotherm studies were carried out in the As(V) concentration range of 0.025 - 7 mg/L. An

equilibrium time of 6 h was chosen based on the kinetic experiment. The amount of As(V) retained in the adsorbent phase was calculated using equation 2 (Mayakaduwa et al., 2016).

$$q_e = [C_0 - C_e]VM^{-1} \quad (2)$$

where q_e is the As(V) amount adsorbed on SUBC hydrogel (mg/g), C_0 and C_e are the initial and equilibrium As(V) concentrations (mg/L), V is the solution volume (L) and M is the hydrogel mass (g).

2.5. Experimental data modeling

Chemical kinetics describes possible reaction pathways as a function of reaction time to reach equilibrium. To investigate the mechanisms of adsorption processes, five different non-linear kinetic models, namely the pseudo-first order, pseudo-second order, Elovich, parabolic diffusion and power function, were applied to the experimental data. Adsorption equilibria generally provides fundamental physio-chemical mechanisms for predicting the applicability and stability of adsorption processes as a unit operation (Ho and McKay, 1998).

The isotherm experimental data were analysed using four non-linear isotherm models (the Langmuir, Freundlich, Temkin and Dubinin-Radushkevich models) (Ho et al., 2002) which were selected because they are the most commonly used mathematical models used to describe the sorption kinetics and isotherms of metals and metalloids on sorbents. These kinetic models have been classified into two main types: reaction-based and diffusion-based models (Ho et al., 2002). While diffusion models are focused on the diffusive transport of metal ions from aqueous solutions into pore networks and active sites of the sorbent, reaction models describe interaction rates between sorbent and specific metal ions. Sorption isotherm models are used to explore how an adsorbate interacts with the adsorbent. Isotherm and kinetic modeling and statistical graphing were done with the Microcal Origin software (Version 6).

2.6. Desorption and re-sorption experiment for exhausted hydrogel composites

Desorption experiments were utilised to evaluate and verify the reusability of SUBC hydrogel. The desorption study was performed with H_2SO_4 , CH_3COOH , $NaOH$ and $NaHCO_3$ with concentrations of 1, 0.1, 0.01 and 0.001 M for each acid/base. The As(V) adsorbed SUBC hydrogel was shaken in the abovementioned solutions for 6, 24 and 48 h. To test the re-sorption capabilities, hydrogel composites were then used for As(V) adsorption. The best desorption

and adsorption method was selected, and two more desorption and re-sorption cycles were conducted to determine the recycling capacity of the SUBC hydrogel composite.

2.7. Comparison of sugarcane bagasse biochar hydrogel composite with rice-hull biochar hydrogel composite

The behaviour of As(V) adsorption of the SUBC hydrogel composite was compared with the results of rice-hull biochar hydrogel composite (RHBC hydrogel). The As(V) adsorption of the RHBC hydrogel has been studied and submitted for journal publication.

3. Results and discussion

3.1. SUBC hydrogel composite synthesis

Synthesis of the SUBC hydrogel underwent several steps: initiation, macro-radical generation, chain propagation and formation of the three-dimensional SUBC hydrogel. In the first step there should be free-radicals to generate monomer radicals for the formation of the polymeric chain. Here, we used ammonium persulfate as the free-radical generator. Under heating conditions, the ammonium persulfate was subjected to the decomposition and generation of sulfate anion radicals. These sulfate radicals hit first on hydroxyl groups of the SUBC and extract hydrogen and formed macro-radicals which are more active than the sulfate anion radicals. The macro-radicals reacted with the acrylamide monomers and generated acrylamide monomer radicals. Generated acrylamide monomer radicals became free-radical donors to neighbouring monomer molecules and with the continuation of the reaction, the polymeric chains formed. Simultaneously, the vinyl groups of N, N'-methylene bisacrylamide, the crosslinkers, reacted with the growing polymeric chains and connected the polymeric chains with each other. Each polymeric chain was connected to the SUBC from one end and the other end connected with N, N'-methylene bisacrylamide. Finally, the 3D SUBC hydrogel structure was formed (Ren et al., 2014; Tanan et al., 2019).

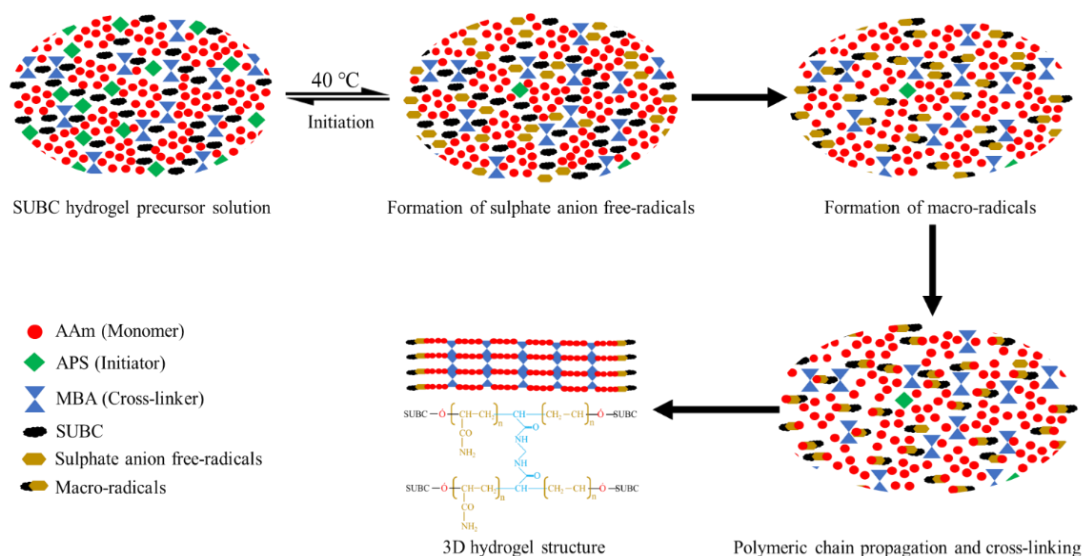


Figure 1 *Process of sugarcane bagasse biochar hydrogel synthesis*

3.2. Characterisation of SUBC hydrogel composite

3.2.1. Swelling behaviour of SUBC hydrogel composite

One of the unique advantages of hydrogel is its high swelling capacity. In aqueous media, hydrogels can adsorb water and swell. Swelling capacity depends on the crosslinking density of the hydrogel. Compared to a low crosslinking density, the hydrogels with a high crosslinking density have a lower swelling capacity. When the crosslinking density is comparatively low, it allows the network chains to have larger-scale movements which facilitate more water adsorption. However, the lower crosslinking density weakens the mechanical strength of the hydrogel which means water adsorption can destroy the structure. Therefore, crosslinking density should be optimised according to the purpose of the hydrogel. The swelling capacity is important for contaminant removal because it directly affects the uptake of a given metal/metalloid.

The selected hydrogel was the 700 °C 0.06 SUBC hydrogel (hydrogel biochar composite synthesised using SUBC produced at 700 °C and sieved through a 0.06 mm sieve). The selection procedure will be discussed with the sorption experiments in Section 3.3. Figure 2 illustrates the swelling of a SUBC hydrogel at various time intervals ranging from 0.5 - 48 h at room temperature. The graph depicts a rapid increase in the swelling ratio up to 24 h when swelling equilibrium is reached without further significant increase. At equilibrium level, the SUBC hydrogel can adsorb water, increasing its weight by about 1050%. Even after 48 h, the

hydrogel did not dissociate, indicating that the cross-linking density was acceptable for the SUBC hydrogel to be used as an adsorbent for contaminant removal.

One of the reasons for such a high swelling capacity is the SUBC hydrogel composite's polymeric chain is made on acrylamide which is considered a highly hydrophilic polymer (Zhao et al., 2010). This water absorption occurs due to repulsion between the hydrophilic groups of the polymer hydrogel and osmotic pressure alteration (Nakhjiri et al., 2021). As depicted in Figure 1, the hydrogel network consists of a large amount of $-NH_2$ functional groups which are hydrophilic. Since the group comes with the crosslinking agent, (N, N'-methylene bisacrylamide) each junction of the three-dimensional structure consisted of the $-NH_2$ group and, therefore, high water adsorption capacity is achieved (Sanyang et al., 2016).

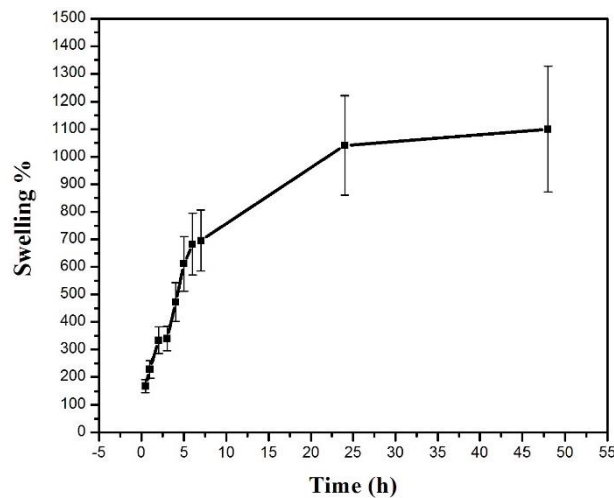


Figure 2 *Percentage of swelling capacity for sugarcane bagasse biochar hydrogel composite in distilled water over the time*

3.2.2. Point of zero charge for SUBC hydrogel composite

The point of zero charge is the pH when the net charge of the surface becomes zero. The point of zero charge helps to determine how the surface charge changes with pH, and to give an idea of active surface functional groups at different pH values. When $pH < pH_{pzc}$, the surface of the material will be negatively charged, whereas when the $pH > pH_{pzc}$, the surface of the material will be positively charged (Herath et al., 2016). Figure 3 shows how the ΔpH changes with the pH_i . Within the researched range of pH (2-10), all the plotted values are negative. However, at pH

2 the plot value is almost zero. Therefore, when the solution pH is higher than 2, the surface charge of the SUBC hydrogel is negative.

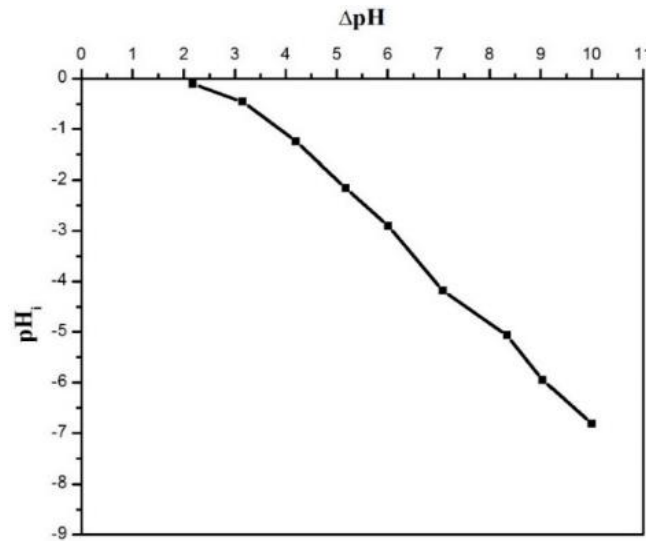


Figure 3 Plot of ΔpH vs pH_i for salt addition method to determine the point of zero charge of sugarcane bagasse biochar hydrogel composite

3.2.3. Physical and chemical characterisation of SUBC hydrogel composite

Figure 4 shows the scanning electron micrographs of the SUBC hydrogel and pure poly(acrylamide) hydrogel. Figure 4(a) shows that the surface of the SUBC hydrogel consisted of macroporous. This macroporous structure provided the solution with easy access to the hydrogel. Further, Figure 4(b) shows the cross-section of the hydrogel and that the hydrogels consisted of multiple layers which were interconnected to make the three-dimensional structure. The pure poly(acrylamide) hydrogel surface was a smooth surface and there was no visible porous structure under scanning electron micrographs.

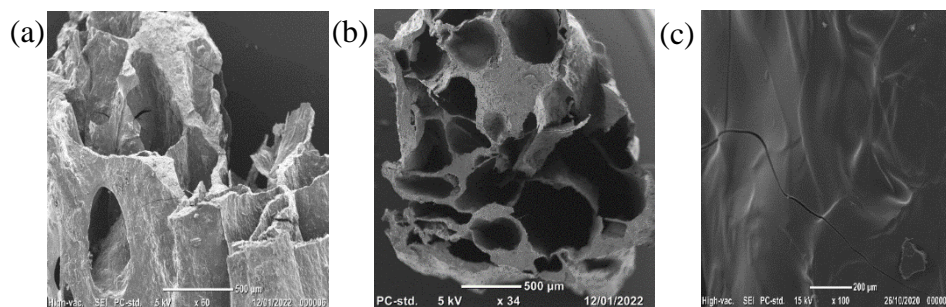


Figure 4 Scanning electron micrographs images of sugarcane bagasse biochar hydrogel composite (a) - Surface, (b) - Cross-section (c) Scanning electron micrographs image of pure poly(acrylamide) hydrogel (surface)

The FTIR spectra of the SUBC, poly(acrylamide) hydrogel and SUBC hydrogel composite are shown in Figure 5. The SUBC hydrogel and poly(acrylamide) hydrogel showed vibration stretching of the -NH_2 group from acrylamide at 3178 and 3170 cm^{-1} , respectively. This functional group was the key advantage for SUBC hydrogel over SUBC for As(V) removal in the pH range of 4-7 and will be further discussed in Section 3.3. The combined stretching vibration of -CH and -CH_2 was shown in both SUBC hydrogel and poly(acrylamide) hydrogel at 1419 and 2924 cm^{-1} respectively, representing the -CH and -CH_2 groups in the polymeric chain which came from the acrylamide. The stretching vibration at 1651 cm^{-1} in both SUBC hydrogel and poly(acrylamide) hydrogel and 1743 cm^{-1} of SUBC represent the stretching vibration C=O functional group. Further, at 1589 cm^{-1} , the SUBC hydrogel showed stretching vibration of the carbonyl group from both acrylamide and NH bending. The peaks at 1419 and 1411 cm^{-1} of SUBC hydrogel and poly(acrylamide) hydrogel respectively, represent the COO^- stretching of the polymeric chain. The stretching vibration of the C-N group is represented by the 1651 cm^{-1} and 1319 cm^{-1} peaks of both SUBC hydrogel and poly(acrylamide) hydrogel respectively. The SUBC showed a peak at 1064 cm^{-1} representing the presence of oxygenated functional groups which could be the alcohol -OH group. This peak shifted to 1095 cm^{-1} . The SUBC hydrogel composite and poly(acrylamide) hydrogel showed peaks at 447 cm^{-1} and 462 cm^{-1} , respectively, which was attributed to the C-H out-of-plane deformation condensing smaller aromatic units into larger sheets.

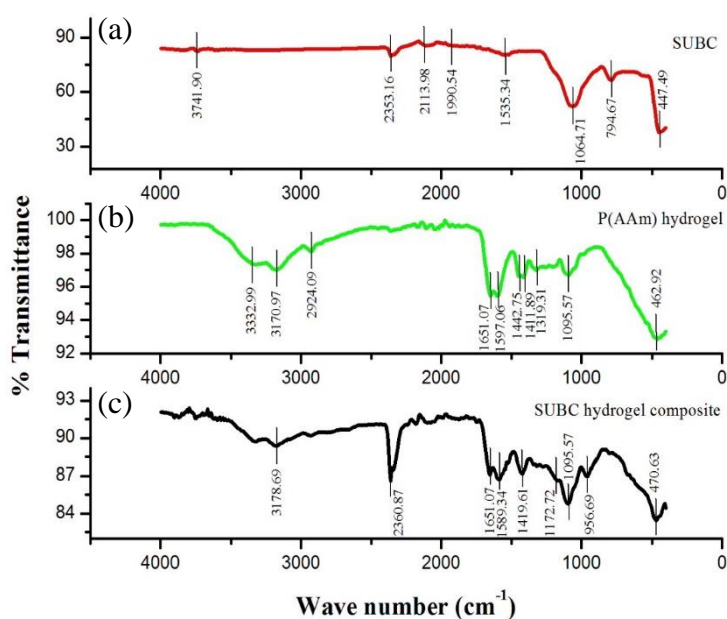


Figure 5 FTIR spectra for (a) Sugarcane bagasse biochar (SUBC), (b) Poly(acrylamide) (P(AAm)) hydrogel, (c) Sugarcane bagasse biochar hydrogel composite (SUBC hydrogel composite)

The powder X-ray diffraction patterns of the SUBC hydrogel composite are given in Figures 6 (a) and (b). Based on the powder X-ray diffraction graph, it can be understood that the SUBC hydrogel had mostly an amorphous structure. However, in the 2θ angles of $22-23^\circ$ area, a significant peak was found related to the silica (identified as SiO_2) which originated from the SUBC (Figure 6(b)). Further, a small number of additional peaks at the 2θ angle ranges of $20.5-21.0$, $49.5-50.0$ and $59.5-60.0^\circ$ were identified as SiO_2 (Figure 6(a)). In hydrogel synthesis, the SUBC bound to the polymeric chain through a free-radical reaction (Figure 1) and, as a result, the silica content bound to the polymeric chain and formed SUBC, as identified with powder X-ray diffraction pattern analysis.

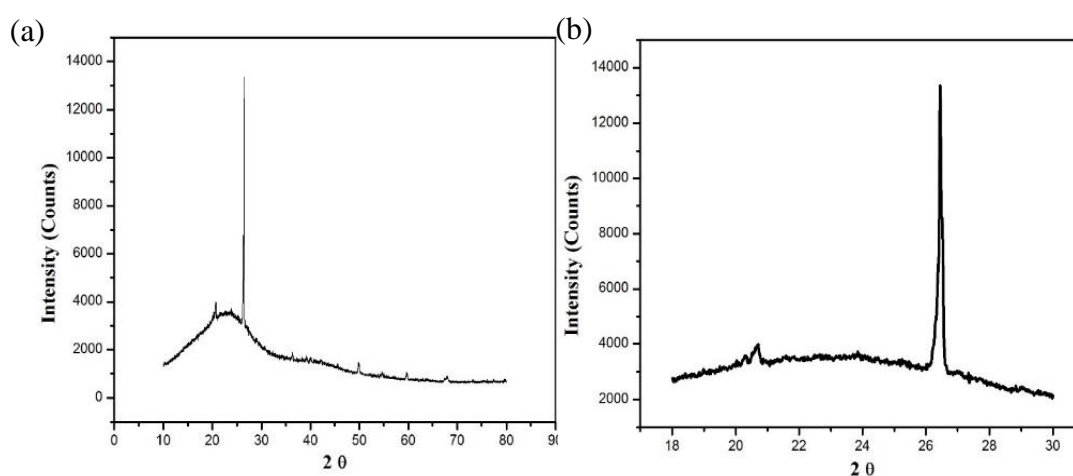


Figure 6 Powder X-ray diffraction pattern for sugarcane bagasse biochar hydrogel composite (a) - Full spectra of the powder X-ray diffraction pattern, (b) - Separated section of the silica peak

The wide-scan X-ray photoelectron spectrometer spectra of the SUBC hydrogel are shown in Figure 7(a). According to Figure 7, the predominant peaks observed in the SUBC hydrogel surface are Si2p, S2p, C1s, N1s and O1s. The binding energy for Si (2p) is between 102.9 and 103.9 eV (Figure 7(f)). The literature shows that SiO_2 has 103.5 eV of X-ray photoelectron spectrometer binding energy and, therefore, here it can be assumed that the form of Si in the SUBC hydrogel was SiO_2 (Wagner et al., 2003). This assumption has also been confirmed by powder X-ray diffraction analysis with Si related peaks (Figure 6). The sugarcane bagasse ash contained 97% of silica by its weight, making Si a major compound (Norsuraya et al., 2016). Figure 7(e) shows a peak in the range of 165.9 and 171.9 eV which is related to S. It should have come from the ammonium persulfate which was the initiator of the process of

hydrogel preparation. The peak related to C appears in the binding energy range of 281.9 and 291.9 eV (Figure 7(b)). Considering the proposed structure in the formation of hydrogel (Figure 1), few C types can be proposed for the above C binding energy range. The literature shows C-C and C-H bonds at 285.0 eV and C=O at 287.8-288.3 eV (Beamson, 1992). A sharp N peak is found in the range of 369.9 and 402.9 eV (Figure 7(c)). Based on the proposed structure (Figure 1) these N peaks are N-(C=O)- and C-NH₂. The literature demonstrates that N-(C=O)- can be found at 399.7 eV and C-NH₂ at 399.4 eV (Beamson, 1992; Mohtasebi et al., 2016; Wagner et al., 2003). The C-NH₂ and N-(C=O)- were the major contributors to the hydrogel structure which rendered the hydrogel surface a positively charged surface within the pH range of 4-7. Therefore, one of the innovative functions of the hydrogel composite was associated with the C-NH₂ group. This is discussed further in Section 3.3. The O peak is found within the range of 528.9 and 536.9 eV (Figure 7(d)). This range refers to several O bonds bond types that the proposed hydrogel structure could explain. Moreover, O bonding in the SiO₂ appears at the binding energy of 532.9 eV which can be explained by the X-ray photoelectron spectrometer O peak.

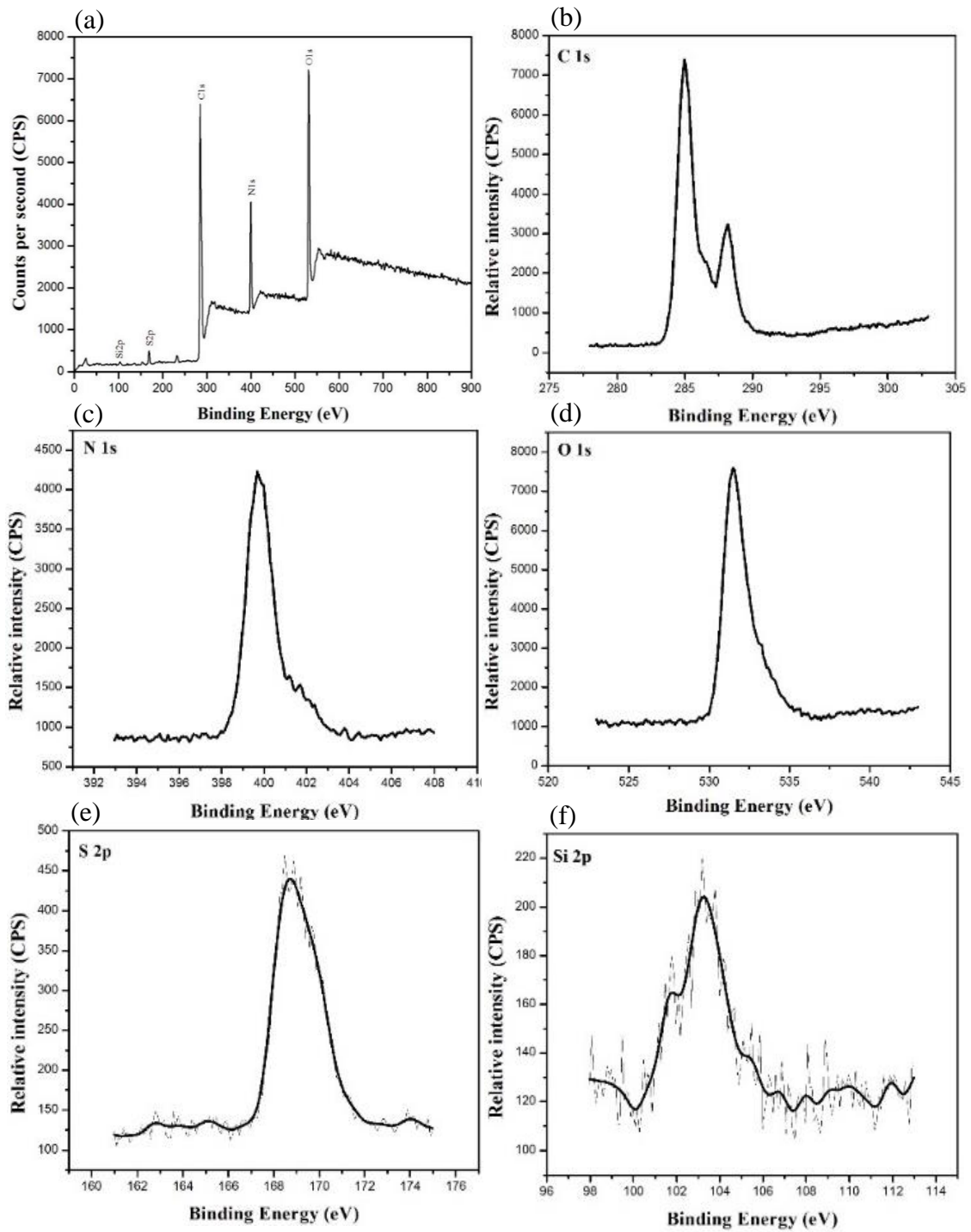


Figure 7 (a) The wide-scan X-ray photoelectron spectrometer spectra of the sugarcane bagasse biochar hydrogel composite, refined X-ray photoelectron spectrometer spectra of (b) C 1s, (c) N 1s, (d) O 1s, (e) S 2p, (f) Si 2p

3.3. Effect of pH on As(V) adsorption and selection of the best hydrogel type

The effect of pH on the As(V) adsorption of nine different SUBC hydrogel types was investigated at various pH values ranging from 4-10 as depicted in Figure 8. Of the nine different hydrogel types, the highest adsorption rate is shown by 7S 0.06 hydrogel (Figure 8(i)) which was elected for continued experimentation as the best hydrogel type. It shows that with the increase in biochar pyrolysis temperature, the adsorption capacity increased. This is because, with the increased pyrolysis temperature, a high amount of volatile matter was discharged from the sugarcane bagasse. This created additional new microporous inside the SUBC, and the surface area of the SUBC also increased.

Considering the size of the SUBC within the hydrogel, the smaller particles easily dispersed into the hydrogel structure while the hydrogel synthesis took place. During hydrogel synthesis, the residual content of the hydrogel was high in the 1.18 mm SUBC hydrogel, and the residual content minimum was 0.06 mm SUBC hydrogel. Therefore, when the particle size was 0.06 mm, the maximum SUBC content was expected to be within the hydrogel structure and the adsorption more efficient. Further, with the 0.06 mm SUBC particles, the unit surface area was higher than those of the 1.18 mm SUBC particles and the adsorption capacity was expected to be high with 0.06 mm SUBC hydrogel compared to the 1.18 mm SUBC hydrogel.

Almost all the hydrogels showed the highest adsorption at the pH range of 6-7. At the acidic pH ranges, the H^+ ions made the biochar surface highly protonated and positively charged (Wu et al., 2018). This positive surface charge was due to the protonation of ionisable functional groups such as $-NH_2$ and $-CO$. The FTIR spectra showed that both the $-NH_2$ and $-CO$ groups were present and, therefore, protonation took place in the SUBC hydrogel. After protonation the $-NH_3^+$ and $-COH^+$ groups converted the hydrogel surface into a positively charged surface. Both the NH_2 and $-CO$ groups were from the acrylamide which was the monomer (Figure 1). Therefore, the three-dimensional polymer structure contained NH_2 and $-CO$ groups in every monomer unit of the polymeric chain and their protonation made the entire hydrogel structure a positively charged surface. When the pH was increasing (>2), the dominant As(V) species became $H_2AsO_4^-$ (pH 2-7) and $HAsO_4^{2-}$ (pH 6-12), and those oxyanions could be easily adsorbed by a positively charged surface. Therefore, the adsorption was expected to be the maximum at the pH range of 6-7. Once the hydrogel was fully swollen, $H_2AsO_4^-$ and $HAsO_4^{2-}$ ions diffused freely into the 3D network structure of the hydrogel through electrostatic interactions between the positively charged surface of the hydrogels and the negatively charged $H_2AsO_4^-$ and $HAsO_4^{2-}$ ions. At the lower pH values (<2), the dominant As(V)

species was H_3AsO_4 which is not an oxyanion and is not able to be attracted by a negatively charged surface (at $\text{pH} < 4$, the surface is negatively charged). Therefore, the As(V) adsorption at the lower pH was low. When the solution pH became higher than 7, the number of hydroxyl ions (OH^-) in the solution increased, and those hydroxyl ions competed with the As(V) species for the adsorption sites, explaining why As(V) adsorption decreased after exceeding pH 7.

Although the point of zero charge of the SUBC hydrogel was negative, the solution pH was crucial to the creation of a positive surface charge which facilitated As(V) adsorption. Therefore, the adsorption of As(V) into the SUBC hydrogel was solely dependent on the solution pH (7R 0.06 hydrogel is now indicated as the SUBC hydrogel).

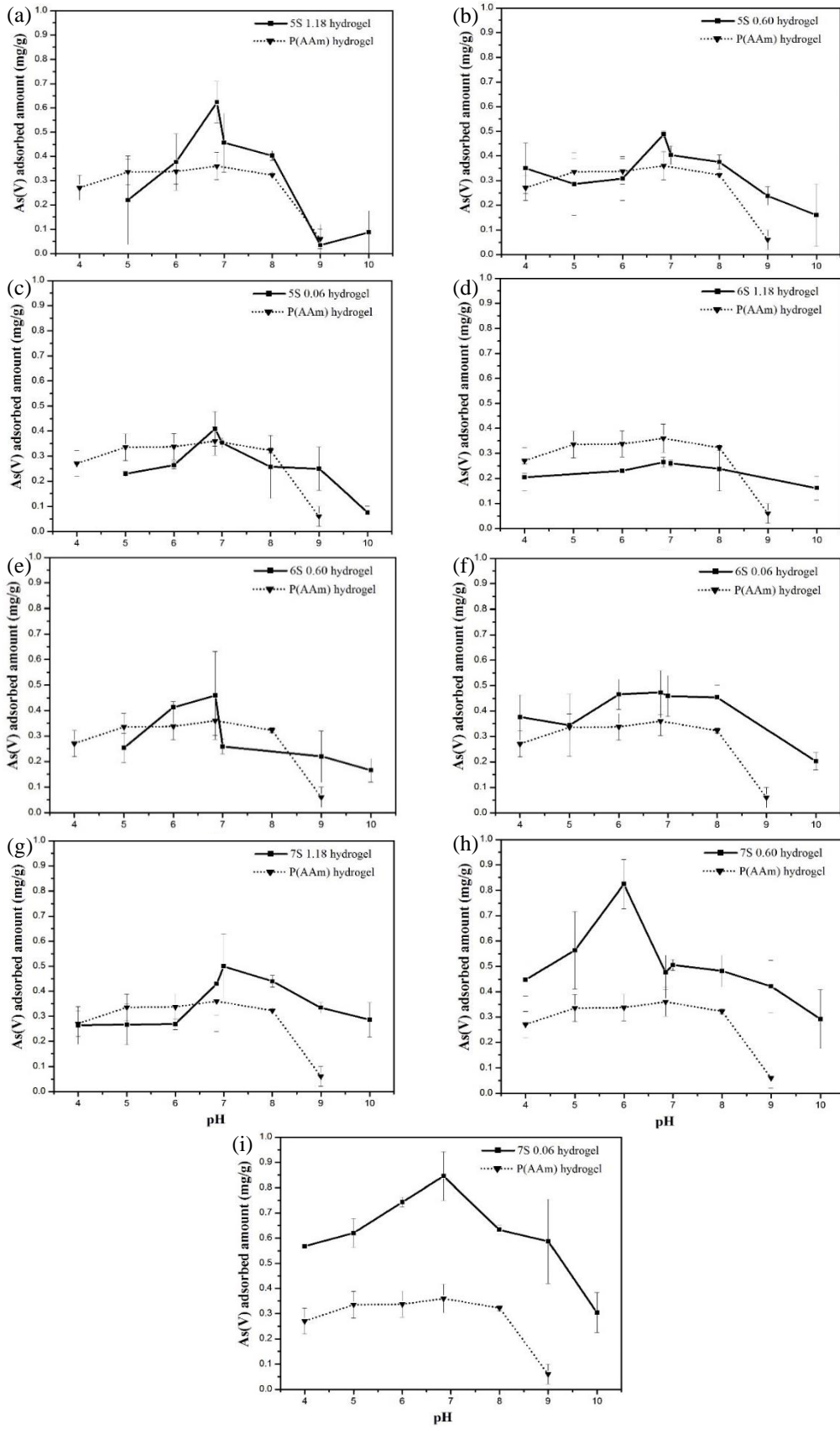


Figure 8 As(V) adsorption patterns of nine different sugarcane bagasse biochar hydrogel composite types with initial pH (a) 5S 1.18 hydrogel, (b) 5S 0.60 hydrogel, (c) 5S 0.06 hydrogel, (d) 6S 1.18 hydrogel, (e) 6S 0.60 hydrogel, (f) 6S 0.06 hydrogel, (g) 7S 1.18 hydrogel, (h) 7S 0.60 hydrogel, (i) 7S 0.06 hydrogel

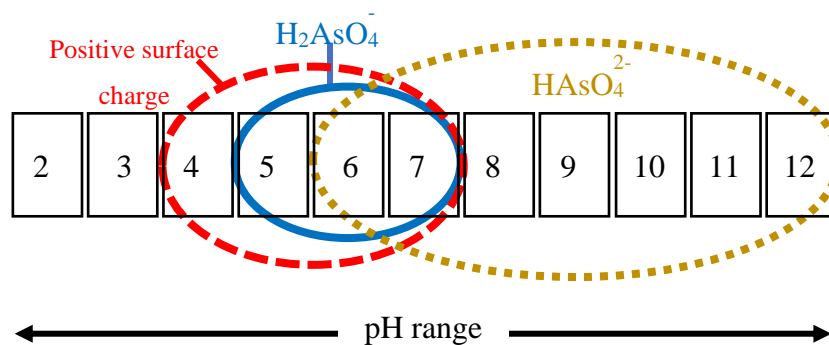


Figure 9 The best pH range for As(V) adsorption (pH 6-7) with sugarcane bagasse biochar hydrogel composite

3.4. Effect of pre-swelling and SUBC hydrogel dosage on As(V) adsorption

Figure 10 shows the effect of hydrogel pre-swelling on adsorption capacity. There was approximately 20-30% increment in As(V) adsorption when the SUBC hydrogel was fully swollen. Once this occurred, H_2AsO_4^- and HAsO_4^{2-} ions diffused freely into the three-dimensional network structure of the hydrogel through electrostatic interactions between the positively charged surface of the hydrogels and the negatively charged H_2AsO_4^- and HAsO_4^{2-} ions. Therefore, the swelling capacity and the pre-swelling also played a significant role in As(V) adsorption by the SUBC hydrogel.

The effective adsorption and optimisation of an adsorbent greatly depends on the sorbent-sorbate ratio. The correct sorbent-sorbate ratio allows sufficient and effective adsorption sites for optimum As(V) removal while ensuring economic efficiency. Figure 11 illustrates the changes of As(V) adsorption per 1 g of SUBC hydrogel composite with different dosages. According to Figure 11, the adsorption capacity for pre-swelled SUBC hydrogel composite was around 0.85 mg/g at 1 g/L, and when the dosage was 5 g/L the adsorption capacity was 0.27 mg/g which is a 0.58 mg/g difference. Between 5 and 10 g/L dosages, this difference was 0.05 mg/g and it decreased further with the rest of the dosages. Considering cost-effectiveness, the production cost for 5 g/L is 5 times higher than 1 g/L hydrogel, but the ratio for adsorption capacity is less than 5 times. Therefore, the most efficient dosage is 1 g/L.

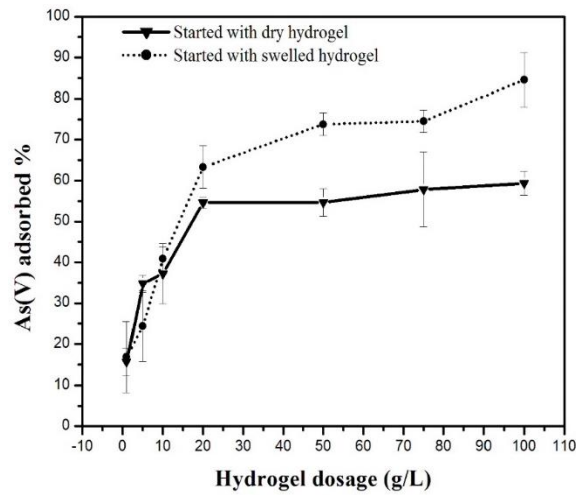


Figure 10 *Effect of pre-swelling of hydrogel on adsorption capacity*

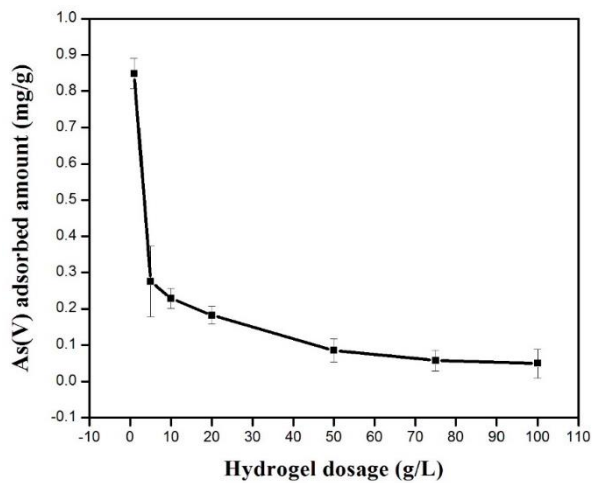


Figure 11 *As(V) adsorption capacity with the different sugarcane bagasse biochar hydrogel composite dosages*

3.5. Adsorption kinetic

Adsorption kinetics details the adsorption rate of a particular adsorbate and the duration of the sorption process to reach equilibrium. Moreover, adsorption kinetics is important for understanding adsorption reaction mechanisms. According to the kinetic graphs, within the first 24 h, the adsorption reached up to 44.3% (0.045 mg/g) and achieved equilibrium. This rapid adsorption in the first 24 h is due to the availability of the positively charged surface sites of the SUBC hydrogel. As the available sites were fully employed by As(V), the adsorption process entered the equilibrium stage.

To understand the adsorption mechanisms and the feasible rate-determining step of the adsorption process, the kinetic data were fitted to the mathematical kinetic models. In the pseudo-first-order model, the adsorption phenomenon was assumed to be non-dissociating molecular adsorption into the adsorbent. The pseudo-second-order model assumed chemical sorption involving valence forces through the sharing or exchange of electrons between the adsorbent and the adsorbate. The Elovich equation describes the kinetics of heterogeneous chemisorption, while the parabolic model indicates that diffusion control phenomena are rate-limiting. The power function model is commonly used to describe homogeneous chemisorption kinetics (Mayakaduwa et al., 2016). The values of kinetic model parameters together with the correlation coefficient (R^2) values are depicted in Table 2.

Figure 12 shows the adsorption kinetics for the adsorption of As(V) into the SUBC hydrogel composite. The calculated R^2 values indicate that the pseudo-second order is the best fit with the experimental data which suggests chemical sorption involving valence forces through the sharing or exchange of electrons between the adsorbent and the adsorbate (Figure 12). It can be suggested that the adsorption of As(V) into the SUBC hydrogel would be more inclined towards the chemisorption mechanism. The goodness of fit of the experimental data to the pseudo-second-order non-linear model is further proven by the value of adsorption capacity evaluated by the pseudo-second-order model (0.045 mg/g) which is similar to the experimental value (0.045 mg/g). However, the pseudo-first order also fits with the experimental data with 0.91 of R^2 and an almost similar equilibrium sorption capacity (Figure 12). Therefore, a physisorption mechanism can also be integrated with the chemisorption mechanism in the As(V) adsorption process into the SUBC hydrogel.

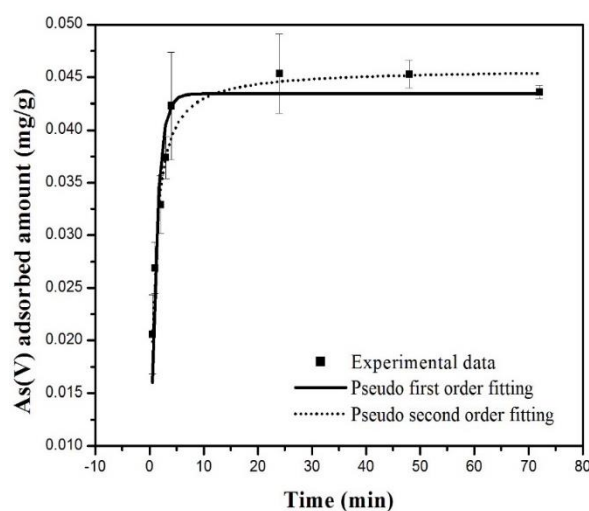


Figure 12 *Best fitted kinetic models on As(V) adsorption*

Table 5 Non-linear kinetic parameters of As(V) adsorption into SUBC hydrogel composite

Model	Non-linear equation	Description	Isotherm parameters	Value	R ²
Pseudo-first order	$q_t = q_e[1 - e^{-K_1 t}]$	K_1 – the rate constant (min^{-1}) q_e, q_t – sorption capacity at equilibrium and at time t , respectively (mg/g)	K_1 q_e	0.91876 0.04342	0.91212
Pseudo-second order	$q_t = \frac{q_e^2 K_2 t}{1 + K_2 t q_e}$	K_2 – the rate constant (g/mg/min) q_e, q_t – sorption capacity at equilibrium and at time t , respectively (mg/g)	K_2 q_e	33.5334 0.04578	0.97296
Elovich	$q_t = b \ln(ab) + \ln(t)$	q_t – sorption capacity at time t (mg/g) a – initial sorption rate (mg/g/min) b – desorption constant (g/mg)	a b	2.90413 222.897	0.79594
Power function	$q_t = b(t^{k_f})$	q_t – sorption capacity at time t (mg/g) b – power function constant k_f – power function rate constant	b k_f	0.02985 0.11128	0.7385
Parabolic	$q_t = a + k_p \sqrt{t}$	q_t – sorption capacity at time t (mg/g) a – parabolic constant k_p – parabolic rate constant	a k_p	0.02895 0.00231	0.55503

3.6. Adsorption isotherm

Work on adsorption isotherm models with experimental data gives details for evaluating and designing the adsorption mechanism of a particular sorbent and sorbate interface. Generally, isotherm mathematical models describe the relationship between the adsorbed amount of a particular substance by a unit weight of adsorbent and the remaining amount of adsorbate at equilibrium. In the present study, isotherm models by Langmuir, Freundlich, Dubinin-Radushkevich and Temkin were used to determine the adsorption mechanism. The Langmuir isotherm model assumes monolayer adsorption when adsorption

can only occur at a fixed number of definite localised sites that are identical and equivalent. The Freundlich isotherm model describes multilayer adsorption with non-uniform distribution of adsorption affinities over the heterogeneous surface (Foo and Hameed, 2010). The Dubinin-Radushkevich model is a semiempirical equation in which the adsorption follows the mechanism of pore filling. This model assumes that a multilayer character, which involves Van der Waal's forces, can be applied to the physical adsorption processes. The Temkin model describes a chemisorption process (Al-Ghouti and Da'ana, 2020).

The isotherm parameters for each isotherm model are given in Table 3. Figure 13(a) shows the adsorption isotherms for the adsorption of As(V) into the SUBC hydrogel. The experimental data were best fitted with the Langmuir, Dubinin-Radushkevich and Freundlich isotherm models with high R^2 values of 0.98, 0.97 and 0.96, respectively (Figure 13). The Langmuir model describes a monolayer coverage, indicating that each site can be held by one adsorbate molecule on a homogeneous substrate. This Langmuir model describes a quantitative interpretation of the solute phase distribution between the solution and the solid and a chemisorption mechanism. The separation factor (R_L), which is based on Langmuir parameters, can be used to determine the favourability of the As(V)-SUBC hydrogel adsorption system. The relationship between the calculated R_L and the initial concentration of As(V) is shown in Figure 13(b). The R_L values were less than 1 for all concentrations of As(V), indicating that the adsorption of As(V) into the SUBC hydrogel is a favourable and feasible process. The Dubinin-Radushkevich model showed R^2 of 0.97, indicating that the adsorption process also involved the pore filling mechanism. Swelled hydrogel is a porous structure and within the hydrogel the SUBC also consisted of a porous structure, confirming that the As(V) adsorption into the SUBC hydrogel facilitates a pore-filing mechanism. According to the Freundlich model, multilayer adsorption occurs on a heterogeneous surface. This further implies that the As(V) was adsorbed into the SUBC hydrogel controls by the physisorption mechanism. The parameter n of the Freundlich model equation was valued at 0.8 which is less than 1, indicating that the adsorption process of As(V) is a favourable process.

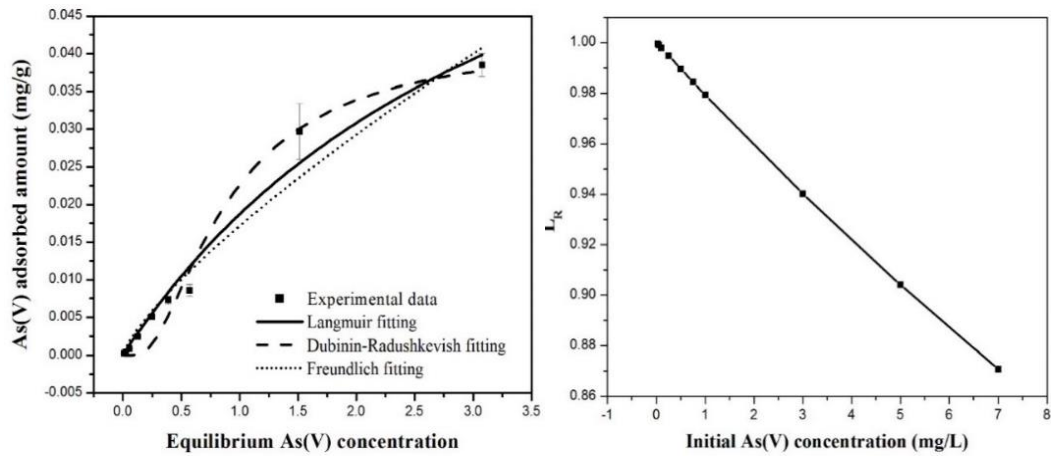


Figure 13 (a) Langmuir, Freundlich and Dubinin-Radushkevich adsorption isotherms of As(V) by sugarcane bagasse biochar hydrogel composite, (b) Separation factor (RL) obtained from the Langmuir isotherm model

Table 6 Non-linear isotherm parameters for As(V) adsorption into SUBC hydrogel composite

Model	Non-linear equation	Description	Isotherm parameters	Value	R ²
Langmuir	$q_{ads} = \frac{q_{max}K_L C_e}{1 + K_L C_e}$	q_{ads} – the amount of adsorbate adsorbed per unit mass of adsorbent (mg/g) q_{max} – the maximum adsorption capacity (mg/g) K_L – the Langmuir affinity parameter (L/mg) C_e – the equilibrium adsorbate aqueous phase concentration (mg/L)	q_{max} K_L	0.08708 0.27385	0.98002
Freundlich	$q_{ads} = K_F C_e^n$	K_F – the Freundlich affinity – capacity parameter ((mg/g)/(mg/L) ⁿ) n – the Freundlich exponent	K_F n	0.01716 0.77028	0.96599
Dubinin-Radushkevich	$q_{ads} = q_D \exp(-B_D [RT \ln(1 + 1/C_e)]^2)$	q_D – Monolayer adsorption capacity (mg/g) B_D – mean free energy sorption (mol ² /kJ)	q_D B_D	0.04175 1.27515	0.97974

3.7. Possible mechanisms for As(V) adsorption into SUBC hydrogel composite

Both isotherm and kinetic modeling data suggest that the As(V) adsorption into the SUBC hydrogel was associated with both physisorption and chemisorption mechanisms. Physical adsorption was mainly caused by the forces of molar interactions including Π^+ - Π electron donor-acceptor interactions and porous diffusion, as well as H-bonding via H-donor-acceptor interactions. The porous diffusion can be identified as the major mechanism as the hydrogel surface held a porous structure as shown in Figure 4, and the hydrogel made a three-dimensional structure as it swelled in the aqueous media. The molecules that are diffused through porous diffusion later underwent further chemisorption and physisorption mechanisms as the swelled hydrogel opened more functional groups and more porous structures within the SUBC particles.

3.8. Desorption and re-sorption of As(V) into SUBC hydrogel

The capability of regeneration of an adsorption material is significant for decreasing the cost of production and enhancing sustainability. Recognition of a reliable method for desorption is one of the most important aspects of this phenomenon. In the present study different acid and base solutions with different concentrations were used to find and select the best method for desorption of adsorbed As(V) from the hydrogel. Further, the resorption capabilities were studied with several adsorption-desorption cycles.

Figure 14 (a)-(e) explains the desorption and resorption capacities of the SUBC hydrogel with different desorption methods for one cycle. The 1 M H_2SO_4 showed 100% of desorption from the adsorbed amount, however the resorption was zero. Therefore, 1 M of H_2SO_4 degraded the SUBC hydrogel structure and all the adsorbed As(V) was released into the solution. With 0.1 M H_2SO_4 , the desorption capacities were around 25-35% while the resorption capacity varied around 20-30%. The 0.01 M H_2SO_4 showed 15-25% of desorption capacity and 35-45% of resorption capacity. The maximum resorption capacity of H_2SO_4 showed with 0.001 M which was 40-50%. However, the desorption capacity for 0.001 M H_2SO_4 was 10-15%. With CH_3COOH , the 0.1-0.001 M showed 10-20% of desorption capacity and 35-45% of resorption capacity. The best concentration for NaOH was 0.1 M and it showed 30-40% desorption capacity and >80% resorption capacity. 1 M NaHCO_3 showed same behaviour as 1 M H_2SO_4 where desorption was 100% but there was no resorption. 0.1, 0.01 and 0.001 M NaHCO_3 showed 10-35% of desorption capacity and 3-40% resorption capacity.

The literature explains that acidic conditions are preferable factors for the desorption of metal ions such as Pb, Cu and Fe from hydrogels (Weerasundara et al., 2021a). However, in the present study, the most suitable condition was alkaline. With the high pH levels of 0.1 M NaOH (12.19), the surface of the SUBC hydrogel becomes negatively charged and the adsorbed As(V) was, therefore, released into the solution. Interestingly, after desorption with 0.1 M NaOH, the adsorption capacity was increased to more than the initial adsorption capacity. Under the alkaline condition with the 0.1 M NaOH, the SUBC hydrogel went through a hydrolysis reaction. The hydrolysed hydrogels tended to change their swelling ratio remarkably. The ionisation equilibrium constant (pKa) of polyacrylic acid was approximately 4.2. Therefore, the hydrolysed poly(acrylamide) hydrogels were further swollen at a pH value higher than 4.2 (pKa). This increased swelling was achieved due to the electrostatic repulsion of the anionic carbonyl groups ($-CO$) (Zhao et al., 2010). Therefore, 0.1 M NaOH further increased its adsorption capacity while showing significant desorption capacity on As(V) with the SUBC hydrogel.

Figure 15 shows images of the SUBC hydrogel (a) dry hydrogel, and (b) after desorption treatment with 0.1 M NaOH. These figures prove the size difference of the same SUBC hydrogel and how it swelled after desorption treatment. Figure 14(f) shows the adsorption, desorption and resorption with 0.1 M NaOH treatment for four cycles. Even after three desorption cycles, the SUBC hydrogel shows around 35% As(V) adsorption capacity. This significant feature reveals that the adsorption capacity of the SUBC hydrogel was not limited to the values reported with one adsorption cycle, but was four or five times higher than the experimental maximum/equilibrium adsorption capacity. The adsorption values with 0.1 M NaOH are as follows: 0.04, 0.08, 0.01 and 0.03 for 1st, 2nd, 3rd and 4th adsorption cycles, respectively. Thus, the total adsorption capacity of the SUBC hydrogel for four adsorption cycles was 0.16 mg/g. Therefore, the SUBC hydrogel can be re-used and recycled for As(V) adsorption, enhancing the effectiveness of the process and its economic and environmental sustainability.

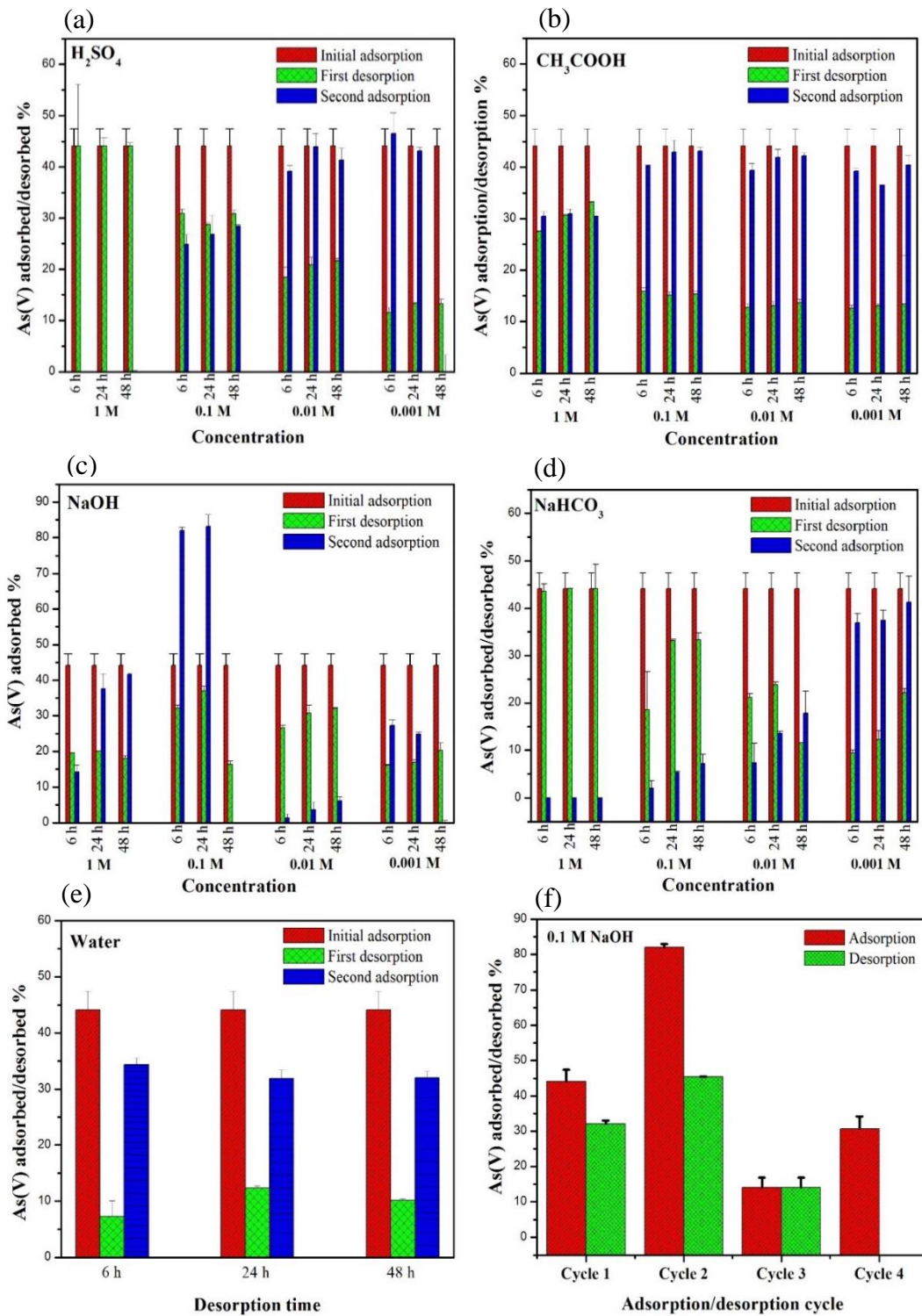


Figure 14 Desorption and resorption capacity for (a) H_2SO_4 , (b) CH_3COOH , (c) $NaOH$, (d) $NaHCO_3$, (e) Distilled water, (f) Selected desorption method and desorption-resorption capacities with four cycles



Figure 15 *Images of sugarcane bagasse biochar hydrogel composite (a) Dry hydrogel, (b) After desorption treatment with 0.1 M NaOH*

3.9. Comparison of sugarcane bagasse biochar hydrogel composite with rice-hull biochar hydrogel composite on As(V) adsorption

Table 4 depicts the conditions and results of both SUBC and RHBC hydrogel on As(V) adsorption. The preparation method was same for both hydrogel composites. The only difference was the biochar type. The data shows that the biochar type did not result in significant differences on As(V) adsorption since the two hydrogel composites showed no significant difference in overall activity. However, both the biochar integrated hydrogels showed enhanced As(V) adsorption capacities compared to the pure poly(acrylamide) hydrogel.

The pore filling mechanism was one of the identified physisorption mechanisms for both the rice-hull biochar and SUBC. Figure 4(c) shows that the pure poly(acrylamide) hydrogel did not have a well-developed porous structure, unlike the rice-hull biochar (Figure S1) and SUBC (Figure 4(a), (b)) hydrogel composites. This was the major reason for the significantly elevated As(V) adsorption capacities of both the rice-hull biochar and SUBC hydrogel composites compared to pure poly(acrylamide) hydrogel. The biochar itself showed a hydrophobic nature. However, after integration of poly(acrylamide) hydrogel at the pH 6-7 range, the surface of the composite showed positive surface charge. As a result, and despite the hydrophobic nature of biochar, the SUBC hydrogel adsorbed As(V) oxyanions in the aqueous media. At this point the porous structure of biochar played a significant role in absorbing As(V) oxyanions via porous diffusion.

Table 4 *Comparison between sugarcane bagasse biochar and rice-hull biochar hydrogel composites*

Condition/results	SUBC hydrogel composite	RHBC hydrogel composite
Biochar pyrolysed temperature and size fraction of best composite	700 °C, 0.06 mm	700 °C, 0.06 mm
Swelling capacity	900%	1100%
Best pH range for As(V) adsorption	6-7	6-7
Best dosage for As(V) adsorption	1 g/L	1 g/L
Dry or swelled condition for maximum As(V) adsorption	Swelled condition	Swelled condition
Equilibrium time for As(V) adsorption	7 h	24 h
Maximum adsorption capacity	0.08 mg/g	0.07 mg/g
Equilibrium adsorption concentration	0.04 mg/g	0.04 mg/g
Mechanisms involved As(V) adsorption	Physisorption and chemisorption	Physisorption and chemisorption
Best method for As(V) desorption	0.1 M NaOH	0.1 M NaOH
Total adsorbed As(V) amount with 4 adsorption cycles	0.16 mg/g	0.16 g/g

4. Conclusion

Sugarcane bagasse biochar hydrogel was successfully developed as a composite of the poly(acrylamide) hydrogel and SUBC to remove As(V) from water. The change in the solution pH affected the adsorption capacity. The highest adsorption was recorded in the range of pH 6-7. This is an advantageous factor of SUBC hydrogel because it is the pH range for most natural water and, therefore, SUBC can be used directly in As(V) contaminated natural water.

The use of swollen SUBC hydrogel for As(V) removal was more efficient than the direct use of dry hydrogel. The hydrogels are three-dimension structured, and this tended to increase pore volumes and the unit surface area in the aqueous environments. Once the SUBC hydrogel became fully swollen, it acted with its maximum capacity to adsorb As(V). Chemisorption and physisorption adsorption mechanisms have been proposed for the adsorption of As(V) into SUBC hydrogel based on kinetic and isotherm data.

The SUBC hydrogel can be considered a revolutionary and innovative solution for removing As(V) from water because of its availability for regeneration and re-use. 0.1 M NaOH was found to be a successful solution for the desorption of As(V) from the SUBC hydrogel and it further increased the adsorption capacity of the SUBC hydrogel for As(V). Further, the SUBC hydrogel can be considered as a solution to overcome classic drawbacks of adsorbents such as adsorbent-water separation which hinders upscaling to a large industrial

scale. Sugarcane bagasse biochar hydrogel composite does not require additional energy (e.g., post filtration) to separate the adsorbent from the water, and so allows up-scaling to industrial large-scale application. The innovative aspects of the proposed hydrogel such as regeneration, re-use, and easy separation from water allow the material to be used for large-scale use. Further, since the adsorbed As(V) is not released when treated with water, it allows the use of SUBC hydrogel as a storage material for As(V) without harming the environment including ground and surface water resources. This makes it of global importance. The comparison of rice-hull biochar and SUBC hydrogel showed that there is no significant difference on A(V) adsorption.

There are further research opportunities related to the optimisation of adsorption capacity and its use at field scale in different aspects such as water filters, surface water bodies, water purification processes, etc. The integration of poly(acrylamide) hydrogel with SUBC expands the application range for contaminant removal as SUBC is a material that can also be used for several other contaminants. This opens the way for further research on the use of SUBC hydrogel as a removal agent for other contaminants. Therefore, this research opens a way to further innovative approaches on contaminant removal in aqueous media.

Acknowledgements

The authors acknowledge the support from Anya J. E. Yago, Dr Craig Stoppiello and Dr Lachlan Casey at the Centre for Microscopy and Microanalysis (CMM) at the University of Queensland.

The authors thank Dr Barbara Harmes and Sandra Cochrane from the University of Southern Queensland, Australia for providing help with language correction and proofreading.

This work was supported by the University of Southern Queensland, QLD, Australia (RTP Stipend Scholarship programme).

Statements and Declarations

Funding: This study was funded by the University of Southern Queensland, QLD, Australia (RTP Stipend Scholarship programme).

Conflicts of interest/Competing interests: The authors declare that they have no conflict of interest.

Author's contributions: Lakshika Weerasundara – Conceptualisation, Methodology, Validation, Formal analysis, Investigation, Resources, Data curation, Writing-Original draft, Writing - Review & editing, Visualisation. Prasanna Kumarathilaka – Formal analysis, Data curation. Alla Marchuk - Formal analysis, Validation, Resources, Supervision. Jochen

Bundschuh – Conceptualisation, Resources, Writing - Review & editing, Supervision, Project administration.

References

- Akl, Z.F., Zaki, E.G. and ElSaeed, S.M., 2021. Green Hydrogel-Biochar Composite for Enhanced Adsorption of Uranium. *ACS omega* 6(50), 34193-34205.
- Al-Ghouti, M.A. and Da'ana, D.A., 2020. Guidelines for the use and interpretation of adsorption isotherm models: a review. *Journal of Hazardous Materials* 393, 122383.
- Asadi, N., Pazoki-Toroudi, H., Del Bakhshayesh, A.R., Akbarzadeh, A., Davaran, S. and Annabi, N., 2021. Multifunctional hydrogels for wound healing: Special focus on biomacromolecular based hydrogels. *International Journal of Biological Macromolecules* 170, 728-750.
- Bakatula, E.N., Richard, D., Neculita, C.M. and Zagury, G.J., 2018. Determination of point of zero charge of natural organic materials. *Environmental Science and Pollution Research* 25(8), 7823-7833.
- Bandara, T., Herath, I., Kumarathilaka, P., Seneviratne, M., Seneviratne, G., Rajakaruna, N., Vithanage, M. and Ok, Y.S., 2017. Role of woody biochar and fungal-bacterial co-inoculation on enzyme activity and metal immobilization in serpentine soil. *Journal of Soils and Sediments* 17(3), 665-673.
- Beamson, G., 1992. High resolution XPS of organic polymers. The Scienta ESCA 300 Database.
- Bibi, S., Kamran, M.A., Sultana, J. and Farooqi, A., 2017. Occurrence and methods to remove arsenic and fluoride contamination in water. *Environmental Chemistry Letters* 15(1), 125-149.
- Das, S.K. and Ghosh, G.K., 2022. Hydrogel-biochar composite for agricultural applications and controlled release fertilizer: A step towards pollution free environment. *Energy J* 242, 122977.
- Foo, K.Y. and Hameed, B.H., 2010. Insights into the modeling of adsorption isotherm systems. *Chemical Engineering Journal* 156(1), 2-10.
- Herath, I., Kumarathilaka, P., Al-Wabel, M.I., Abduljabbar, A., Ahmad, M., Usman, A.R. and Vithanage, M., 2016. Mechanistic modeling of glyphosate interaction with rice husk derived engineered biochar. *Microporous and Mesoporous Materials* 225, 280-288.

- Ho, Y. and McKay, G., 1998. A comparison of chemisorption kinetic models applied to pollutant removal on various sorbents. *Process Safety and Environmental Protection* 76(4), 332-340.
- Ho, Y., Porter, J. and McKay, G., 2002. Equilibrium isotherm studies for the sorption of divalent metal ions onto peat: copper, nickel and lead single component systems. *Water Air and Soil Pollution* 141(1), 1-33.
- Ji, M., Wang, X., Usman, M., Liu, F., Dan, Y., Zhou, L., Campanaro, S., Luo, G. and Sang, W., 2022. Effects of different feedstocks-based biochar on soil remediation: A review. *Environmental Pollution* 294, 118655.
- Karakoyun, N., Kubilay, S., Aktas, N., Turhan, O., Kasimoglu, M., Yilmaz, S. and Sahiner, N., 2011. Hydrogel–Biochar composites for effective organic contaminant removal from aqueous media. *Desalination* 280(1-3), 319-325.
- Kumarathilaka, P., Bundschuh, J., Seneweera, S., Marchuk, A. and Ok, Y.S., 2021. Iron modification to silicon-rich biochar and alternative water management to decrease arsenic accumulation in rice (*Oryza sativa* L.). *Environmental Pollution* 286, 117661.
- Liang, Y., He, J. and Guo, B., 2021. Functional hydrogels as wound dressing to enhance wound healing. *ACS nano* 15(8), 12687-12722.
- Mandal, A., Clegg, J.R., Anselmo, A.C. and Mitragotri, S., 2020. Hydrogels in the clinic. *Bioengineering and Translational Medicine* 5(2), e10158.
- Mayakaduwa, S., Kumarathilaka, P., Herath, I., Ahmad, M., Al-Wabel, M., Ok, Y.S., Usman, A., Abduljabbar, A. and Vithanage, M., 2016. Equilibrium and kinetic mechanisms of woody biochar on aqueous glyphosate removal. *Chemosphere* 144, 2516-2521.
- Mohtasebi, A., Chowdhury, T., Hsu, L.H., Biesinger, M.C. and Kruse, P., 2016. Interfacial charge transfer between phenyl-capped aniline tetramer films and iron oxide surfaces. *Journal of Physical Chemistry C* 120(51), 29248-29263.
- Nakhjiri, M.T., Marandi, G.B. and Kurdtabar, M., 2021. Preparation of magnetic double network nanocomposite hydrogel for adsorption of phenol and p-nitrophenol from aqueous solution. *Journal of Environmental Chemical Engineering* 9(2), 105039.
- Norsuraya, S., Fazlena, H. and Norhasyimi, R., 2016. Sugarcane bagasse as a renewable source of silica to synthesize Santa Barbara Amorphous-15 (SBA-15). *Procedia Engineering* 148, 839-846.
- Peppas, N.A. and Hoffman, A.S. (2020) *Biomaterials Science* pp. 153-166, Elsevier.
- Ren, J., Kong, W. and Sun, R., 2014. Preparation of sugarcane bagasse/poly (acrylic acid-co-acrylamide) hydrogels and their application. *Bioresources* 9(2), 3290-3303.

- Sanyang, M., Ghani, W.A.W.A.K., Idris, A. and Ahmad, M.B., 2016. Hydrogel biochar composite for arsenic removal from wastewater. *Desalination and Water Treatment* 57(8), 3674-3688.
- Simeng, L. and Chen, G., 2018. Using hydrogel-biochar composites for enhanced cadmium removal from aqueous media. *Material Science & Engineering* 2(6), 294-298.
- Tanan, W., Panichpakdee, J. and Saengsuwan, S., 2019. Novel biodegradable hydrogel based on natural polymers: Synthesis, characterization, swelling/reswelling and biodegradability. *European Polymer Journal* 112, 678-687.
- Wagner, C., Naumkin, A., Kraut-Vass, A., Allison, J., Powell, C. and Rumble Jr, J., 2003. NIST standard reference database 20, Version 3.4 (Web version). National Institute of Standards and Technology: Gaithersburg, MD 20899.
- Weerasundara, L., Gabriele, B., Figoli, A., Ok, Y.-S. and Bundschuh, J., 2021a. Hydrogels: Novel materials for contaminant removal in water—A review. *Critical Reviews in Environmental Science and Technology* 51(17), 1970-2014.
- Weerasundara, L., Ok, Y.-S. and Bundschuh, J., 2021b. Selective removal of arsenic in water: a critical review. *Environmental Pollution* 268, 115668.
- Wu, J., Huang, D., Liu, X., Meng, J., Tang, C. and Xu, J., 2018. Remediation of As (III) and Cd (II) co-contamination and its mechanism in aqueous systems by a novel calcium-based magnetic biochar. *Journal of Hazardous Materials* 348, 10-19.
- Zhang, L. and Guan, Y., 2022. Microbial investigations of new hydrogel-biochar composites as soil amendments for simultaneous nitrogen-use improvement and heavy metal immobilization. *Journal of Hazardous Materials* 424, 127154.
- Zhao, Q., Sun, J., Lin, Y. and Zhou, Q., 2010. Study of the properties of hydrolyzed polyacrylamide hydrogels with various pore structures and rapid pH-sensitivities. *Reactive and Functional Polymers* 70(9), 602-609.

4.3. Concluding remarks

Sugarcane bagasse biochar hydrogel was a successful answer to the classic drawbacks of traditional adsorbent materials as the hydrogel does not require additional energy to separate from water after the treatment. Further, the same hydrogel can be regenerated and re-used for As(V) removal several times. The As(V) adsorption by SUBC hydrogel was pH dependent where the highest adsorption was recorded in the range of pH 6-7. Within the pH 6-7 range, the hydrogel surface became positively charged due to protonation of the $-NH_2$ and $-CO$ groups in the polymer chain, and the positive surface attracted As(V) oxyanions. This is an advantageous factor because it is also the pH range for most natural water and, as a result, SUBC can be used directly in As(V) contaminated natural water. The use of swelled SUBC hydrogel for As(V) removal was found to be more efficient than the direct use of dry hydrogel. The hydrogels are three-dimension structured, and this tended to increase pore volumes and the unit surface area in the aqueous environments. Once the SUBC hydrogel became fully swollen, it acted with its maximum capacity to adsorb As(V). The chemisorption and physisorption adsorption mechanisms that have been proposed for the adsorption of As(V) into SUBC hydrogel is based on kinetic and isotherm data.

CHAPTER 5: PAPER 5 – ASSESSMENT AND OPTIMISATION OF As(V) ADSORPTION ON HYDROGEL COMPOSITE INTEGRATING CHITOSAN-POLYVINYL ALCOHOL AND Fe₃O₄ NANOPARTICLES AND EVALUATION OF THEIR REGENERATION AND RE-USABLE CAPABILITIES IN AQUEOUS MEDIA

5.1. Introduction

Fe₃O₄ nanoparticles incorporated with modified chitosan-polyvinyl alcohol hydrogel was developed for As(V) removal in water. This hydrogel does not dissolve or dissociate in water so an additional filtration step is not necessary to separate the hydrogel from water. Four chitosan-Fe₃O₄ (ChFe) hydrogel types were developed based on chitosan:Fe₃O₄ ratios of 1:0, 1:1, 1:0.5 and 1:0.25. Batch sorption experiments were conducted with different pH, dosages, kinetics and isotherms. The exhausted ChFe hydrogels were evaluated for their regeneration and re-use capability with different acids and bases. The hydrogel showed reusability features that enable it to overcome one of the common drawbacks of traditional adsorbents.

This article cannot be displayed due to copyright restrictions. See the article link in the Related Outputs field on the item record for possible access.

5.3. Concluding remarks

A modified chitosan hydrogel was developed through the integration with Fe_3O_4 nanoparticles to remove $\text{As}(\text{V})$ from water. In addition to efficient $\text{As}(\text{V})$ removal, two major objectives were considered for the ChFe hydrogel composite. First, easy removal of adsorbent from water after the $\text{As}(\text{V})$ removal without high-tech or energy requirements. Second, reusability to minimise the waste load. The material preparation was successful, and the solution pH affected the adsorption capacity. The highest adsorption was recorded at pH 4 and, with this increment of solution pH, the adsorption capacity declined. Swollen ChFe hydrogel was more efficient for $\text{As}(\text{V})$ removal than dry hydrogel. The chemisorption adsorption mechanisms have been proposed for the adsorption of $\text{As}(\text{V})$ into the ChFe hydrogel composite based on kinetic and isotherm data. 0.1 M CH_3COOH is a successful solution for the regeneration of the ChFe hydrogel composite, and it further increases the adsorption capacity of the ChFe hydrogel composite for $\text{As}(\text{V})$.

CHAPTER 6: PAPER 6 – Cu(II)-LOADED CHITOSAN-POLYVINYL ALCOHOL AND Fe₃O₄ NANOPARTICLE INTEGRATED HYDROGEL COMPOSITE FOR ENHANCED AND EFFICIENT As(V) ADSORPTION

6.1. Introduction

Use of metal ions to remove As in water has gained interest due to their high As adsorption capacities. A chitosan-PVA hydrogel was integrated with Fe₃O₄ nanoparticles, and the material showed successful As(V) removal capacities. However, the material is still open for more modification since there are several functional groups that provide binding agents for more metal ions. Cu(II) is a strong Lewis-acid and several works of literature have been reported on the use of Cu(II) ions to modify the adsorbent materials to enhance the As adsorption capacity. Considering this the ChFe hydrogel composite was incorporated with Cu(II) ions to achieve further enhanced As(V) removal in water. The loaded Cu(II) ions could bind with -NH₂ groups of the chitosan structure and hold three hydroxyl groups. Each of these hydroxyl groups provided an active site for As(V) sorption. Therefore, each Cu bound site within the hydrogel structure created three potential binding sites for As(V).

Cu(II)-loaded chitosan-polyvinyl alcohol and Fe₃O₄ nanoparticle integrated hydrogel composite for enhanced and efficient As(V) adsorption

Lakshika Weerasundara^a, Prasanna Kumarathilaka^a, Alla Marchuk^b Jochen Bundschuh^{*a,c}

^a*School of Civil Engineering and Surveying, Faculty of Health, Engineering and Sciences, University of Southern Queensland, West Street, Toowoomba, Queensland, 4350, Australia*

^b*Institute for Life Sciences and the Environment, University of Southern Queensland, West Street, Toowoomba, Queensland, 4350, Australia*

^c*Doctoral Program in Science, Technology, Environment, and Mathematics, Department of Earth and Environmental Sciences, National Chung Cheng University, 168 University Rd., Min-Hsiung, Chiayi County, 62102, Taiwan*

*Corresponding author

E-mail address: jochen.bundschuh@usq.edu.au (Jochen Bundschuh), School of Civil Engineering and Surveying, Faculty of Health, Engineering and Sciences, University of Southern Queensland, Toowoomba, Queensland 4350, Australia. Doctoral Program in Science, Technology, Environment, and Mathematics, Department of Earth and Environmental Sciences, National Chung Cheng University, 168 University Rd., Min-Hsiung, Chiayi County, 62102, Taiwan.

Abstract

To further enhance the arsenic (V) (As(V)) adsorption capacity from water, a modified chitosan Fe₃O₄ nanoparticles (ChFe) hydrogel was re-modified by loading Cu(II) ions onto the chitosan structure. Kinetic and isotherm batch sorption experiments, and regeneration and re-use experiments were then undertaken. The Cu(II) loaded chitosan Fe₃O₄ nanoparticles (ChFe-Cu) hydrogel showed 6.8 mg/g adsorption capacity at the initial adsorption cycle. The adsorption was pH dependant, and the highest adsorption was in the range of pH 3-4. The adsorption capacity gradually decreased with an increasing solution pH. Within the pH 4 range, the hydrogel surface became positively charged due to protonation of the -NH₂ and -OH groups in the polymer chain, and the positive surface attracted H₂AsO₄⁻ and HAsO₄²⁻ oxyanions. The experimental kinetic and isotherm data suggest a chemisorption mechanism onto a heterogeneous surface. The Cu(II) loading enhanced the As(V) adsorption capacity by increasing the active sites for As(V). The loaded Cu(II) ions bound with the chitosan structure's -NH₂ groups and held three hydroxyl groups. Each of these hydroxyl groups provided an active site for As(V) sorption. Electrostatic attractions with -NH₃⁺ and -OH₂⁺, ligand-exchange inner-sphere complexes formation and bidentate corner-sharing (²C) and bidentate edge-sharing (²E) trimetric surface complexes formation has been proposed as the adsorption mechanism of As(V) into ChFe-Cu hydrogel. 0.1 M CH₃COOH was used for the regeneration of the ChFe-Cu hydrogel, and it offered a successful re-usable capability where the second to fourth adsorption showed 50% (3.4 mg/g) of As(V) removal in each cycle. The cumulative adsorption capacity of ChFe-Cu hydrogel composite for four adsorption cycles was 17 mg/g. This modified hydrogel composite expanded its adsorption horizons with an innovative aspect. Since the Cu(II) loading did not adversely affect on As(V) adsorption, the ChFe hydrogel can be used for adsorption of Cu(II) and then, without further processing, be used for As(V) adsorption in water. The overall process overcomes the classic drawbacks of traditional adsorbent materials with significant adsorption capacity, easy water-adsorption separation, very tiny size when dried making storage and disposal easy, reusability, and ability to remove several contaminants simultaneously or separately. This fact will enhance the environmental and economical sustainability giving the material global advantage in terms of water safety.

Keywords: Arsenic(V), hydrogel, Cu(II), chitosan, Fe₃O₄, nanoparticles, adsorption

1. Introduction

Adsorption is a well-known method for the removal of contaminants from water. It is an operation involving a liquid and solid phase. In the liquid phase, the dissolved contaminants are transferred to the solid phase, creating the adsorbent. Adsorption has been considered an effective method for water purification over the last decades due to several advantages such as low cost, high efficiency, easy operation, easy implementation, and the availability of various materials as potential adsorbents. Adsorption has potential application over a vast range (ng/L to mg/L). However, most adsorbent materials have several drawbacks such as requiring additional energy to separate the adsorbate from water after the adsorption process, inability to be regenerated or re-used, and the failure of a single adsorbent to remove more than one contaminant. Therefore, to achieve sustainable outcomes, the adsorbent materials should overcome the abovementioned drawbacks in an efficient manner.

Arsenic (As) in water originates from a variety of sources: geochemical reactions, industrial waste discharges and agricultural use of As-containing pesticides (Bundschuh et al., 2022; Kumarathilaka et al., 2020). Arsenic can be found in water in different oxidation states such as +5, +3, 0 and -3 with the influence of different redox conditions (Bundschuh et al., 2021; Weerasundara et al., 2021). A significant interest in As arises due to its carcinogenic nature. Acute and chronic As poisoning has been reported in several parts of the world requiring potential mitigation methods (Kumarathilaka et al., 2021d; Morales-Simfors and Bundschuh, 2021). Arsenic removal by adsorption has gained significant interest over the last decades. Efficient As removal by adsorption depends on various factors such as pH, availability of functional groups for chemical adsorption, surface characteristics for physical and chemical adsorptions, cost of production, cost of operation, the requirement of additional adsorbent-water separation techniques etc. However, simultaneous optimisation of all these factors is a challenging or even impossible task. Despite this, if the type of material used as the adsorbent is available for modification, the above task can be achieved.

In water, As can be found as H_3AsO_4 , H_2AsO_4^- , HAsO_4^{2-} , H_3AsO_3 , H_2AsO_3^- , and HAsO_3^{2-} . Since most of these are oxyanions, Lewis-Acid-Base interactions and electrostatic interactions can be easily employed as adsorption mechanisms if there are compatible functional groups. As(V) oxyanions can be considered strong anionic ligands (Lewis-base) that can be removed through both Lewis-acid and electrostatic interactions. Therefore, to enhance the As(V) removal capacity of a potential adsorbent, the above interaction can be used to modify the hydrogel.

Metal ions are considered to be Lewis-acids that can be used to modify any adsorbent to achieve enhanced As(V) removal if the adsorbent material is available for modification. Fe(III) and Cu(II) have been used to remove As(V) from water through adsorption (Kumarathilaka et al., 2021b; Yan et al., 2018). According to the Irving Williams order, Cu(II) is a much stronger Lewis-acid than Fe(III) (An et al., 2005). Several works of literature have reported the use of Cu(II) ions to modify adsorbent materials to enhance As adsorption capacity (An et al., 2010; An et al., 2005; Luan et al., 2019; Ramana and Sengupta, 1992; Wu et al., 2019; Wu et al., 2018; Yamani et al., 2016; Zhao and Sengupta, 1998).

Chitosan is a well-known organic waste product from the shellfish industry. Its unique molecular characteristics and bio-degradable nature have led to use as an adsorbent in different ways. Chitosan-based hydrogel is one of the most promising ways to remove several contaminants including As (Weerasundara et al., 2021). The presence of amide groups and hydroxyl groups in the chitosan structure make it a favourable material for As(V) adsorption. In our previous study, we developed and modified a chitosan based hydrogel with the integration of Fe₃O₄ nanoparticles (ChFe hydrogel composite) to remove As(V) from water. Our study showed around 15 mg/g adsorption capacity over five adsorption cycles (Weerasundara et al., 2022).

The present study focuses on the re-modification of the modified ChFe hydrogel composite by loading Cu(II) to further increase the adsorption capacity. The ChFe hydrogel has an amide group which has nitrogen as an electron donor atom. The Cu(II) ions interact with this nitrogen atom in the amide group and a Cu(II) integrated ChFe hydrogel composite was obtained. As nitrogen atoms are predominantly in their free base form at pH > 3, the positive charges of loaded Cu(II) ions are still available to interact with anions in the aqueous phase. Moreover, since only a fraction of the copper's six coordination bonding sites is consumed for binding copper to the polymer surface, the immobilised Cu(II) ions remain capable of complexing with target ligands from the aqueous phase. Considering this as the null hypothesis: the Cu(II) loaded ChFe hydrogel composite (ChFe-Cu) hydrogel was synthesised and optimised for As(V) adsorption in aqueous media. The present study focused on the synthesis of a novel material as well as the possibility of overcoming the classic drawbacks of traditional adsorbent materials. This adsorbate will facilitate easy water-adsorption separation after completion of the adsorption process to a very tiny size when dried which makes for easy storage and disposal, reusability, and the ability to remove several contaminants simultaneously or separately.

2. Materials and Methods

2.1. Materials

FeCl₃.6H₂O, FeCl₂.4H₂O, trisodium citrate, chitosan (from shrimp shells, ≥75% deacetylated), poly-vinyl alcohol (PVA) and Cu(II) acetate monohydrate were purchased from Sigma-Aldrich Pty Ltd. A stock solution (1000 mg/L) of As(V) was prepared by dissolving sodium arsenate dibasic heptahydrate (Na₂HAsO₄.H₂O) in distilled water. This stock solution was used for the preparation of the As(V) solutions with required concentrations, and the solutions were freshly prepared for each study.

2.2. Laboratory analysis

After every experiment, samples were separated from the hydrogels and the solutions were filtered through a glass fibre filtration technique (0.6 μm), and the remaining As(V) concentrations were measured using Inductively Coupled Plasma Mass Spectrometry (ICP-MS) (PerkinElmer NexION™ 300X). Calibration blanks, laboratory reagent blanks and calibration standards were measured as part of the quality assurance and quality control measures. Experiments were conducted and analysed in triplicates. Calibration curves were set up and ensured that the residual mean square (R^2) was greater than or equal to 0.98. The calibration blank was de-ionised distilled water used to prepare the calibration standards.

2.3. Preparation of Fe₃O₄ nanoparticles

The Fe₃O₄ nanoparticle preparation was done according to the method described in Yan et al. (2017). In brief, 5.4 g of FeCl₃.6H₂O was dissolved in <10 mL of distilled water. 2.0 g of FeCl₂.4H₂O was also dissolved in <10 mL of distilled water separately. After a complete dissolve, two solutions were mixed and made the final volume as 25 mL with distilled water. Then N₂ was purged through the solution for 5 min to remove the dissolved O₂ from the solution. While continuing the N₂ purging, 2.0 g of trisodium citrate was added to the solution to stabilise the precipitation within the solution. 12.5 mL of aqueous ammonia was added to the solution drop by drop under vigorous mechanical stirring and N₂ purging. N₂ purging and stirring continued for the next 3 h. After 3 h, the solution was dialysed with 14 mm dialysis tubing in deionised water to remove the impurity ions. This solution was frozen at minus 70 °C for about 72 h (Snijders Evosafe, VF-620) and dried in a freeze dryer (Martin Christ, Alpha 2-4 LDPlus). The final Fe₃O₄ nanoparticle products were stored in airtight containers until use.

2.4. Synthesis of ChFe-Cu hydrogel composite

The synthesis of the ChFe-Cu hydrogel composite was undertaken based on the methods described in Jin and Bai (2002), Wu et al. (2019) and Yamani et al. (2016), and the procedures were combined and slightly modified. First, Cu(II) acetate was dissolved in 100 mL of acetic acid (w/w). The weight ratio was selected as 1:20 chitosan:Cu(II) ions. After dissolving completely, 4.2 g of chitosan flakes was added into the solution. The solution was placed in a thermostatic water bath shaker at 120 rpm and 60 °C for 12 h. After 12 h, if the solution still had raw chitosan, shaking was continued for another 6 h. 100 mL of PVA solution was prepared by dissolving 8.5 g of PVA using a magnetic stirrer at 800 rpm and 70 °C. The chitosan-Cu and PVA solutions were then mixed on a magnetic stirrer at 800 rpm, 70 °C. 2.1 g of Fe₃O₄ nanoparticles were added to the gel blend and shaking continued for 48 h at 800 rpm and 70 °C. After 48 h, the solution was stirred again for another 48 h at room temperature. This solution was then introduced dropwise to a solution of 0.1 M NaOH in methanol while shaking in a mechanical shaker to form the hydrogel beads. The shaking continued for another 30 mins after the hydrogel beads' formation. The hydrogel beads were then separated from the NaOH-methanol solution and allowed to partially air-dry. The hydrogel beads were thoroughly washed in distilled water until a neutral pH was obtained. The washed hydrogel beads were air-dried for 24 h and stored in an airtight container until use.

2.5. Characterisation of ChFe-Cu hydrogel composite

2.5.1. Swelling percentage

The swelling percentage was measured by immersing the ChFe-Cu hydrogel in distilled water, and the weight increase was recorded at room temperature. The first measurement was recorded at 0.5 h and then once an hour until 6 h. Then the weight was recorded once every 24 h until the weight gain became nearly constant. The percentage of swelling was calculated using equation 1.

$$\text{Swelling \%} = \frac{W_{\text{swollen}} - W_{\text{dry}}}{W_{\text{dry}}} \times 100 \quad (1)$$

where W_{swollen} and W_{dry} are the weight of the swollen and dry samples, respectively.

2.5.2. Point of zero charge

To determine the point of zero charge (PZC) of the ChFe-Cu hydrogel composite the salt-addition method was employed. The 0.05 g of ChFe-Cu hydrogel composite sample was introduced to 10 mL of 0.1 M NaNO₃ solution. Separate samples were prepared for each pH and the pH of the samples was adjusted as 2, 3, 4, 5, 6, 7, 8, 9 and 10 (± 0.1) using 0.1 M HNO₃ and 0.1 M NaOH solutions. Samples were shaken for 24 h in a shaker at room temperature at 200 rpm (Orbital shaker OM15, RATEK). Initial pH (pH_i) and the final pH (pH_f) were measured and the PZC was obtained from the plot of ΔpH (pH_f – pH_i) against pH_i (Bakatula et al., 2018).

2.5.3. Physical and chemical characterisation

Fourier Transform Infrared Spectroscopy (FTIR) analysis, Scanning Electron Microscopy (SEM) (JCM-6000, JEOL) analysis, X-ray Photoelectron Spectrometer (XPS) analysis (Kratos Axis Ultra XPS, Centre for Microscopy and Microanalysis, The University of Queensland) were conducted for the identification of functional groups, chemical status and surface morphology of the ChFe-Cu hydrogel composite.

2.6. Batch sorption experiments for ChFe-Cu hydrogel composite

Kinetic and isotherm experiments were conducted. For kinetic experiments a 5 mg/L As(V) was used at 1 g/L ChFe-Cu dosage and the samples were taken at predetermined time intervals from 0.5 - 72 h. Batch isotherm studies were carried out in the As(V) concentration range of 0.025 - 7 mg/L. An equilibrium time of 24 h was chosen based on the kinetic experiment. The amount of As(V) retained in the adsorbent phase was calculated using equation 2 (Mayakaduwa et al., 2016).

$$q_e = [C_0 - C_e]VM^{-1} \quad (2)$$

where q_e is the As(V) amount adsorbed on ChFe-Cu hydrogel (mg/g), C_0 and C_e are the initial and equilibrium As(V) concentrations (mg/L), V is the solution volume (L) and M is the hydrogel mass (g).

2.7. Experimental data modeling

For the kinetic data, five different non-linear kinetic models, namely the pseudo-first order, pseudo-second order, Elovich, parabolic diffusion and power function, were applied.

Kinetic models give ideas about the rate limiting factors of the adsorption process as well as the mechanism. In an adsorption process there are three basic steps. The first step is the external mass transfer of the adsorbate to the external surface of the adsorbent. Then the internal diffusion occurs on the sorption sites, and finally, the adsorption occurs (Largitte and Pasquier, 2016). With the surface characteristics, availability of functional groups and types of the adsorbate, the adsorption rate is determined. Therefore, with the adsorption rate of a particular adsorbent, the adsorption mechanism can be decided. And for that, the above models and their mathematical equations are used (Wang and Guo, 2020).

In the pseudo-first order, it is assumed that adsorption occurs on the adsorbent surface as a monolayer adsorption process. Therefore, the basic and rate limiting step is the external mass transfer or internal diffusion. Therefore, the pseudo-first order describes the physisorption mechanism between the adsorbate and the adsorbent (Li, 1999). In the pseudo-second order the adsorption occurred with external mass transfer, internal diffusion and adsorption into active sites. Therefore, the amount of active sites decides the rate of the adsorption process. Therefore, the adsorption into active sites is the rate controlling step. With that, the pseudo-second order assumes that the adsorption process is a chemical sorption process where the valance forces are involved through sharing or exchanging of electrons between the adsorbent and the adsorbate. The Elovich model describes the chemical adsorption mechanism onto a heterogeneous adsorbent. Further, the model assumes that the activation energy increases with adsorption time. The parabolic diffusion model is used to decide whether the rate limiting factor is a diffusion-controlled step. The power function describes a homogeneous chemisorption mechanism.

The adsorption isotherms describe how the adsorbates in water interact with adsorbent material and help to explain the adsorption mechanisms. The Langmuir adsorption isotherm model assumes monolayer adsorption which means the adsorption occurs in a single layer with one molecule of thickness. Further, the Langmuir model explains that adsorption occurs at a fixed number of adsorption sites. These adsorption sites are identical to one another, and no lateral interactions are formed. The Freundlich isotherm model is used to describe a multilayer adsorption process onto a heterogeneous surface with a chemisorption mechanism (Foo and Hameed, 2010). The Dubinin-Radushkevich model is a semiempirical equation in which the adsorption of this model follows the mechanism of pore filling. This model assumes that a multilayer character, which involves Van der Waal's forces, can be applied to the physical adsorption processes (Al-Ghouti and Da'ana, 2020). Isotherm and kinetic modeling and statistical graphing were done with the Microcal Origin software (Version 6).

2.8. Desorption and re-adsorption experiment for exhausted hydrogel composites

The ChFe-Cu hydrogel samples that were used for As(V) adsorption then underwent four adsorption-desorption experiments with a 0.1 M CH₃COOH (shaken for 6 h) solution to assess the recyclability and reusability of ChFe-Cu hydrogel composite.

3. Results and discussion

3.1. ChFe-Cu hydrogel composite synthesis and proposed structure

The synthesis of the ChFe hydrogel and the structure formation is well described in our previous work (Weerasundara et al., 2022). Briefly, ChFe-Cu synthesis occurs through a gel blending process. In the hydrogel the chitosan acts as the backbone of the structure. The PVA binds with chitosan via -OH groups and the PVA acts as the binding agent or a crosslinker of the 3D structure of the hydrogel. The Fe₃O₄ nanoparticles bind through -OH bonds and Fe-NH₂ bonds to the hydrogel structure.

The novel component in the ChFe-Cu hydrogel composite is Cu(II) which generally binds with the chitosan via the Lewis-acid-based interaction. The functional group-containing nitrogen as electron donor atoms is employed as the metal hosting site. Since the nitrogen atoms are predominantly in their free base form (at pH>3) the positive charges of loaded Cu(II) ions remain available to interact with anions in the aqueous phase. Moreover, since only a fraction of the copper's six coordination bonding sites is consumed to bind it to the polymer surface, the immobilised Cu(II) ions remain capable of complexing with target ligands from the aqueous phase. Consequently, the Cu(II) loaded ChFe-Cu hydrogel composite can interact with As(V) oxyanions in the water through concurrent Lewis-acid-base interaction and electrostatic interactions. Further, the Cu(II) can connect two parallel chitosan chains together through -NH₂ functional groups and act as a cross-linker (Lü et al., 2008). The proposed structure of the ChFe-Cu hydrogel composite is illustrated in Figure 1.

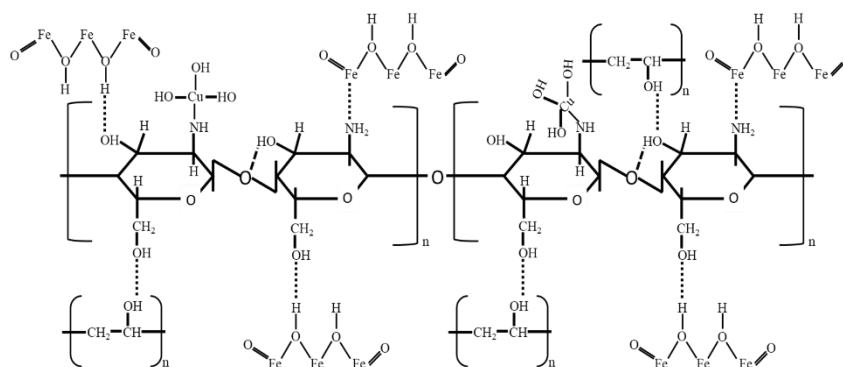


Figure 1 Proposed structure of ChFe-Cu hydrogel composite

3.2. Characterisation of ChFe-Cu hydrogel composite

3.2.1. Swelling behaviour of ChFe-Cu hydrogel composite

A significant characteristic behaviour of hydrogels is their ability to swell in the presence of water and shrink when drying. The factors affecting this feature are the hydrophilicity of the hydrogel backbone and cross-link density. The swelling capacity directly affects the As(V) adsorption on the ChFe-Cu hydrogel as the availability of the functional groups within the hydrogel depends on the swelling capacity of the hydrogel. Figure 2(a) illustrates the swelling percentage of the ChFe-Cu hydrogel composite. There is a rapid increase in swelling up to 6 h. After 6 h the swelling percentage increases at a slow rate and, when it comes to 48 h, it is in its maximum swollen status.

The maximum swollen percentage of ChFe-Cu hydrogel composite is around 263%. To compare the changes, Figure 2(b) illustrates the swelling capacity of ChFe hydrogel composite and pure chitosan hydrogel composite (Weerasundara et al., 2022). The maximum swelling percentages of ChFe hydrogel composite and pure chitosan hydrogel are 482 and 293% respectively. This shows that the ChFe-Cu hydrogel has a lower swelling percentage compared to both the ChFe hydrogel composite and pure hydrogel. This is due to the cross-linking effect of the Cu(II) ions between the parallel chitosan chains of the ChFe-Cu hydrogel. This means the cross-link density of ChFe-Cu hydrogel composite is higher than the ChFe hydrogel composite. Generally, the increasing cross-link density decreases the swelling capacity and may be effect on adsorption capacity. However, here the Cu(II) acts not only as a cross-linker, but also as a possible binding site for the As(V) oxyanions. Therefore, the lower swelling capacity can be expected but the adsorption capacity may not be affected in the same way. This fact can be confirmed with the adsorption experiments in the following sections (Sections 3.3 and 3.4).

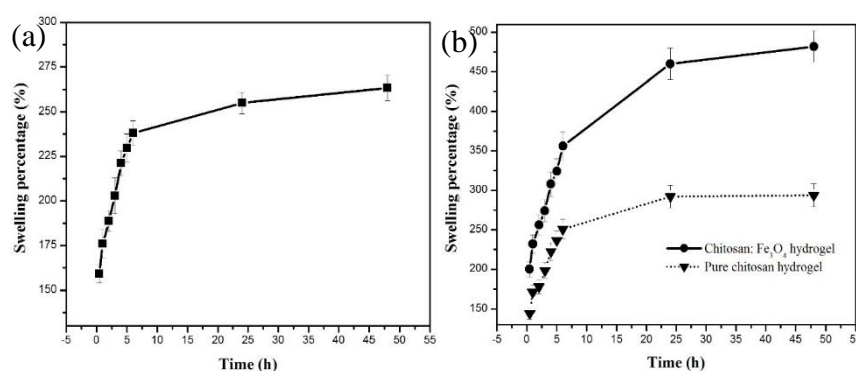


Figure 2 (a) Swelling percentage of ChFe-Cu hydrogel composite over the time, (b) Swelling percentage of ChFe hydrogel composite and pure chitosan hydrogel (Weerasundara et al., 2022)

3.2.2. Point of zero charge for ChFe-Cu hydrogel composite

Depending on the pH of the solution, the surface of the absorbent material can bear net negative, net positive, or no charge. Adsorption of the As(V) occurred via As(V) oxyanions and, therefore, it is important to know when the adsorbent material holds a net positive charge. The PZC is a pH dependant measurement, and it indicates the pH value that is required to give a zero net surface charge. And when the $pHPZC < pH$ of the solution, the surface of the material will be negatively charged, whereas when the $pHPZC > pH$ of the solution, the surface of the material will be positively charged (Herath et al., 2016). Figure 3 shows that when the solution pH is at 6, the net surface charge of the ChFe-Cu hydrogel is zero. Therefore, when the solution pH is higher than 6, the surface charge of the ChFe-Cu hydrogel is negative and at a higher solution pH than 6, and the surface charge of the ChFe-Cu hydrogel composite is positive. Considering the As(V) adsorption, the best pH range is <6 since the As(V) adsorption occurs through $H_2AsO_4^-$ and $HAsO_4^{2-}$ oxyanions.

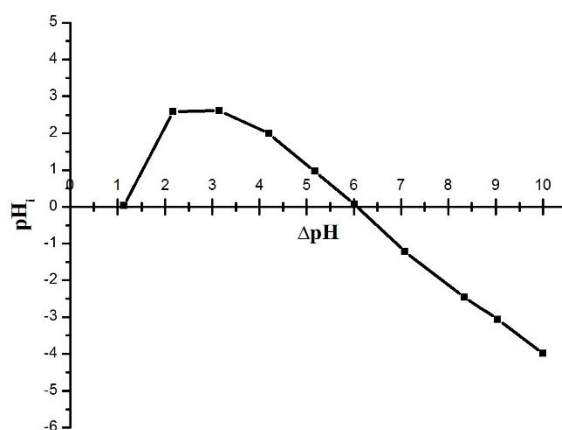


Figure 3 Plot of ΔpH vs pH_i for salt addition method to determine the PZC of ChFe-Cu hydrogel composite

3.2.3. Physical and chemical characterisation of ChFe-Cu hydrogel composite

The macrographs and SEM micrographs of the ChFe-Cu hydrogel composite are shown in Figure 4. The ChFe-Cu hydrogel has a rough outer surface. This surface morphology shows a significant difference to the surface morphology of ChFe hydrogel composite (Weerasundara et al., 2022). The surface roughness increased to a greater extent with Cu(II) loading. The Cu(II) loading has been affected on the cross-linking of the ChFe-Cu hydrogel composite and

this is a reason for increasing the roughness of the surface. The increased cross-link density may cause a shrinking effect of the hydrogel and make the rough surface.

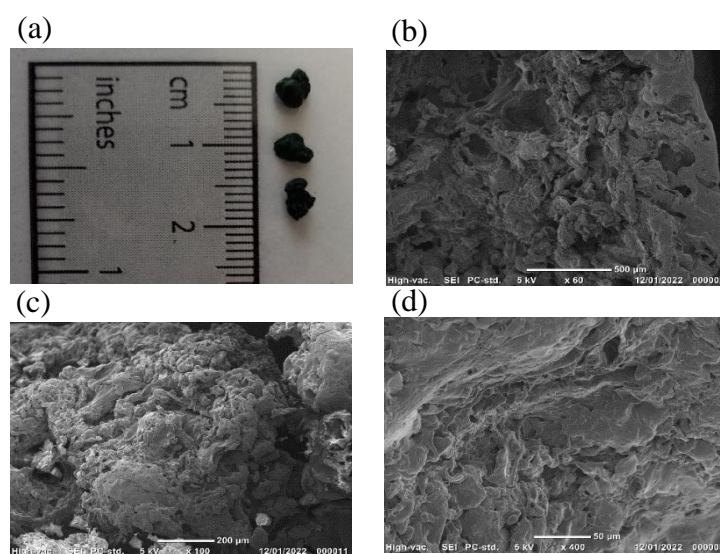


Figure 4 (a) Image of ChFe-Cu hydrogel composites, (b)-(d) SEM images of ChFe-Cu hydrogel composite

The FTIR spectra of the ChFe-Cu hydrogel composite is shown in Figure 5(a). For comparison, Figure 5(b) shows the FTIR spectra of the ChFe hydrogel composite and pure chitosan hydrogel (Weerasundara et al., 2022). As can be seen in Figure 5(a), the broad absorption band at 3278 cm^{-1} is attributed to the stretching vibration of -OH groups in the chitosan and PVA. The absorption peak at 2908 cm^{-1} in the ChFe-Cu hydrogel composite describe -CH₃ groups in the chitosan and PVA. This peak shows reduced band intensity compared to ChFe hydrogel. The absorption peak at 1705 cm^{-1} in the ChFe-Cu hydrogel composite is assigned to the C-H bending vibration and amide C=O stretching vibration in the chitosan. The absorption peak at 1643 cm^{-1} in the ChFe-Cu hydrogel composite belongs to the N-H bending in chitosan. This peak also showed significant band reduction compared to the ChFe hydrogel. The -NH₃ groups are the binding sites for Cu(II) and, therefore, most of the -NH₂ groups are employed by Cu(II). The amide II bands of chitosan which is C-N stretching coupled to N-H bending can be found around 1550 cm^{-1} in the ChFe-Cu hydrogel composite. The absorption peak at 1411 cm^{-1} in the ChFe-Cu hydrogel composite is attributed to the C-N bending in the chitosan. The peak around 1373 cm^{-1} in the ChFe-Cu hydrogel composite describes the O-H bending in PVA. The peaks at 1311 cm^{-1} in the ChFe-Cu hydrogel composite represent the stretching of aromatic amine in the chitosan structure. The C-O-C group in the ChFe-Cu hydrogel composite can be seen at 1018 cm^{-1} . A peak at 894 cm^{-1} appeared in the

ChFe-Cu hydrogel composite which can be attributed to the amide ring stretching in the chitosan. Small absorption peaks at 825 cm^{-1} in the ChFe-Cu hydrogel composite belong to the free -NH_2 in the chitosan. This peak is not clear in the ChFe-Cu hydrogel composite as it contains fewer free -NH_2 groups compared to the ChFe and pure chitosan hydrogel. There is a peak assigned to 570 cm^{-1} in ChFe-Cu hydrogel composite which is attributed to the Fe-O bond of the Fe_3O_4 nanoparticles.

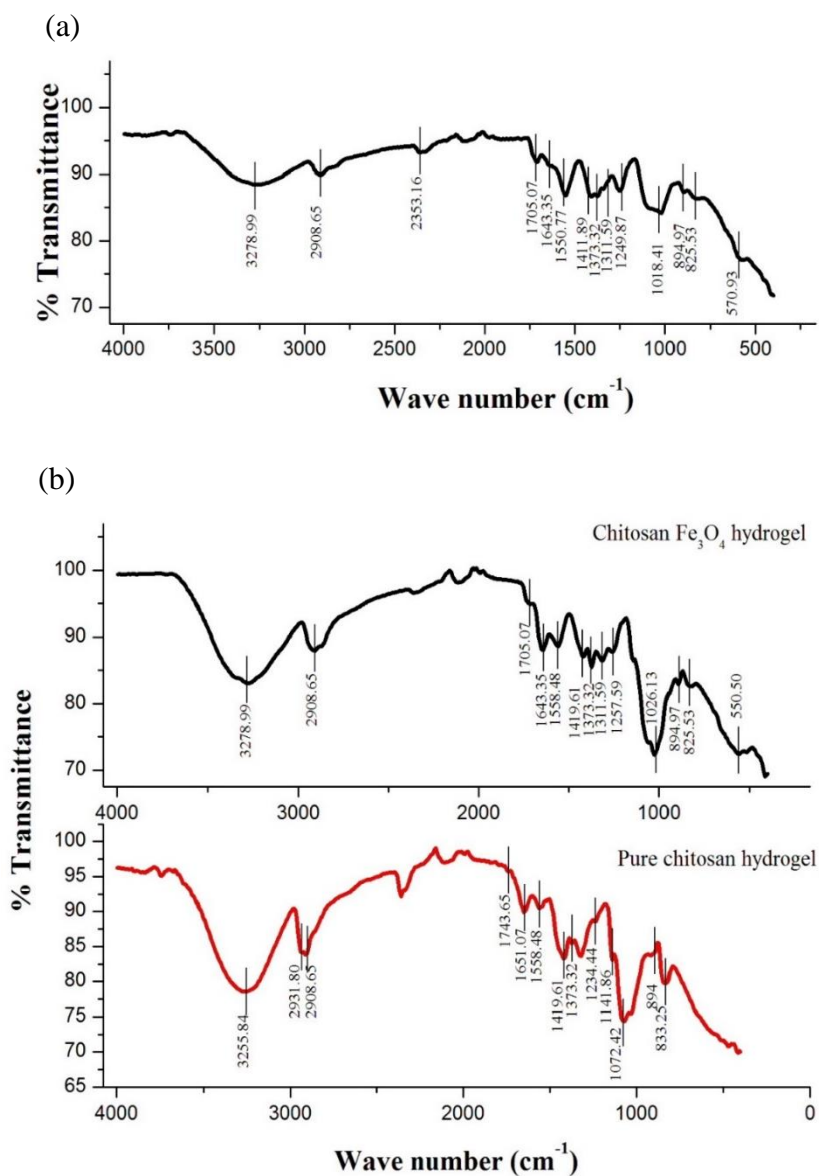


Figure 5 (a) FTIR spectra of ChFe-Cu hydrogel composite, (b) FTIR spectra of pure chitosan hydrogel and ChFe hydrogel composite (Weerasundara et al., 2022)

The wide-scan XPS spectra of the ChFe-Cu hydrogel composite and the elemental percentages are shown in Figure 6(a). The peaks found in the ChFe-Cu hydrogel composite surface are C1s, N1s O1s and Cu2p (Figure 6(b)-(e)). The peak related to C1s appears in the binding energy range of 281.9 and 291.9 eV (Figure 6(b)). Considering the proposed structure of the ChFe-Cu hydrogel composite, a few C types can be proposed for the above C binding energy range: C-C and C-H bonds and C=O. The N 1s peak found at the binding energy 400 eV range (Figure 6(c)). This is attributed to the N atom in the R-NH₂ group of the chitosan. The O peak was found within the range of 529 and 535 eV (Figure 6(d)). This range refers to C-OH of PVA and chitosan and Fe-O of Fe₃O₄ nanoparticles. The Cu2p peak in the range of 900-950 eV (Figure 6(e)) confirms the Cu loading into the hydrogel composite. The composition of Cu(II) in the ChFe-Cu hydrogel is 3.41%.

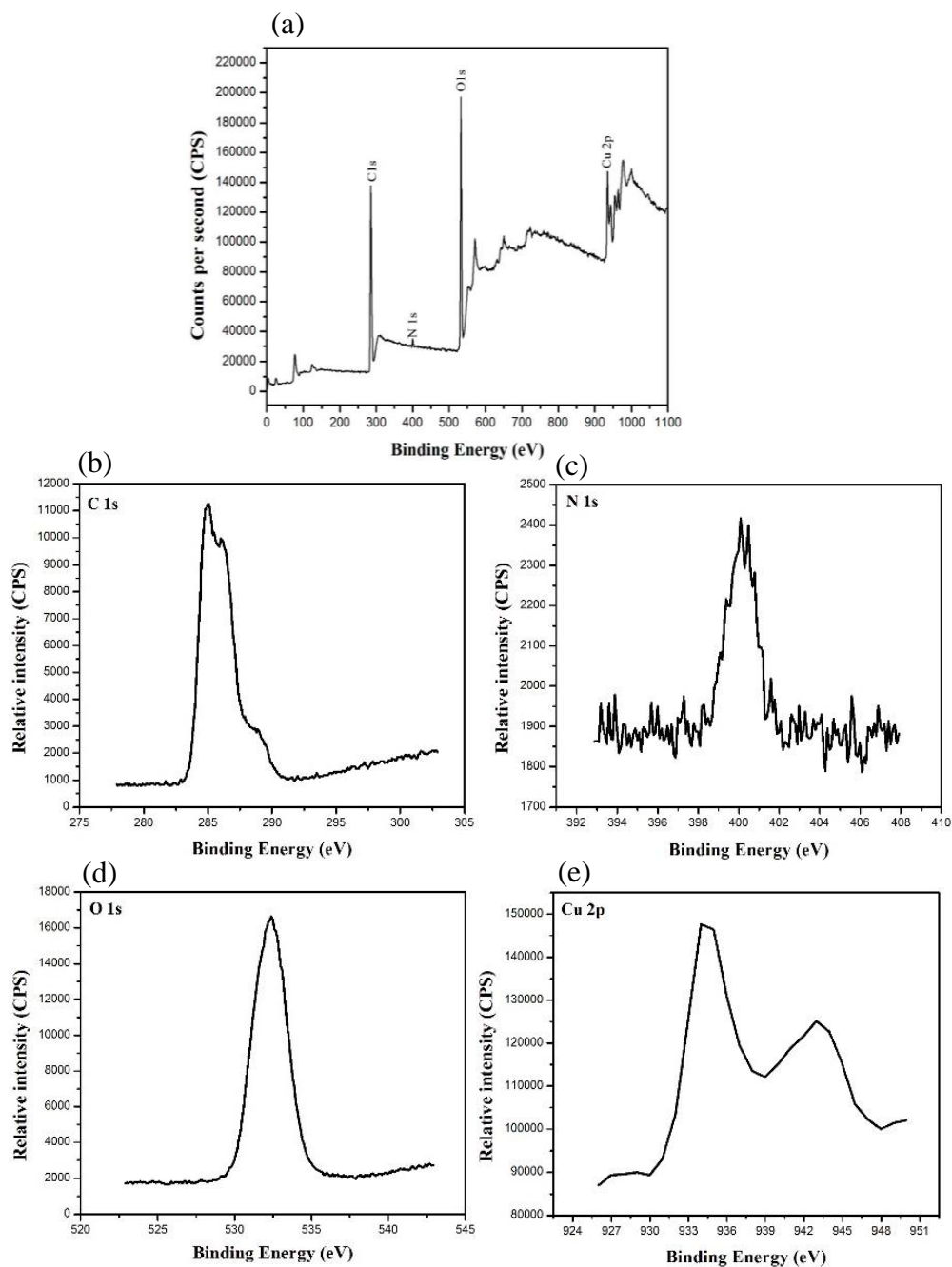


Figure 6 (a) The wide-scan XPS spectra of the ChFe-Cu hydrogel composite, refined XPS spectra of (b) C 1s, (c) N 1s, (d) O 1s, (e) Cu 2p

3.3. Effect of pH on As(V) adsorption

pH is one of the crucial factors in As adsorption as the speciation of As is highly dependent on the solution pH and the redox potential. The ChFe hydrogel composite showed pH dependent characteristics on As(V) adsorption and, at the range of pH 4-5, the maximum adsorption was recorded while the adsorption declined with the increasing solution pH. Figure 7 shows the behaviour of As(V) adsorption into the ChFe-Cu hydrogel composite with different

solution pH. The pattern of the As(V) adsorption on to the ChFe-Cu hydrogel composite is same as that of the ChFe hydrogel composite, where the maximum adsorption is at the range of pH 4-5. This pH dependent adsorption feature can be explained with PZC and the available As(V) oxyanions in the particular pH range. At the pH range of 2-7 the dominant As(V) oxyanion is H_2AsO_4^- . Since the available As(V) species is negatively charged, it can be adsorbed through a positively charged surface. Figure 3 shows that pHPZC for the ChFe-Cu hydrogel composite is 6 and, therefore, a positive surface charge can be expected at $\text{pH} < 6$. At the pH range of 4-5, the surface charge is positive, and it is at full capacity for adsorption of As(V), therefore a maximum adsorption can be expected.

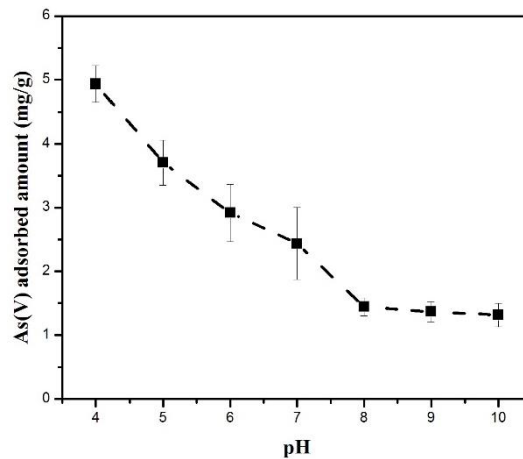


Figure 7 Effect of solution pH on As(V) adsorption into ChFe-Cu hydrogel composite

3.4. Adsorption kinetics

The kinetic data and the non-linear curve fittings are shown in Figure 8. The kinetic data shows that until 6 h the adsorption of As(V) into the ChFe-Cu hydrogel composite has a rapid rate and gained 4.86 mg/g (97%) of As(V) adsorption. After 6 h the adsorption showed no significant difference as it reached the equilibrium stage, and at the maximum adsorption it showed 4.92 mg/g (98%) of As(V) adsorption at 72 h.

To understand the adsorption mechanisms and the feasible rate-determining step of the adsorption process, the kinetic data were fitted to the mathematical kinetic models: pseudo first-order, pseudo second order, Elovich, parabolic diffusion and power function. The values of the kinetic model parameters together with the correlation coefficient (R^2) values are

depicted in Table 1. The calculated R^2 values (0.97) indicate that the pseudo second order is the best fit with experimental data which suggests chemisorption mechanism. The goodness of fit of the experimental data to the pseudo-second-order non-linear model is further proven by the value of adsorption capacity evaluated by the pseudo-second-order model (4.82 mg/g), as it is similar to the experimental value (4.86 mg/g). It can be suggested that adsorption can occur through external mass transfer, internal diffusion, and finally, adsorption into active sites.

Figure 8 shows a rapid adsorption up to 6 h, followed by equilibrium because all the active sites of the ChFe-Cu hydrogel by As(V) oxyanions are employed. According to the proposed structure there are several kinds of active site that can be employed by As(V) oxyanions such as protonated -OH and -NH₂ sites, Cu(II) sites and Fe₃O₄ sites.

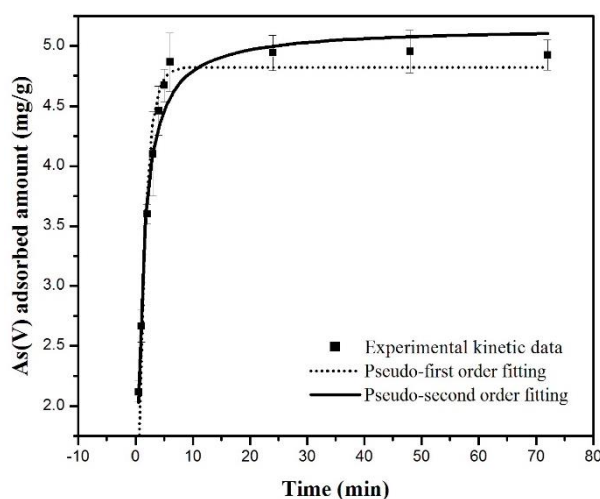


Figure 8 *Best fitted kinetic models on As(V) adsorption into the ChFe-Cu hydrogel composite*

Table 1 *Non-linear kinetic parameters of As(V) adsorption into a ChFe-Cu hydrogel composite*

Model	Non-linear equation	Description	Isotherm parameters	Value	R ²
Pseudo-first order	$q_t = q_e[1 - e^{-K_1 t}]$	K_1 – the rate constant (min^{-1}) q_e, q_t – sorption capacity at equilibrium and at time t , respectively (mg/g)	K_1 q_e	0.79097 4.82161	0.95
Pseudo-second order	$q_t = \frac{q_e^2 K_2 t}{1 + K_2 t q_e}$	K_2 – the rate constant (g/mg/min) q_e, q_t – sorption capacity at equilibrium and at time t , respectively (mg/g)	K_2 q_e	0.25204 5.15734	0.97
Elovich	$q_t = b \ln(ab) + \ln(t)$	q_t – sorption capacity at time t (mg/g) a – initial sorption rate (mg/g/min) b – desorption constant (g/mg)	a b	198.9244 1.84666	0.74
Power function	$q_t = b(t^{k_f})$	q_t – sorption capacity at time t (mg/g) b – power function constant k_f – power function rate constant	b k_f	3.34136 0.11506	0.66
Parabolic	$q_t = a + k_p \sqrt{t}$	q_t – sorption capacity at time t (mg/g) a – parabolic constant k_p – parabolic rate constant	a k_p	3.31478 0.25608	0.45

3.5. Adsorption isotherm

Work on adsorption isotherm models with experimental data provides details for designing and evaluating the adsorption mechanism of a particular sorbent and sorbate interface. The isotherm parameters for each isotherm model are given in Table 2. Figure 9 shows the adsorption isotherms for the adsorption of As(V) into the ChFe-Cu hydrogel composite. The experimental data were best fitted with the Freundlich isotherm model with

high R^2 values of 0.97 (Figure 9). The Freundlich model describes a multilayer adsorption that occurs on a heterogeneous surface. The proposed structure shows that the Fe_3O_4 nanoparticles are immersed into the hydrogel structure rather than being attached to the outer surface. The chemical and physical characterisation data indicates that the ChFe-Cu hydrogel is contained with -OH, -NH₂, Fe and Cu related functional groups which can be described as the active sites responsible for As(V) oxyanion adsorption. The data matches with the kinetic modeling which describes the heterogeneous chemisorption mechanism. The parameter n of the Freundlich model equation is valued at 0.56 which is less than 1, and this indicates that the adsorption process of As(V) into ChFe-Cu hydrogel composite is a favourable process.

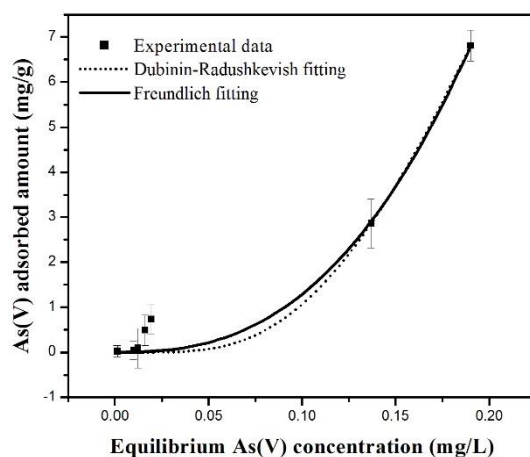


Figure 9 *Freundlich and Dubinin-Radushkevich isotherm model fitting for ChFe-Cu hydrogel composite on As(V) adsorption*

Table 2 *Non-linear isotherm parameters for As(V) adsorption into a ChFe-Cu hydrogel composite*

Model	Non-linear equation	Description	Isotherm parameters	Value	R ²
Langmuir	$q_{\text{ads}} = \frac{q_{\text{max}}K_L C_e}{1+K_L C_e}$	q_{ads} – the amount of adsorbate adsorbed per unit mass of adsorbent (mg/g) q_{max} – the maximum adsorption capacity (mg/g) K_L – the Langmuir affinity parameter (L/mg) C_e – the equilibrium adsorbate aqueous phase concentration (mg/L)	q_{max} K_L	5.81524 0.17174	0.95
Freundlich	$q_{\text{ads}} = K_F C_e^n$	K_F – the Freundlich affinity – capacity parameter ((mg/g)/(mg/L) ⁿ) n – the Freundlich exponent	K_F n	1.04231 0.56775	0.97
Dubinin-Radushkevich	$q_{\text{ads}} = q_D \exp(-B_D [RT \ln(1 + 1/C_e)]^2)$	q_D – Monolayer adsorption capacity (mg/g) B_D – mean free energy sorption (mol ² /kJ)	q_D B_D	1.82659 4.44x10 ⁻⁸	0.97

3.6. Possible mechanisms for As(V) adsorption into ChFe-Cu hydrogel composite

Both isotherm and kinetic modeling data suggested that the As(V) adsorption into the ChFe-Cu hydrogel composite is associated with the chemisorption mechanism. The chemical and physical characterisation data on the ChFe-Cu hydrogel composite further support the chemisorption mechanism proposal demonstrating that there are several kinds of functional groups that can attract As(V) oxyanions. The possible mechanisms can be identified as electrostatic interactions, Lewis-acid-base interactions, inner-sphere ligand exchange complex formation, bidentate corner-sharing (²C) and bidentate edge-sharing (²E) trimetric surface complex formation. In the pH range, which is lower than the PZC, the -NH₂ and -OH groups in the PVA and chitosan become protonated, making the surface of the hydrogel more positive. At the protonated state the negatively charged H₂AsO₄⁻ and HAsO₄²⁻ ions create electrostatic attractions with -NH₃⁺ and -OH₂⁺. The Fe₃O₄ nanoparticles form ligand-exchange inner-sphere complexes and bidentate corner-sharing (²C) and bidentate edge-sharing (²E) trimetric surface complexes with the H₂AsO₄⁻ and HAsO₄²⁻ ions. With the ligand-exchange inner-sphere complex

formation, the -OH^- groups in Fe_3O_4 become protonated and form -OH_2^+ and are then replaced with the H_2AsO_4^- and HAsO_4^{2-} ions. The Cu(II) ions interact with the As(V) oxyanions via both Lewis-acid-base interactions and electrostatic interactions. It should be noted that the Lewis-acid-base interactions further enhance the electrostatic interactions between Cu(II) ions and As(V) oxyanions due to short distanced inner-sphere complex formation and these short distance complexes enhance the electrostatic interactions (An et al., 2005).

3.7. Desorption and re-sorption of As(V) on ChFe-Cu hydrogel

From the viewpoint of cost-effectiveness and environmental sustainability, it is beneficial if an adsorbent material can be regenerated and re-used. Multiple re-uses will reduce the production cost as well as the amount of waste generation. In our earlier study (Weerasundara et al., 2022), a reliable method was identified (0.1 M CH_3COOH for 6 h shaking duration) for regeneration of the ChFe hydrogel composite, and in the present study the same method was used for assessing the regeneration capability of the ChFe-Cu hydrogel composite and its potential for re-use.

Figure 10 shows the adsorption, desorption, and resorption of the ChFe-Cu hydrogel composite with 0.1 M CH_3COOH treatment for four cycles. The adsorption capacities were 4.9, 2.5, 2.5, and 2.5 mg/g from first to fourth adsorption cycles, respectively. During the adsorption process the solution pH tended to increase, and the final pH was in the range of 5-6. Therefore, during the adsorption process the surface charge of the ChFe-Cu hydrogel shifted towards negative or weak positive status. With that, the affinity towards As(V) became weak, and it can be assumed that all of the adsorption sites had not been employed for As(V) . This is the reason that even with insignificant desorption capacity, the adsorption in second, third and fourth cycles showed constant resorption capacities. Maintaining a constant pH level throughout the whole adsorption process may facilitate higher adsorption capacity than 4.9 mg/g during the first cycle, but pH maintenance will make the adsorption process more expensive and complex. Therefore, in practical situations, maintaining a constant pH to achieve enhanced adsorption capacity is not efficient practice. However, the re-usable feature reveals that the ChFe-Cu hydrogel composite has a cumulative adsorption capacity. The adsorption values with 0.1 M CH_3COOH are as follows: 6.8, 3.4, 3.4 and 3.4 mg/g for 1st, 2nd, 3rd and 4th adsorption cycles respectively. Thus, the total adsorption capacity of the ChFe-Cu hydrogel composite for four adsorption cycles is 17 mg/g. Therefore, the ChFe-Cu hydrogel composite

can be re-used and recycled for As(V) adsorption, enhancing the effectiveness of the process and, therefore, its economic and environmental sustainability.

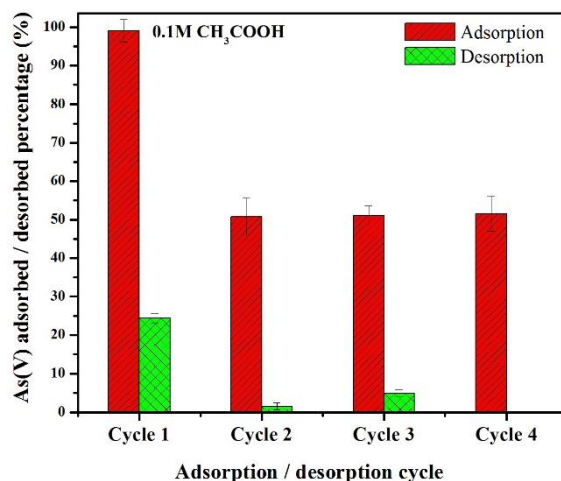


Figure 10 Reusable capacities of ChFe-Cu hydrogel composite over four adsorption cycles

3.8. Comparison of ChFe-Cu hydrogel composite with ChFe hydrogel composite on As(V) adsorption

Table 3 depicts the conditions and results of both the ChFe-Cu and ChFe hydrogel composites on As(V) adsorption. The basic preparation method was the same for both hydrogel composites. The only difference was that the ChFe-Cu hydrogel composite was loaded with Cu(II) ions. The data show that Cu(II) loading significantly decreased the swelling percentage of the ChFe-Cu hydrogel. The Cu(II) acted as a crosslinker between chitosan chains, and this limited the mobility of the hydrogel complex due to increased crosslinking density. Despite this, the adsorption capacity was significantly increased with the ChFe-Cu hydrogel, and there was a 4.6 mg/g difference compared to the ChFe hydrogel composite. Similar adsorption mechanisms were involved in both hydrogel composites, however the number of active sites was higher in the ChFe-Cu hydrogel than in the ChFe hydrogel composite. The reason behind the increased active sites number is that the loading of Cu(II) into chitosan makes more -OH sites for As(V) adsorption.

Table 3 Comparison between ChFe-Cu and ChFe hydrogel composites

Condition/results	ChFe-Cu hydrogel composite	ChFe hydrogel composite
Swelling capacity	263 %	482 %
Best pH range for As(V) adsorption	< 6	<6.6
Equilibrium time for As(V) adsorption	6 h	6 h
Maximum adsorption capacity (First adsorption cycle)	6.8 mg/g	2.2 mg/g
Mechanisms involved As(V) adsorption	chemisorption	chemisorption
Total adsorbed As(V) amount with 4 adsorption cycles	17 mg/g	15.1 mg/g

4. Conclusion

The ChFe-Cu hydrogel was developed as a composite of the Cu(II) loaded chitosan-PVA hydrogel and Fe₃O₄ nanoparticles to remove As(V) from water. The Cu(II) loading was achieved by a Lewis-acid-base interaction between Cu(II) ions and -NH₂ ions in the chitosan structure. The change in the solution pH affected the adsorption capacity. The highest adsorption was recorded in the range of pH 4-5 and, with an increment of solution pH, the adsorption capacity declined. Within the pH 3-6 range, the hydrogel surface became positively charged due to protonation of the -NH₂ and -OH groups in the hydrogel composite, and the positive surface attracted H₂AsO₄⁻ and HAsO₄²⁻ oxyanions. Further, within pH 3-6, the Fe₃O₄ nanoparticles formed inner and outer surface complexes with H₂AsO₄⁻ and HAsO₄²⁻ oxyanions and adsorbed As(V). The Cu(II) created more binding sites for As(V) oxyanions since the Cu(II) contained three -OH groups. With the presence of these functional groups, both kinetic and isotherm modeling suggest the chemisorption adsorption mechanisms for the adsorption of As(V) into the ChFe-Cu hydrogel composite.

The ChFe-Cu hydrogel composite is available for regeneration and re-use. 0.1 M CH₃COOH is a successful solution for regeneration of the ChFe-Cu hydrogel composite. Further, the ChFe-Cu hydrogel composite can be considered as a solution to overcome the characteristic drawbacks of adsorbents such as adsorbent-water separation which hinders upscaling to a large industrial scale. The ChFe-Cu hydrogel composite does not require additional energy (i.e., post filtration) to separate the adsorbent from water and, as a result, allows up-scaling to industrial large-scale applications. The innovative aspects of the proposed hydrogel such as regeneration, re-use and easy separation from water allow large-scale

application of the material. This emphasises the global importance of the ChFe-Cu hydrogel composite.

There are further research opportunities for optimising adsorption capacity and its use at the field scale in different aspects such as water filters and water purification processes. The ability of Cu(II) to load onto the ChFe hydrogel composite further expands the application range for contaminant removal. The possibility exists to use ChFe hydrogel for Cu(II) ion removal, and then use it for As(V) removal from water. The adsorption of Cu(II) from Cu contaminated water will facilitate the Cu loading onto the ChFe hydrogel composite, and the Cu adsorbed ChFe hydrogel composite can then be used for As(V) removal. However, a detailed experiment is required to conduct to assess the potential. This will further enhance the sustainability of the material by supporting environmentally friendly aspects and decreasing the amount of waste products.

Acknowledgements

The authors acknowledge the support from Katelynn Hadzi at the University of Southern Queensland, Anya J. E. Yago, Dr Craig Stoppiello and Dr Lachlan Casey at the Centre for Microscopy and Microanalysis (CMM) at the University of Queensland.

The authors thank Dr Barbara Harmes and Sandra Cochrane from the University of Southern Queensland, Australia for providing help with language correction.

This work was supported by the University of Southern Queensland, QLD, Australia (RTP Stipend Scholarship programme).

References

- Al-Ghouti, M.A. and Da'ana, D.A. 2020. Guidelines for the use and interpretation of adsorption isotherm models: a review. *Journal of Hazardous materials* 393, 122383.
- An, B., Fu, Z., Xiong, Z., Zhao, D. and SenGupta, A.K. 2010. Synthesis and characterization of a new class of polymeric ligand exchangers for selective removal of arsenate from drinking water. *Reactive and Functional Polymers* 70(8), 497-507.
- An, B., Steinwinder, T.R. and Zhao, D. 2005. Selective removal of arsenate from drinking water using a polymeric ligand exchanger. *Water Research* 39(20), 4993-5004.
- Bakatula, E.N., Richard, D., Neculita, C.M. and Zagury, G.J. 2018. Determination of point of zero charge of natural organic materials. *Environmental Science and Pollution Research* 25(8), 7823-7833.

- Bundschuh, J., Armenta, M.A., Morales-Simfors, N., Alam, M.A., López, D.L., Delgado Quezada, V., Dietrich, S., Schneider, J., Tapia, J. and Sracek, O. 2021. Arsenic in Latin America: New findings on source, mobilization and mobility in human environments in 20 countries based on decadal research 2010-2020. *Critical Reviews in Environmental Science and Technology* 51(16), 1727-1865.
- Bundschuh, J., Niazi, N.K., Alam, M.A., Berg, M., Herath, I., Tomaszewska, B., Maity, J.P. and Ok, Y.S. 2022. Global arsenic dilemma and sustainability. *Journal of Hazardous Materials* 436, 129197.
- Foo, K.Y. and Hameed, B.H. 2010. Insights into the modeling of adsorption isotherm systems. *Chemical engineering journal* 156(1), 2-10.
- Herath, I., Kumarathilaka, P., Al-Wabel, M.I., Abduljabbar, A., Ahmad, M., Usman, A.R. and Vithanage, M. 2016. Mechanistic modeling of glyphosate interaction with rice husk derived engineered biochar. *Microporous and mesoporous materials* 225, 280-288.
- Jin, L. and Bai, R. 2002. Mechanisms of lead adsorption on chitosan/PVA hydrogel beads. *Langmuir* 18(25), 9765-9770.
- Kumarathilaka, P., Bundschuh, J., Seneweera, S., Marchuk, A. and Ok, Y.S. 2021a. Iron modification to silicon-rich biochar and alternative water management to decrease arsenic accumulation in rice (*Oryza sativa* L.). *Environmental Pollution* 286, 117661.
- Kumarathilaka, P., Bundschuh, J., Seneweera, S. and Ok, Y.S. 2021b. Rice genotype's responses to arsenic stress and cancer risk: the effects of integrated birnessite-modified rice hull biochar-water management applications. *Science of the Total Environment* 768, 144531.
- Kumarathilaka, P., Seneweera, S., Ok, Y.S., Meharg, A.A. and Bundschuh, J. 2020. Mitigation of arsenic accumulation in rice: an agronomical, physico-chemical, and biological approach—a critical review. *Critical Reviews in Environmental Science and Technology* 50(1), 31-71.
- Largitte, L. and Pasquier, R. 2016. A review of the kinetics adsorption models and their application to the adsorption of lead by an activated carbon. *Chemical Engineering Research and Design* 109, 495-504.
- Li, Z. 1999. Sorption kinetics of hexadecyltrimethylammonium on natural clinoptilolite. *Langmuir* 15(19), 6438-6445.
- Lü, R., Cao, Z. and Shen, G. 2008. Comparative study on interaction between copper (II) and chitin/chitosan by density functional calculation. *Journal of Molecular Structure: THEOCHEM* 860(1-3), 80-85.

- Luan, H., Teychene, B. and Huang, H. 2019. Efficient removal of As (III) by Cu nanoparticles intercalated in carbon nanotube membranes for drinking water treatment. *Chemical Engineering Journal* 355, 341-350.
- Mayakaduwa, S., Kumarathilaka, P., Herath, I., Ahmad, M., Al-Wabel, M., Ok, Y.S., Usman, A., Abduljabbar, A. and Vithanage, M. 2016. Equilibrium and kinetic mechanisms of woody biochar on aqueous glyphosate removal. *Chemosphere* 144, 2516-2521.
- Morales-Simfors, N. and Bundschuh, J. 2021. Arsenic-rich geothermal fluids as environmentally hazardous materials—A global assessment. *Science of The Total Environment*, 152669.
- Ramana, A. and Sengupta, A.K. 1992. Removing selenium (IV) and arsenic (V) oxyanions with tailored chelating polymers. *Journal of Environmental Engineering* 118(5), 755-775.
- Wang, J. and Guo, X. 2020. Adsorption kinetic models: Physical meanings, applications, and solving methods. *Journal of Hazardous materials* 390, 122156.
- Weerasundara, L., Ok, Y.S. and Bundschuh, J. 2021. Selective removal of arsenic in water: a critical review. *Environmental Pollution* 268, 115668.
- Weerasundara, L., Ok, Y.S., Kumarathilaka, P., Marchuk, A. and Bundschuh, J. 2022. Assessment and optimization of As (V) adsorption on hydrogel composite integrating chitosan-polyvinyl alcohol and Fe₃O₄ nanoparticles and evaluation of their regeneration and reusable capabilities in aqueous media. *Science of The Total Environment*, 158877.
- Wu, K., Jing, C., Zhang, J., Liu, T., Yang, S. and Wang, W. 2019. Magnetic Fe₃O₄@ CuO nanocomposite assembled on graphene oxide sheets for the enhanced removal of arsenic (III/V) from water. *Applied Surface Science* 466, 746-756.
- Wu, L.K., Wu, H., Zhang, H.-B., Cao, H.Z., Hou, G.Y., Tang, Y.P. and Zheng, G.Q. 2018. Graphene oxide/CuFe₂O₄ foam as an efficient absorbent for arsenic removal from water. *Chemical Engineering Journal* 334, 1808-1819.
- Yamani, J.S., Lounsbury, A.W. and Zimmerman, J.B. 2016. Towards a selective adsorbent for arsenate and selenite in the presence of phosphate: Assessment of adsorption efficiency, mechanism, and binary separation factors of the chitosan-copper complex. *Water Research* 88, 889-896.
- Yan, E., Cao, M., Jiang, J., Gao, J., Jiang, C., Ba, X., Yang, X. and Zhang, D. 2017. A novel adsorbent based on magnetic Fe₃O₄ contained polyvinyl alcohol/chitosan composite nanofibers for chromium (VI) removal. *Solid State Sciences* 72, 94-102.

- Yan, E., Cao, M., Ren, X., Jiang, J., An, Q., Zhang, Z., Gao, J., Yang, X. and Zhang, D. 2018. Synthesis of Fe₃O₄ nanoparticles functionalized polyvinyl alcohol/chitosan magnetic composite hydrogel as an efficient adsorbent for chromium (VI) removal. *Journal of Physics and Chemistry of Solids* 121, 102-109.
- Zhao, D. and Sengupta, A.K. 1998. Ultimate removal of phosphate from wastewater using a new class of polymeric ion exchangers. *Water Research* 32(5), 1613-1625.

6.3. Concluding remarks

The Fe₃O₄ integrated chitosan hydrogel was developed for As(V) removal from water. In this study the hydrogel was further modified with Cu(II) ions to introduce more As adsorption sites to the ChFe hydrogel. With modification, the Cu(II) ions attached with Fe₃O₄ nanoparticles and created three more As adsorption sites with each Cu(II) ion. Here, the chitosan hydrogel was loaded with two different metal ions to enhance the As(V) adsorption. As with the ChFe hydrogel, the ChFe-Cu hydrogel can also be re-used several times. At the first adsorption, the ChFe-Cu hydrogel showed a three-fold increase in As(V) adsorption capacity compared to the ChFe hydrogel. This further confirms that enhanced adsorption has occurred due to the binding site that was created through Cu(II) ions.

CHAPTER 7: PAPER 7 – ASSESSMENT OF As(III) REMOVAL FROM WATER WITH BIOCHAR HYDROGEL COMPOSITES WHICH WERE SUCCESSFUL IN As(V) REMOVAL FROM WATER AND OVERCAME THE CLASSIC DRAWBACKS OF ADSORBENT MATERIALS

7.1. Introduction

Over 200 million people worldwide have been reported at risk of arsenic poisoning from drinking water. Lung, kidney, liver, and skin cancers are common health conditions associated with chronic arsenic exposure. In aquatic environments, inorganic arsenic species can be found as As(III) and As(V). This arsenic speciation is determined by pH and redox potential. Alkaline ($\text{pH} > 7.5$) and reduced conditions are favourable for As(III), while acidic and oxidised conditions are favourable for As(V). The As(III) is known to be 60 times more toxic than As(V), and highly toxic compared to organic arsenic species (Kumarathilaka et al., 2019). It is also more mobile than As(V).

As(III) removal has been a significant research topic over the last few decades. Several removal methods have been used: nano-filtration, lime softening, coagulation/flocculation, electrochemical techniques, chemical precipitation, ion exchange and membrane separation. However, when used alone, these methods have several disadvantages such as a significant amount of waste generation, high production and processing cost, additional pre- and post-treatment needs, and high energy requirements. Taking these factors into account, the abovementioned methods cannot be considered efficient and sustainable methods for As(III) removal.

This study focused on two major aspects. First, the synthesis of potential, low cost and novel material to remove As(III) from aqueous media. Second, to overcome the classic drawbacks of adsorption methods by achieving low or no energy requirements on water-adsorbent separation after the adsorption and to enhance the sustainability by regeneration and re-used of the material.

Assessment of As(III) removal from water with biochar hydrogel composites which were successful in As(V) removal from water and overcame the classic drawbacks of adsorbent materials

Lakshika Weerasundara^a, Prasanna Kumarathilaka^a, Alla Marchuk^b Jochen Bundschuh^{*a,c}

^a*School of Civil Engineering and Surveying, Faculty of Health, Engineering and Sciences, University of Southern Queensland, West Street, Toowoomba, Queensland, 4350, Australia*

^b*Institute for Life Sciences and the Environment, University of Southern Queensland, West Street, Toowoomba, Queensland, 4350, Australia*

^c*Doctoral Program in Science, Technology, Environment, and Mathematics, Department of Earth and Environmental Sciences, National Chung Cheng University, 168 University Rd., Min-Hsiung, Chiayi County, 62102, Taiwan*

*Corresponding author

E-mail address: jochen.bundschuh@usq.edu.au (Jochen Bundschuh), School of Civil Engineering and Surveying, Faculty of Health, Engineering and Sciences, University of Southern Queensland, Toowoomba, Queensland 4350, Australia. Doctoral Program in Science, Technology, Environment, and Mathematics, Department of Earth and Environmental Sciences, National Chung Cheng University, 168 University Rd., Min-Hsiung, Chiayi County, 62102, Taiwan.

Abstract

Rice-hull biochar hydrogel composite (RHBC hydrogel) and sugarcane bagasse biochar hydrogel composite (SUBC hydrogel) were successfully synthesised and their capacity for arsenic (III) (As(III)) adsorption was assessed. The As(III) adsorption into RHBC and SUBC hydrogels was pH dependent and the solution pH affected both adsorbent and adsorbate functions. Non-linear kinetic and isotherm modeling on the experimental data revealed that both physisorption and chemisorption mechanisms are involved in As(III) adsorption into RHBC and SUBC hydrogels. Based on the surface morphology identified with scan electron microscopy analysis, pore filling is proposed as the physisorption mechanism while the monodentate complexation is proposed as the chemisorption mechanism. The surface charge of the RHBC and SUBC hydrogels was negative when the solution pH was > 2 based on the point of zero charge analysis. When the solution pH was < 9 , the available As(III) compound was HAsO_2 which is a neutral compound. With these conditions, the hydrogels' -OH groups formed monodentate complexes with HAsO_2 ; the only functional group available in the RHBC and SUBC surfaces that can attract As(III) in the solution. The data shows that, at the equilibrium state, the adsorption capacities of RHBC and SUBC hydrogels in a single adsorption cycle were 0.03 and 0.05 mg/g respectively. The hydrogels can be regenerated with 0.1 M NaOH and re-used in up to two adsorption cycles. The cumulative adsorption capacities for two adsorption cycles were 0.16 mg/g for both the RHBC and SUBC hydrogels. RHBC and SUBC hydrogel adsorption capacities were lower for As(III) compared to arsenic (V) (As(V)). However, the hydrogels can be used to adsorb both As(III) and As(V) simultaneously as there is no competition on adsorption sites. The As(V) adsorption occurred via -CO and - NH_2 , and the As(III) adsorption occurred via -OH groups. Both RHBC and SUBC hydrogels were successful in terms of overcoming the classic drawbacks of traditional adsorptive materials due to their reusability and easy water-adsorbent separation feature. Further, after adsorption, the hydrogels shrink in dry conditions and, thus, reduce the amount of waste produced in the As(III) removal process. Therefore, the RHBC and SUBC can be considered for large-scale water purification systems because of their sustainable and environmentally friendly characteristics.

Keywords: Arsenic (III), adsorption, hydrogel, biochar, recycle

1. Introduction

Arsenic is a metalloid which can be found naturally in the Earth's crust and, due to natural weathering processes, it is a prominent geogenic groundwater contaminant (Amen et al., 2020; Bundschuh et al., 2021; Kumarathilaka et al., 2021c). Industrialisation and urbanisation have triggered many anthropogenic sources of arsenic in the environment such as mining, coal ash disposal, pesticide application, wood preservation and metallurgy (Bundschuh et al., 2022; Kumarathilaka et al., 2018b; Martinson and Reddy, 2009).

Worldwide, over 200 million people have been reported at risk of arsenic poisoning via ingestion; mainly through drinking water. Lung, kidney, liver and skin cancers are common health conditions associated with chronic arsenic exposure (Kumarathilaka et al., 2021d; Li et al., 2022). Other than carcinogenic impacts, various chronic diseases such as papillary and cortical necrosis, diabetes mellitus, cardiovascular diseases, skin lesions, cirrhosis, melanosis and black foot disease have been identified as impacts of arsenic contamination.

In aquatic environments, inorganic arsenic species can be found as arsenic (III) (As(III)) and arsenic (V) (As(V)) (Kumarathilaka et al., 2020; Martinson and Reddy, 2009). This arsenic speciation is decided by the pH and redox potential. Alkaline ($\text{pH} > 7.5$) and reduced conditions are favourable for As(III), while acidic and oxidised conditions are favourable for As(V). As(III) is known to be 60 times more toxic than As(V). As(III) is highly toxic compared to organic arsenic species. Further, As(III) is more mobile than As(V) (Mensah et al., 2022). Therefore, the removal of As(III) from water requires greater attention.

Due to its toxicity and solubility, As(III) removal has been a significant research topic over the last few decades. Several As(III) removal methods have been in use: nano-filtration, lime softening, coagulation/flocculation, electrochemical techniques, chemical precipitation, ion exchange and membrane separation (Vithanage et al., 2019; Weerasundara et al., 2021). However, these methods have several disadvantages such as a significant amount of waste generation, high production and processing cost, additional pre- and post-treatment needs, and high energy requirements. The adsorption method can be identified as overcoming one or more of these disadvantages.

The adsorption method is comparatively cheap, and it does not need significant amounts of energy or processing technologies. Therefore, the adsorption method can be identified as a user-friendly method. CuO nanoparticles, biochar, clay minerals, siderite, magnetite, TiO₂ nanocrystals and metal-organic frameworks are a few of the many adsorbents that can be found in the literature addressing adsorbent materials for As(III) removal (Ahmed et al., 2021; Guo

et al., 2007; Manning and Goldberg, 1997; Martinson and Reddy, 2009; Ohe et al., 2005; Zhang et al., 2019).

Even though the general concept of adsorption provides an advantage in terms of low cost, low energy requirements and user-friendliness, adsorption itself also has several disadvantages. The biochar and nanoparticles like materials are difficult to separate from water after adsorption completion, and require additional energy which increases the cost and complexity of the overall process and hinders upscaling to an industrial scale. Further, once adsorption is complete, the adsorbent has no re-use capability, thus reducing its economic and environmental sustainability.

Considering these facts, the present study focused on two major aspects. First, the synthesis of potential, low cost and novel material to remove As(III) from aqueous media. Second, overcome the classic drawbacks of adsorption methods by achieving low or no energy requirements on water-adsorbent separation after the adsorption, and enhance sustainability by regeneration and re-use of the material. Moreover, waste generation will be reduced by reusing the material.

Biochar has been identified as a low cost and easily accessible material for contaminant removal. It is a potential adsorptive material for As(III) removal due to the presence of favourable functional groups that attract As(III). However, due to its hydrophobic nature, using biochar by itself hinders the adsorption of As(III) in water. The present study focuses on embedding biochar particles into a hydrophilic hydrogel structure, opening up the biochar's functional groups to adsorb As(III) in the aqueous environment. The hydrogels themselves are emerging materials in contaminant removal from water. The hydrogel structure is not only used for biochar embedding, but also to enhance the adsorption capacity (Weerasundara et al., 2021b). With this goal, we have selected a poly acrylamide hydrogel (PAAm hydrogel) as the hydrogel structure.

The most fundamental advantages of using a hydrogel for contaminant removal from aqueous media is its non-destructive three-dimensional structure and its swelling and deswelling capacity in the presence of water and dry conditions, respectively (Weerasundara et al., 2021b). This feature facilitates easy water-adsorbent separation with reduced additional energy demand.

The present study focused on two different biochar hydrogel composites, rice-hull biochar hydrogel composite (RHBC hydrogel) and sugar cane bagasse biochar hydrogel composite (SUBC hydrogel), for removal of As(III) from aqueous media. They showed significant adsorption impacts on As(V) adsorption.

2. Materials and Methods

2.1. Preparation of biochar and hydrogel biochar composites

Rice-hull biochar and sugarcane bagasse biochar were used for the synthesis of the RHBC hydrogel and SUBC hydrogel respectively. A complete and detailed procedure for synthesis of biochar and hydrogels is explained in our previous studies. In brief, the rice-hull and sugarcane bagasse biochar were produced using a slow pyrolysis method with the following program: 7 °C/min heating rate, 2 h holding time at 700 °C under continuous nitrogen flow of 2 L/min. The prepared biochar was demineralised with 0.1 mol/L HCl, and the dried biochar was ground and sieved through a 0.06 mm mesh. For hydrogel synthesis, a 1.0 mL of acrylamide (1.0 g) solution was mixed with 0.6 g of biochar and 0.001 g of N, N'-methylene bis-acrylamide. In the next step, 0.2 mL of ammonium persulfate (0.1 g) was added and mixed. The solutions were placed in 5 mm vinyl tubes and kept at 40 °C for 30 mins. The tubes were kept at room temperature for another 24 h and the hydrogel samples were obtained.

2.2. Basic characterisation of RHBC and SUBC hydrogels

The physical and chemical characterisations and methods are described and discussed in detail, and can be found in our previous studies. A brief discussion can be found in the Results and discussion section (Section 3.1).

2.3. Laboratory analysis and batch sorption studies

A 1000 mg/L As(III) in 2% HCl high purity standard solution (purchased from Sigma Aldrich Pvt Ltd) was used for the preparation of the As(III) experimental and calibration standard solutions. Fresh solutions were prepared for each study. After each experiment, the total arsenic concentrations were measured using Inductively Coupled Plasma Mass Spectrometry (ICP-MS) (PerkinElmer NexION™ 300X). All the experiments were conducted in triplicate.

As part of the quality assurance and quality control measures, control experiments were conducted for each study. Further, calibration blanks and laboratory reagent blanks were measured. Calibration curves were set up and it was ensured that the residual mean square (R^2) was greater than or equal to 0.98. The calibration standards were measured once for each of the twelve samples as a quality assurance and quality control measure.

For all experiments, the hydrogel dosage of 1 g/L was used. This dosage was selected from the previous studies of RHBC and SUBC hydrogels on As(V) removal from water as the

1 g/L was effective in terms of cost of production and As(V) adsorption. For pH edge experiments, kinetic experiments and adsorption/re-sorption studies 5 g/L of As(III) solutions were used.

To determine the effect of pH on As(III) adsorption into the RHBC and SUBC hydrogels, pH edge experiments were conducted separately within the pH range of 4 to 10. The selected pH range from the pH edge experiments was used as the initial pH for kinetic, isotherm and adsorption/resorption studies. The kinetic studies were conducted for both the RHBC and SUBC hydrogels to determine the equilibrium duration, rate limiting factor and potential adsorption mechanisms. In the kinetic study, samples were removed at predetermined time intervals from 0.5 - 48 h. The isotherm studies were conducted with different initial As(III) concentrations within the range of 0.025 - 7 mg/L. An equilibrium time of 6 h was chosen based on the kinetic experiment. The amount of total arsenic retained in the adsorbent phase was calculated using equation 1 (Mayakaduwa et al., 2016).

$$q_e = [C_0 - C_e]VM^{-1} \quad (2)$$

where q_e is the As(III) amount adsorbed on the RHBC and SUBC hydrogels separately (mg/g), C_0 and C_e are the initial and equilibrium arsenic concentrations (mg/L), V is the solution volume (L) and M is the hydrogel mass (g).

2.4. Experimental data modeling and graphing

The kinetic and isotherm data modeling and statistical graphing were done with the Microcal Origin software (Version 6). Five non-linear kinetic models of pseudo-first order, pseudo-second order, Elovich, parabolic diffusion and power function were tested for modeling the adsorption kinetics of RHBC and SUBC on As(III) adsorption from an aqueous solution. The non-linear modeling was considered to be a better technique over linear modeling considering the realistic parameters, which means the non-linear models do not assume the data is independent.

Pseudo-first-order and pseudo-second-order are the most employed kinetic models to describe solid-liquid phase adsorptions (Benjelloun et al., 2021). Pseudo-first order describes the physisorption mechanism between adsorbate and adsorbent (Li, 1999). The pseudo-second order assumes that the adsorption process is a chemical sorption process where the valance forces are involved through the sharing or exchanging of electrons between adsorbent and adsorbate. The Elovich model describes the chemical adsorption mechanism into a

heterogeneous adsorbent. The parabolic diffusion model is used to decide whether the rate limiting factor is diffusion-controlled step. The power function describes a homogeneous chemisorption mechanism.

Adsorption isotherms describe the way adsorbates interact with adsorbents. Therefore, isotherm modeling is essential to optimise the use of adsorbents on any kind of adsorbates. In the present study, to identify the adsorption mechanisms, three isotherm models were used: Langmuir, Freundlich and Dubinin-Radushkevich. The Langmuir isotherm model assumes monolayer adsorption. The Freundlich isotherm model is used to describe a multilayer adsorption process into a heterogeneous surface with a chemisorption mechanism (Foo and Hameed, 2010). The Dubinin-Radushkevich model describes the mechanism of pore filling with a multilayer character (Al-Ghouti and Da'ana, 2020).

2.5. Desorption and resorption experiment on RHBC and SUBC hydrogels

The adsorption, desorption and resorption experiments were conducted to study the re-use capacities of the RHBC and SUBC hydrogels. With our previous studies on As(V) removal, the 0.1 NaOH was identified as a reliable method for efficient desorption of As(V) from both the RHBC and SUBC hydrogel composites. Based on the results of those studies, the same desorption method was also used for As(III). In total, three adsorption cycles were conducted to assess reusability.

3. Results and discussion

3.1. RHBC and SUBC hydrogel synthesis and characterisation

The synthesis of the RHBC and SUBC hydrogels and the structure formation is well described in our previous works. Both hydrogels were synthesised by grafting copolymerisation. The synthesis procedure consisted of four major steps: initiation, macro-radical generation, chain propagation and development of a three-dimensional structure by crosslinking of polyacrylamide chains. The maximum swelling capacities of the RHBC and SUBC hydrogels were 900 and 1050%, respectively. The equilibrium duration needed to achieve these swelling capacities were 7 and 24 h, respectively. The difference of swelling capacity is directly related to the hydrophilicity/hydrophobicity of the biochar.

The literature shows that the hydrophobicity of the biochar is directly related to the amount of carboxylic groups presence in the biochar (Mao et al., 2019). The carboxylic groups enhance the hydrophobicity of the biochar. The FTIR analysis of the rice-hull biochar and sugarcane bagasse biochar shows in the rice-hull biochar as a visible carboxylic group peak

but not in the sugarcane bagasse biochar (Figures S1 and S2). Therefore, the difference of swelling capacity between the RHBC and SUBC hydrogels can be understood with an FTIR analysis. The point of zero charge (PZC) analysis showed that both the RHBC and SUBC hydrogels have a negative surface charge in the range of $2 < \text{pH}$ (Figures S3 and S4).

The FTIR spectra of RHBC and SUBC hydrogel composites show that both hydrogel types have similar functional groups. The XRD pattern analysis showed that both the RHBC and SUBC hydrogels contain silica, and that the SUBC hydrogels contain a higher amount of silica compared to the RHBC hydrogel (Figures S5 and S6). The wide-scan XPS spectra of both the RHBC and SUBC hydrogels showed the predominant peaks of Si2p, S2p, C1s, N1s and O1s with similar patterns, and a similar chemical composition of the surface functional groups (Figures S7 and S8). This supports the FTIR analysis as well.

3.2. Effect of pH on As(III) adsorption into RHBC and SUBC hydrogels

The effects of pH on As(III) adsorption into RHBC and SUBC hydrogels are illustrated in Figure 1. For both hydrogel composites, the best pH range for adsorption can be identified as 6-7.5 where only neutral As(III) species (HAsO_2) can be found. The PZC analysis indicates that the surface charge of both RHBC and SUBC hydrogel is negative within the entire experimental pH range (Figures S3 and S4). However, it has been identified that, in the pH range of 4-7, the surface can have positive ions due to the protonation of $-\text{NH}_2$ and $-\text{CO}$ ionisable functional groups. This protonation is an advantage for As(V) adsorption but not for As(III) adsorption as there are no As(III) oxyanions available below pH 9.2 (Li et al., 2010). Therefore, electrostatic interactions cannot be employed for As(III) adsorption on to RHBC and SUBC hydrogels. Under these conditions, As(III) removal can only take place through $-\text{OH}$ groups via the formation of monodentate complexes. The presence of $-\text{OH}$ functional groups on both the RHBC and SUBC hydrogels can be confirmed with FTIR spectra of both hydrogels. The stretching vibrations at 3741.90 cm^{-1} on both the RHBC and SUBC hydrogel composites represents the $-\text{OH}$ groups. HAsO_2 can only be found within the pH range of 6-7.5, and this is the reason for elevated As(III) adsorption within the pH 6-7.5.

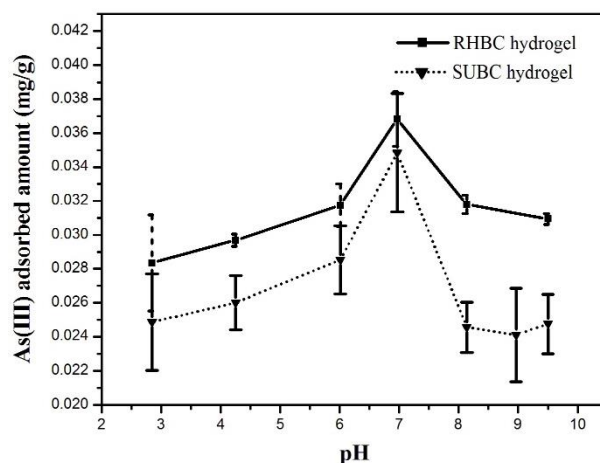


Figure 1 *Effect of pH on As(III) adsorption into RHBC and SUBC hydrogels*

3.3. Adsorption kinetics

The kinetic data and the best fitted non-linear kinetic models on the RHBC and SUBC hydrogels are illustrated in Figures 2 (a) and (b), respectively. The kinetic data for both hydrogels show that, within the first 6 h, adsorption occurred at a rapidly increasing rate and, following that, the increasing rate was slow. At the equilibrium state, the RHBC hydrogel achieved 0.031 mg/g As(III) adsorption, and for the SUBC hydrogel it was 0.05 mg/g. Regarding non-linear curve fitting, the values of kinetic model parameters and correlation coefficient (R^2) values on the RHBC and SUBC hydrogels are depicted in Table 1. The kinetic data of the RHBC hydrogel showed a best fit with the Elovich model, with an R^2 value of 0.90.

The Elovich model describes the heterogeneous chemisorption kinetics on adsorbents. Considering the SUBC hydrogel, the best fitted model was the power function with a R^2 value of 0.97 which describes the homogeneous chemisorption kinetics. This supports the phenomena that was explained with the pH study (Section 3.2). The surface charge of the RHBC and SUBC hydrogels are negative and the available As(III) compound is neutral. Therefore, electrostatic interactions are impossible. The -OH groups of the hydrogels can form monodentate complexes with HAsO_2 . Kinetic, FTIR and pH studies strongly supported the phenomena and, therefore, it can be confirmed the chemisorption mechanism is prominent in As(III) adsorption into RHBC and SUBC hydrogels.

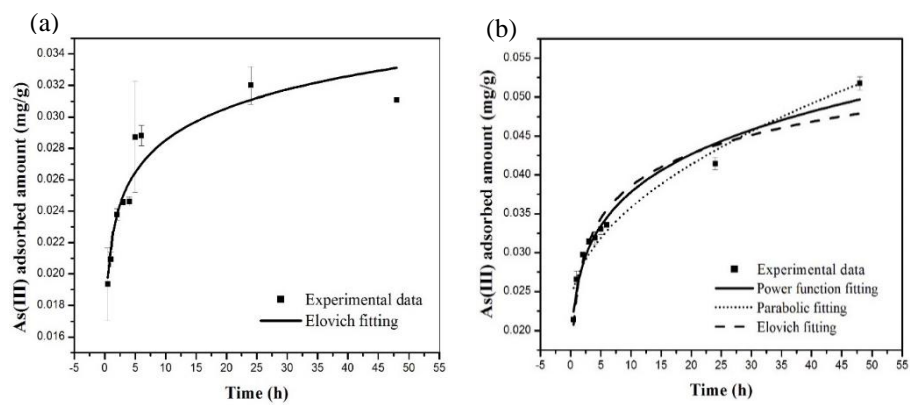


Figure 2 Kinetic data and the best fitting kinetic models on (a) RHBC hydrogel, (b) SUBC hydrogel

Table 1 Non-linear kinetic parameters of As(III) adsorption into RHBC and SUBC hydrogel composites

Model	Non-linear equation	Description	Isotherm parameters	Value			R ²	
				RHBC hydrogel	SUBC hydrogel	RHBC hydrogel		
Pseudo-second order	$q_t = \frac{q_e^2 K_2 t}{1 + K_2 t q_e}$	K ₂ – the rate constant (g/mg/min)	K ₂	82.48	28.99	0.82	0.71	
			q _e , q _t – sorption capacity at equilibrium and at time t, respectively (mg/g)	q _e	0.03	0.04		
Pseudo-first order	$q_t = q_e [1 - e^{-K_1 t}]$	K ₁ – the rate constant (min ⁻¹)	K ₁	1.78	1.22	0.53	0.43	
			q _e , q _t – sorption capacity at equilibrium and at time t, respectively (mg/g)	q _e	0.02	0.03		
Elovich	$q_t = b \ln(ab) + \ln(t)$	q _t – sorption capacity at time t (mg/g)	a	4.99	0.38	0.90	0.95	
			a – initial sorption rate (mg/g/min)	b	341.69	168.05		
			b – desorption constant (g/mg)	b	0.02	0.02	0.87	0.97
Power function	$q_t = b(t^{k_f})$	b – power function constant	k _f	0.10	0.17			
			k _f – power function rate constant	a	0.02	0.02	0.70	0.96
Parabolic	$q_t = a + k_p \sqrt{t}$	q _t – sorption capacity at time t (mg/g)	a	0.02	0.02	0.70	0.96	
			a – parabolic constant	k _p	0.001	0.004		
		k _p – parabolic rate constant						

3.4. Adsorption isotherm

The isotherm parameters of the RHBC and SUBC hydrogels for three different non-linear isotherm models are given in Table 2. Figures 3 (a) and (b) show the best-fitted adsorption isotherms for the adsorption of As(III) into the RHBC and SUBC hydrogels, respectively.

According to the model parameters, the RHBC hydrogel is best fitted with the Langmuir isotherm model, with a R^2 value of 0.99. The model parameters and the best-fitted model further confirm and explain the chemisorption mechanism of As(III) adsorption into the RHBC hydrogel. Further, the Langmuir model assumes monolayer adsorption where adsorption can only occur at a fixed number of definite localised sites that are identical and equivalent. As(III) adsorption can only occur with complexation with -OH functional groups and, as a result, adsorption sites can be found with a fixed number, and they are identical and equivalent. Thus, the chemisorption mechanism can be strongly proposed for As(III) adsorption into the RHBC hydrogel. Further, the Freundlich model (R^2 0.98) also shows good fitting parameters that explain heterogeneous multilayer adsorption with physisorption mechanisms. The surface morphology of the RHBC hydrogel (Figure S9) explains that the RHBC hydrogel has a porous outer and inner structure. Therefore, a pore filling mechanism can be a part of the As(III) adsorption process for the RHBC hydrogel.

Regarding the SUBC hydrogel, the best-fitted isotherm model is the Freundlich model (R^2 0.96) which explains heterogeneous multilayer adsorption with a physisorption mechanism. Considering the surface morphology of the hydrogel (Figure S10), pore filling can be proposed as the physisorption mechanism that facilitates the diffusion of As(III) into the hydrogel structure. The Langmuir model also shows a good fit with the experimental data with an R^2 value of 0.96. Therefore, it confirms the monolayer chemisorption mechanism of As(III) into the SUBC hydrogel through monodentate complex formation.

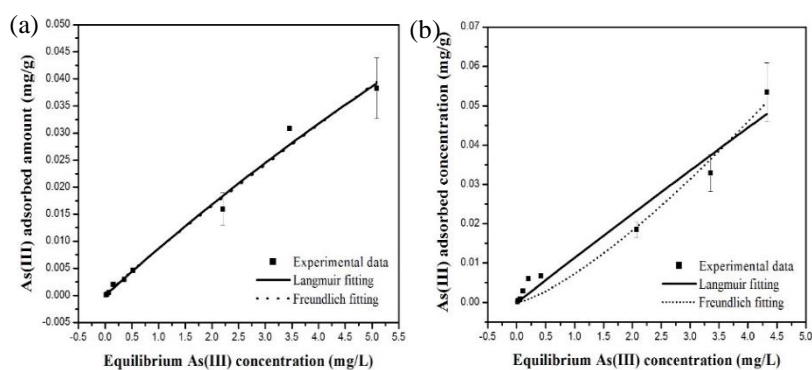


Figure 3 Isotherm data and best fitted isotherm models on (a) RHBC hydrogel and (b) SUBC hydrogel

Table 2 Non-linear isotherm parameters for As(III) adsorption into RHBC and SUBC hydrogel composite

Model	Non-linear equation	Description	Isotherm parameters	Value			R ²
				RHBC hydrogel	SUBC hydrogel	SUBC hydrogel	
Freundlich	$q_{ads} = K_F C_e^n$	K_F – the Freundlich affinity – capacity parameter (mg/g)/(mg/L) ⁿ n – the Freundlich exponent	K_F 0.008	0.007	0.98	0.97	
Langmuir	$q_{ads} = \frac{q_{max} K_L C_e}{1 + K_L C_e}$	Q_{max} – the amount of adsorbate adsorbed per unit weight of adsorbent (mg/g) Q_{max} – the maximum adsorption capacity (mg/g) K_L – the Langmuir affinity parameter (L/mg) C_e – the equilibrium adsorbate aqueous phase concentration (mg/L)	n 0.93	1.33	0.99	0.96	
Dubinin-Radushkevich	$q_{ads} = q_D \exp \left(-B_D \left[RT \ln \left(1 + \frac{1}{C_e} \right) \right]^2 \right)$	q_D – Monolayer adsorption capacity (mg/g) B_D – mean free energy sorption (mol ² /kJ)	q_D 0.05	0.07	0.98	0.95	
			B_D 7.95	10.54			

3.5. Desorption and re-adsorption of As(V) on RHBC and SUBC hydrogel

One of the major objectives of the present study was overcoming the classic drawbacks of the adsorption method such as additional energy requirements on water-adsorbent separation and unavailability for re-use. The re-use of adsorptive materials can reduce waste generation. As a result, production and processing costs can be reduced; enhancing financial efficiency. In previous studies of RHBC and SUBC hydrogels on As(V) removal, 0.1 M NaOH was identified as a reliable method for regeneration of these particular hydrogels, thus facilitating their re-use.

Figure 3 shows the adsorption, desorption and resorption capacities of RHBC and SUBC hydrogels over three cycles. One of the identical characteristics of the regeneration of RHBC and SUBC hydrogels with 0.1 M NaOH is enhancement of the adsorption capacities of the hydrogel in the second cycle. When the hydrogel is treated with 0.1 M NaOH, the Na^+ ions, they can retain the hydrogel surface and diffuse into the hydrogel structure. The 0.1 M NaOH can replace $-\text{NH}_2$ groups with Na^+ of the hydrogel structure and form strongly ionisable carboxylic acid groups. These Na^+ ions create electrostatic repulsive effects between As(III) oxyanions. This increases the surface pH of the hydrogel up to the range of pH 11-12. With that, in the next cycle it can activate the $\text{H}_2\text{AsO}_3^{3-}$ oxyanions and the electrostatic repulsive effects between $\text{H}_2\text{AsO}_3^{3-}$ oxyanions, and the hydrogel negative surface increases the adsorption capacity of the hydrogel.

Furthermore, the alkalinity of 0.1 M NaOH with the RHBC hydrogel leads to the adsorption increasing by 20%, and with SUBC hydrogel it is a 45% increment. However, when it reaches the third cycle, the adsorption capacity is decreased significantly in the RHBC hydrogel and in SUBC hydrogel the adsorption is zero. Therefore, with the proposed 0.1 M NaOH regeneration method, the hydrogel can only be used for two cycles of As(III) removal.

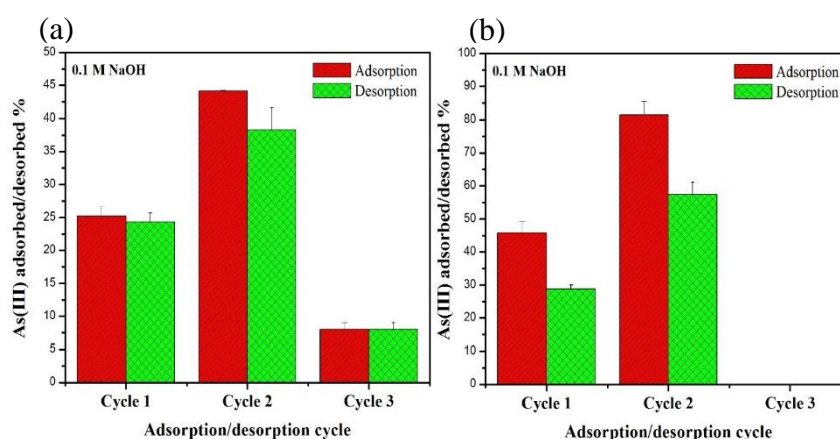


Figure 4 Adsorption and desorption capacities of (a) RHBC hydrogel, (b) SUBC hydrogel

3.6. Comparison of As(III) removal with As(V) removal by RHBC and SUBC hydrogels

The solution pH and the redox potential decides the availability of As form in the water. Therefore, the two forms of same metalloid act in different ways in terms of adsorption. As a result, most adsorptive materials are not effective for simultaneous As(III) and As(V) removal, and most show a low adsorption capacity for As(III) compared to As(V) (Deng et al., 2008; Goh et al., 2009; Li et al., 2010). The adsorptive materials used in the present study have been used for As(V), and Table 3 depicts the comparison of As(III) and As(V) adsorption by the RHBC and SUBC hydrogels.

Regarding As(V) removal, two kinds of functional groups are involved: $-NH_2$ and $-CO$ groups. For As(III) removal, only $-OH$ groups are available for attracting the As(III) compounds. The protonated surface facilitates As(V) adsorption since oxyanions are available for binding with protonated functional groups. However, regarding As(III), when the solution pH is < 9 , only the neutral $HAsO_2$ form can be found and, therefore, the affinity towards As(III) is comparatively low in both the RHBC and SUBC hydrogels compared to those of As(V).

The regeneration and re-use of RHBC and SUBC hydrogels on As(III) is less effective compared to As(V). As(V) shows significant adsorption capabilities for four adsorption cycles, and the cumulative adsorption capacity is 0.16 mg/g for both RHBC and SUBC hydrogels. However, regarding As(III) adsorption, reusability is limited to two adsorption cycles and the cumulative As(III) adsorptions were 0.08 and 0.13 mg/g into RHBC and SUBC hydrogel respectively.

Table 3 Comparison between As(III) and As(V) removal with RHBC and SUBC hydrogels

Condition/results	RHBC hydrogel		SUBC hydrogel	
	As(III)	As(V)	As(III)	As(V)
Optimum pH range	6-7.5	6-7	6-7.5	6-7
Best fitted kinetic model	Elovich	Pseudo-first order	Power-function	Pseudo-second order
Best fitted isotherm model	Langmuir	Langmuir	Langmuir	Langmuir
Mechanisms involved in adsorption	monodentate complex formation	Electrostatic interaction, porous diffusion, H-bonding	monodentate complex formation	Electrostatic interaction, porous diffusion, H-bonding
Cumulative arsenic adsorption	0.08 mg/g	0.16 mg/g	0.13 mg/g	0.16 g/g

4. Conclusion

The biochar-hydrogel composites were successfully synthesised and showed efficient removal and re-usable capacities for As(V). In the present study, the two different biochar-hydrogel composites known as RHBC and SUBC hydrogels were assessed for their capacity for As(III) removal. In terms of toxicity, As(III) is more concerning than As(V). Just as the As(V) the As(III) adsorption was pH dependent; the pH 6-7.5 range was identified as the optimum pH range. The kinetic and isotherm experiments proved the chemisorption and physisorption mechanisms of As(III) adsorption into the RHBC and SUBC hydrogels. The porous structure facilitated porous diffusion of As(III) into the RHBC and SUBC hydrogels.

Regarding the chemisorption mechanism, the only possible mechanism was monodentate complexation of the -OH groups of the hydrogels with HAsO_2 . The surface protonation in both the RHBC and SUBC hydrogels with the change of solution pH facilitated As(V) adsorption into the RHBC and SUBC hydrogels. But, regarding As(III) adsorption on the protonated surface, this is not possible. At the pH levels of less than 9 the neutral HAsO_2 exists and only the -OH groups can attract HAsO_2 which limit the As(III) adsorption into the RHBC and SUBC hydrogels.

The RHBC and SUBC hydrogels are available for re-use in terms of As(III) adsorption. However, this is limited to only two cycles which results in low As(III) adsorption capacity. When compared to As(V) adsorption, As(III) adsorption into both the RHBC and SUBC hydrogels was low. However, the adsorption can be enhanced if a self-oxidisation process is implanted into the RHBC and SUBC hydrogels. Hence, further research opportunities are open with RHBC and SUBC hydrogels to enhance the removal capacities of As(III).

Most importantly, the RHBC and SUBC hydrogels can be used for simultaneous removal of As(III) and As(V) as the optimum pH range is the same for both. Moreover, the two arsenic species do not compete for adsorptive sites as As(III) and As(V) binding sites are different from each another. The RHBC and SUBC hydrogels do not dissociate in the water and, after the adsorption process, the hydrogels can simply be removed from water without any particles or colour remaining. After employment in the adsorption process, the hydrogels shrink with dry conditions. Further, the RHBC and SUBC hydrogels can also be applied to the large-scale water purification process with its re-usable and easy separation characteristics.

Acknowledgements

The authors acknowledge the support from Anya J. E. Yago, Dr Craig Stoppiello and Dr Lachlan Casey at the Centre for Microscopy and Microanalysis (CMM) at the University of Queensland.

The authors thank Dr Barbara Harmes and Sandra Cochrane from the University of Southern Queensland, Australia for providing help with language correction.

Financial support of this work by the University of Southern Queensland, QLD, Australia (RTP Stipend Scholarship programme) is gratefully acknowledged.

References

- Ahmed, W., Mehmood, S., Núñez-Delgado, A., Ali, S., Qaswar, M., Shakoor, A., Maitlo, A.A. and Chen, D.-Y. 2021. Adsorption of arsenic (III) from aqueous solution by a novel phosphorus-modified biochar obtained from *Taraxacum mongolicum* Hand-Mazz: Adsorption behavior and mechanistic analysis. *Journal of Environmental Management* 292, 112764.
- Al-Ghouti, M.A. and Da'ana, D.A. 2020. Guidelines for the use and interpretation of adsorption isotherm models: a review. *Journal of Hazardous materials* 393, 122383.
- Amen, R., Bashir, H., Bibi, I., Shaheen, S.M., Niazi, N.K., Shahid, M., Hussain, M.M., Antoniadis, V., Shakoor, M.B. and Al-Solaimani, S.G. 2020. A critical review on arsenic removal from water using biochar-based sorbents: the significance of modification and redox reactions. *Chemical Engineering Journal* 396, 125195.
- Benjelloun, M., Miyah, Y., Evrendilek, G.A., Zerrouq, F. and Lairini, S. 2021. Recent advances in adsorption kinetic models: their application to dye types. *Arabian Journal of Chemistry* 14(4), 103031.
- Bundschuh, J., Armienta, M.A., Morales-Simfors, N., Alam, M.A., López, D.L., Delgado Quezada, V., Dietrich, S., Schneider, J., Tapia, J. and Sracek, O. 2021. Arsenic in Latin America: New findings on source, mobilization and mobility in human environments in 20 countries based on decadal research 2010-2020. *Critical Reviews in Environmental Science and Technology* 51(16), 1727-1865.
- Bundschuh, J., Niazi, N.K., Alam, M.A., Berg, M., Herath, I., Tomaszewska, B., Maity, J.P. and Ok, Y.S. 2022. Global arsenic dilemma and sustainability. *Journal of Hazardous Materials* 436, 129197.

- Deng, S., Yu, G., Xie, S., Yu, Q., Huang, J., Kuwaki, Y. and Iseki, M. 2008. Enhanced adsorption of arsenate on the aminated fibers: sorption behavior and uptake mechanism. *Langmuir* 24(19), 10961-10967.
- Foo, K.Y. and Hameed, B.H. 2010. Insights into the modeling of adsorption isotherm systems. *Chemical Engineering Journal* 156(1), 2-10.
- Goh, K.-H., Lim, T.-T. and Dong, Z. 2009. Enhanced arsenic removal by hydrothermally treated nanocrystalline Mg/Al layered double hydroxide with nitrate intercalation. *Environmental Science & Technology* 43(7), 2537-2543.
- Guo, H., Stüben, D. and Berner, Z. 2007. Adsorption of arsenic (III) and arsenic (V) from groundwater using natural siderite as the adsorbent. *Journal of Colloid and Interface Science* 315(1), 47-53.
- Kumarathilaka, P., Bundschuh, J., Seneweera, S. and Ok, Y.S. 2021a. An integrated approach of rice hull biochar-alternative water management as a promising tool to decrease inorganic arsenic levels and to sustain essential element contents in rice. *Journal of Hazardous materials* 405, 124188.
- Kumarathilaka, P., Bundschuh, J., Seneweera, S. and Ok, Y.S. 2021b. Rice genotype's responses to arsenic stress and cancer risk: the effects of integrated birnessite-modified rice hull biochar-water management applications. *Science of the Total Environment* 768, 144531.
- Kumarathilaka, P., Seneweera, S., Meharg, A. and Bundschuh, J. 2018. Arsenic speciation dynamics in paddy rice soil-water environment: sources, physico-chemical, and biological factors-a review. *Water Research* 140, 403-414.
- Kumarathilaka, P., Seneweera, S., Ok, Y.S., Meharg, A.A. and Bundschuh, J. 2020. Mitigation of arsenic accumulation in rice: an agronomical, physico-chemical, and biological approach—a critical review. *Critical Reviews in Environmental Science and Technology* 50(1), 31-71.
- Li, C., Bundschuh, J., Gao, X., Li, Y., Zhang, X., Luo, W. and Pan, Z. 2022. Occurrence and behavior of arsenic in groundwater-aquifer system of irrigated areas. *Science of The Total Environment*, 155991.
- Li, Z. 1999. Sorption kinetics of hexadecyltrimethylammonium on natural clinoptilolite. *Langmuir* 15(19), 6438-6445.
- Li, Z., Deng, S., Yu, G., Huang, J. and Lim, V.C. 2010. As (V) and As (III) removal from water by a Ce–Ti oxide adsorbent: behavior and mechanism. *Chemical Engineering Journal* 161(1-2), 106-113.

- Manning, B.A. and Goldberg, S. 1997. Adsorption and stability of arsenic (III) at the clay mineral– water interface. *Environmental science & technology* 31(7), 2005-2011.
- Mao, J., Zhang, K. and Chen, B. 2019. Linking hydrophobicity of biochar to the water repellency and water holding capacity of biochar-amended soil. *Environmental Pollution* 253, 779-789.
- Martinson, C.A. and Reddy, K. 2009. Adsorption of arsenic (III) and arsenic (V) by cupric oxide nanoparticles. *Journal of Colloid and Interface Science* 336(2), 406-411.
- Mayakaduwa, S., Kumarathilaka, P., Herath, I., Ahmad, M., Al-Wabel, M., Ok, Y.S., Usman, A., Abduljabbar, A. and Vithanage, M. 2016. Equilibrium and kinetic mechanisms of woody biochar on aqueous glyphosate removal. *Chemosphere* 144, 2516-2521.
- Mensah, A.K., Marschner, B., Wang, J., Bundschuh, J., Wang, S.-L., Yang, P.-T., Shaheen, S.M. and Rinklebe, J. 2022. Reducing Conditions Increased the Mobilisation and Hazardous Effects of Arsenic in A Highly Contaminated Gold Mine Spoil. *Journal of Hazardous Materials*, 129238.
- Ohe, K., Tagai, Y., Nakamura, S., Oshima, T. and Baba, Y. 2005. Adsorption behavior of arsenic (III) and arsenic (V) using magnetite. *Journal of Chemical Engineering of Japan* 38(8), 671-676.
- Vithanage, M., Weerasundara, L. and Ghosh, A. (2019) *Environmental Arsenic in a Changing World*, pp. 561-562, CRC Press.
- Weerasundara, L., Gabriele, B., Figoli, A., Ok, Y.-S. and Bundschuh, J. 2021a. Hydrogels: Novel materials for contaminant removal in water—A review. *Critical Reviews in Environmental Science and Technology* 51(17), 1970-2014.
- Weerasundara, L., Ok, Y.-S. and Bundschuh, J. 2021b. Selective removal of arsenic in water: a critical review. *Environmental Pollution* 268, 115668.
- Zhang, T., Wang, J., Zhang, W., Yang, C., Zhang, L., Zhu, W., Sun, J., Li, G., Li, T. and Wang, J. 2019. Amorphous Fe/Mn bimetal–organic frameworks: outer and inner structural designs for efficient arsenic (iii) removal. *Journal of Materials Chemistry A* 7(6), 2845-2854.

Supplementary materials

Assessment of As(III) removal from water with biochar hydrogel composites which were successful in As(V) removal in water and overcome the classical drawbacks of adsorbent materials

Lakshika Weerasundara, Prasanna Kumarathilaka, Alla Marchuk Jochen

Bundschuh *

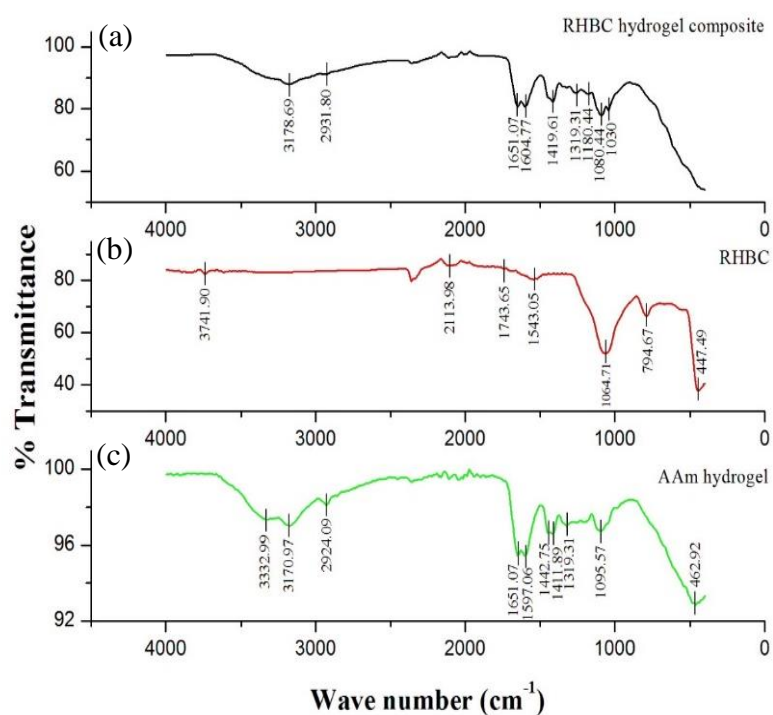


Figure S1 FTIR spectra for (a) RHBC hydrogel composite, (b) RHBC, (c) Acrylamide hydrogel without RHBC

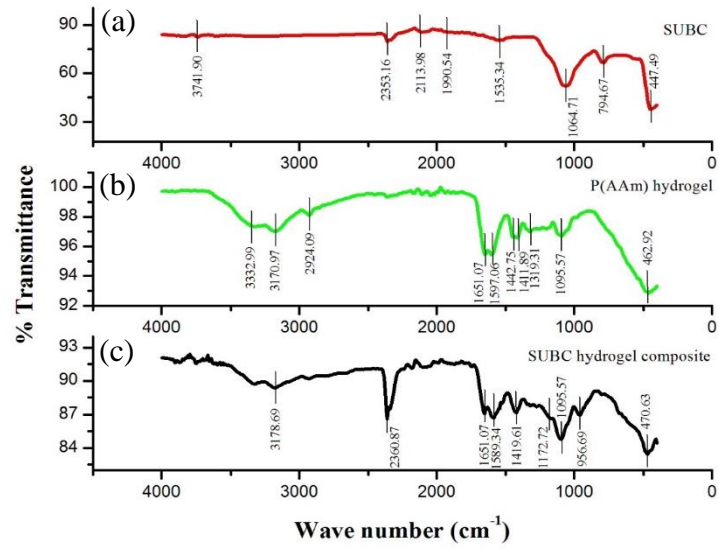


Figure S2 FTIR spectra for (a) SUBC, (b) Acrylamide hydrogel, (c) SUBC hydrogel composite

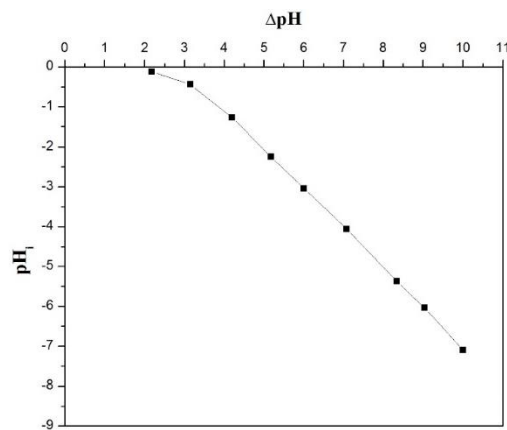


Figure S1 Plot of ΔpH vs pH_i for salt addition method to determine the PZC of RHBC hydrogel composite

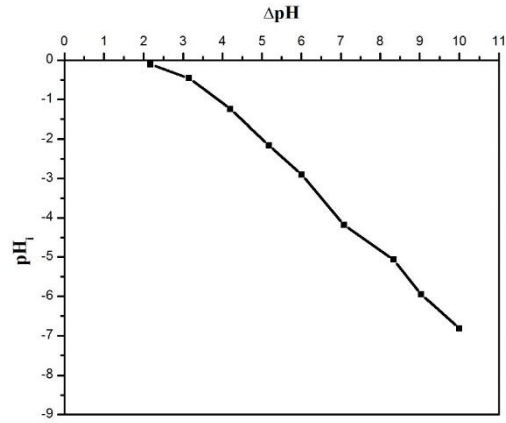


Figure S4 Plot of ΔpH vs pH_i for salt addition method to determine the PZC of SUBC hydrogel composite

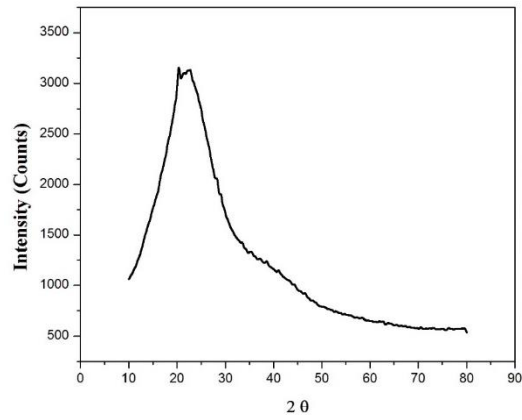


Figure S5 XRD pattern for RHBC hydrogel composite

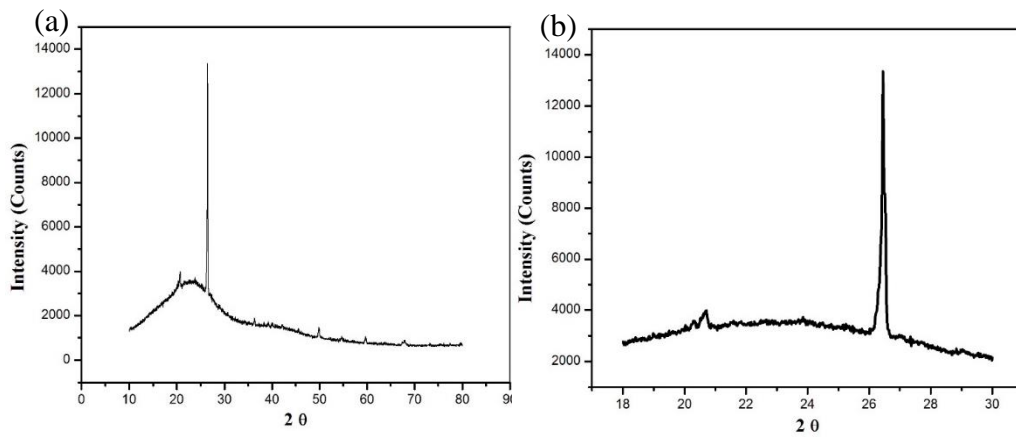


Figure S6 XRD pattern for SUBC hydrogel composite (a) Full spectra of the XRD pattern, (b) Separated section of the Silica peak

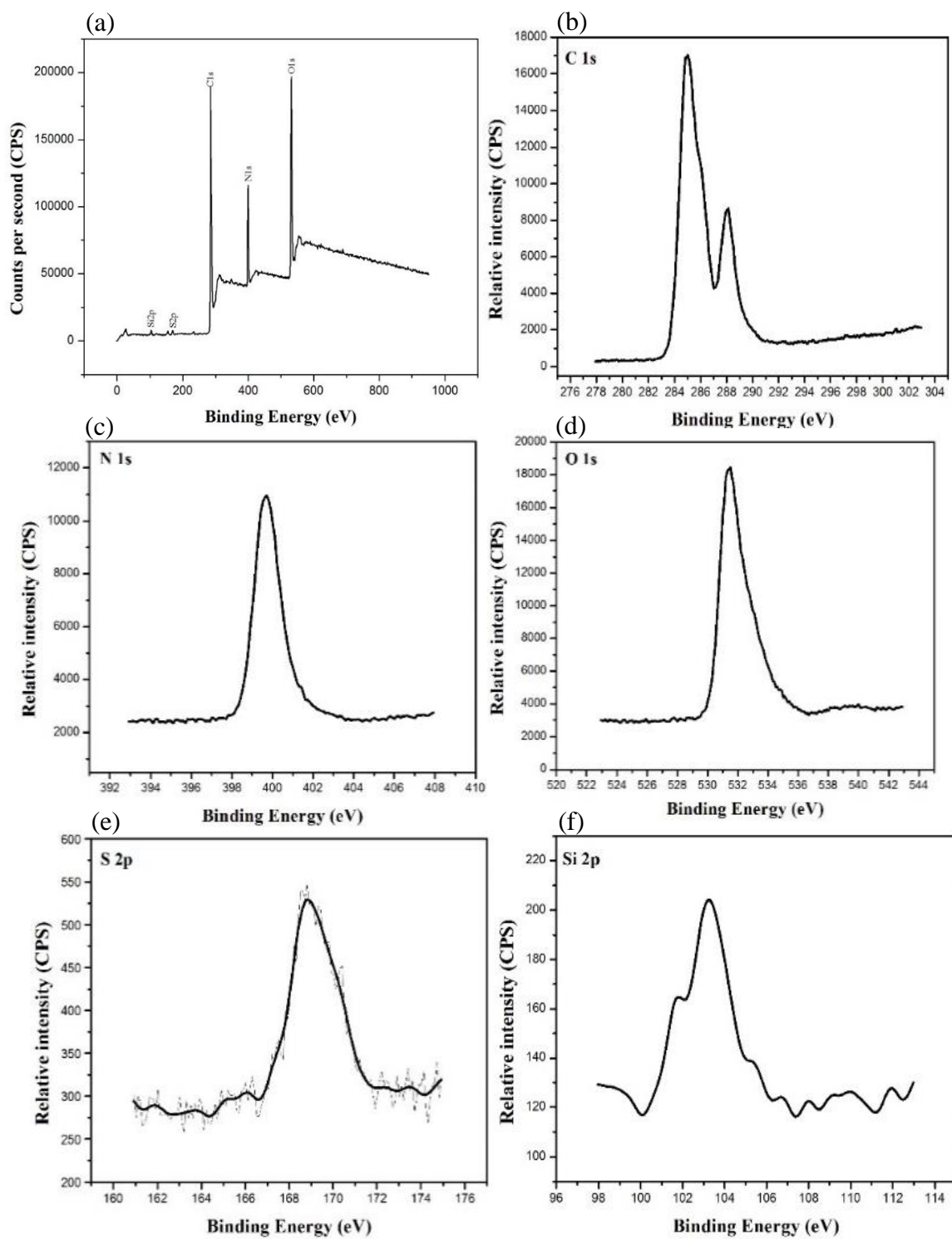


Figure S2 XPS spectra of RHBC hydrogel composite (a) The wide-scan XPS spectra, refined XPS spectra of (b) C 1s, (c) N 1s, (d) O 1s, (e) S 2p, (f) Si 2p

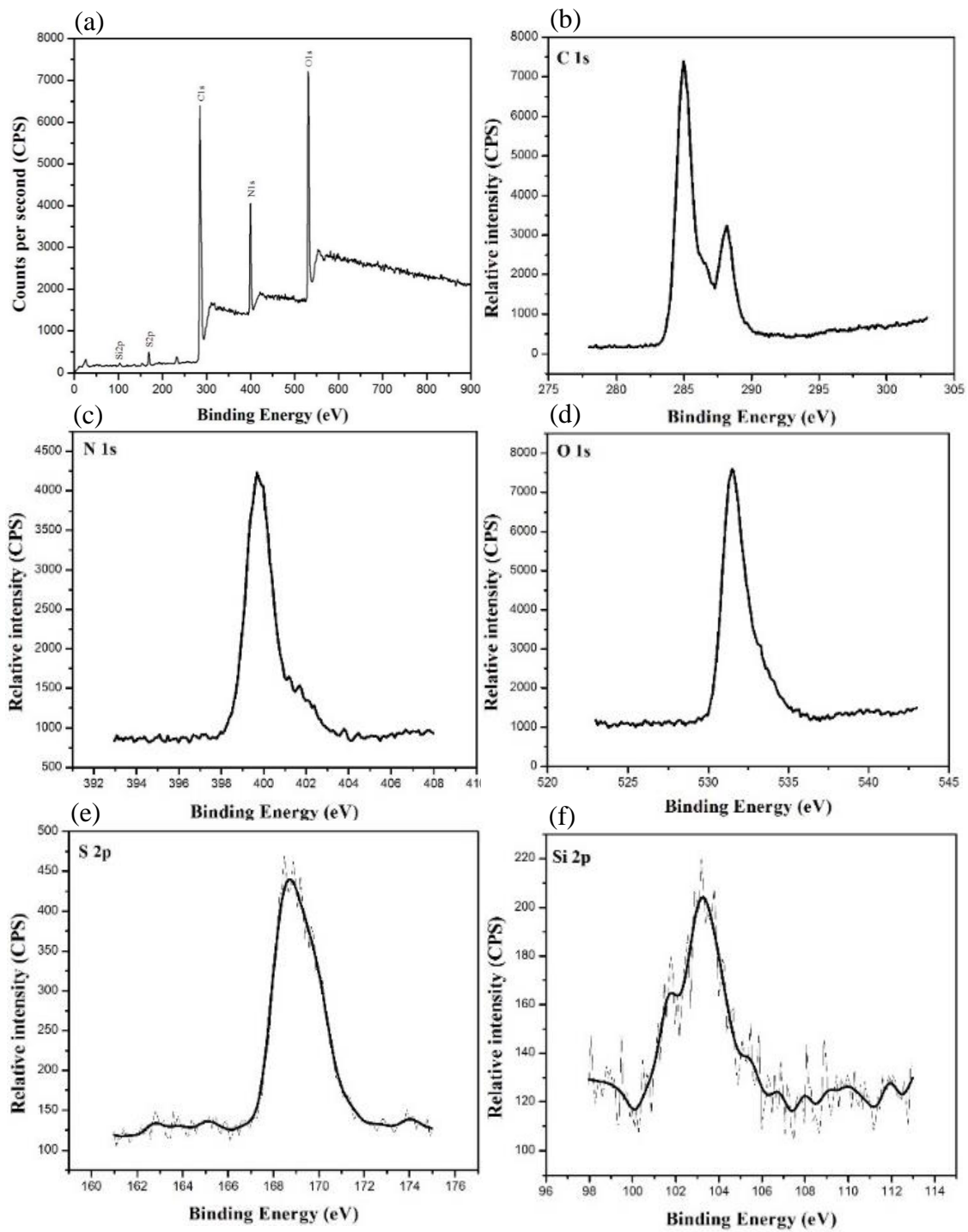


Figure S8 (a) The wide-scan XPS spectra of the SUBC hydrogel composite, refined XPS spectra of (b) C 1s, (c) N 1s, (d) O 1s, (e) S 2p, (f) Si 2p

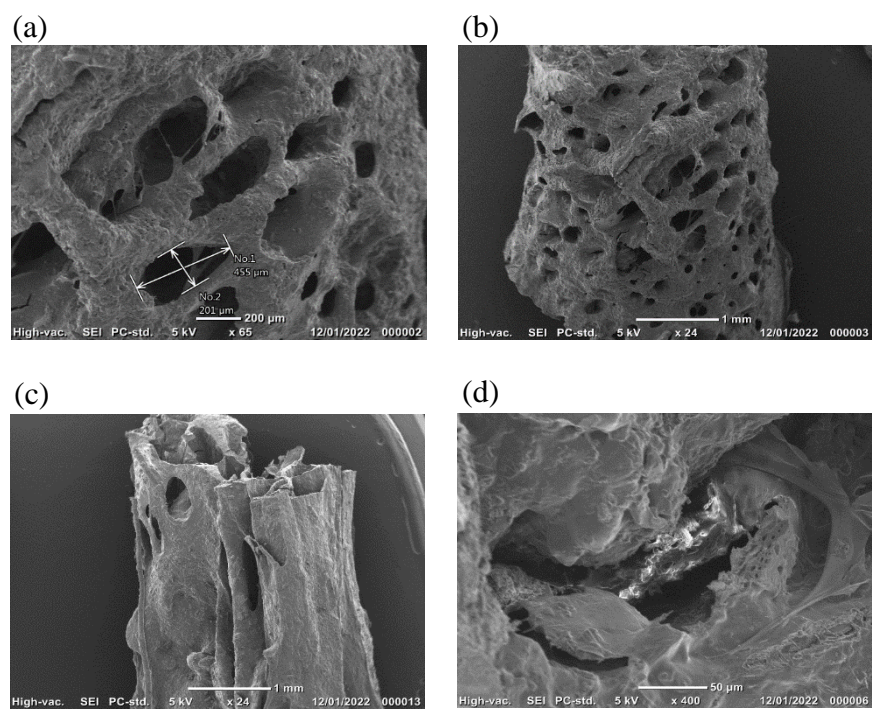


Figure S9 SEM images of RHBC hydrogel composite (a), (b), (c) Surface (d) Inside a pore

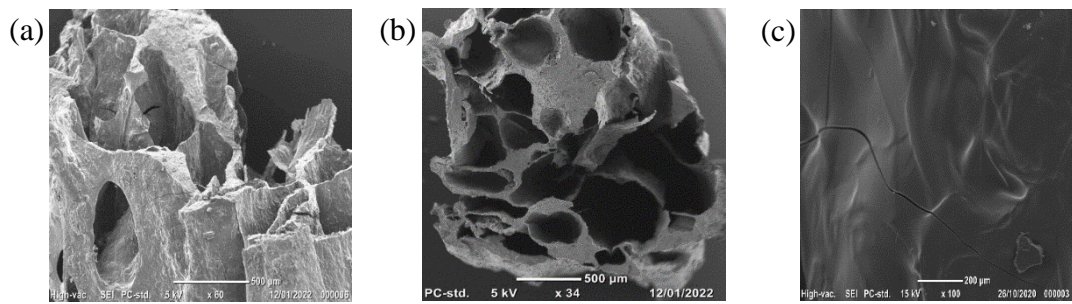


Figure S10 SEM images of SUBC hydrogel composite (a) Surface, (b) Cross-section (c) SEM image of pure acrylamide hydrogel (surface)

7.3. Concluding remarks

This study conducted to assess the As(III) removal capabilities of RHBC and SUBC hydrogels. The kinetic and isotherm experiments proved the chemisorption and physisorption mechanisms of As(III) adsorption into RHBC and SUBC hydrogels. The RHBC and SUBC hydrogels were available for re-use in terms of As(III) adsorption. However, this is limited only to two cycles which results in low As(III) adsorption capacity. Considering As(V), both hydrogel composites showed efficient adsorption capacities for five adsorption cycles. When compared to As(V) adsorption, the As(III) adsorption onto both RHBC and SUBC hydrogels was low. However, adsorption can be enhanced if a self-oxidization process is implanted into the RHBC and SUBC hydrogels. Hence, further modifications of both hydrogel composites are required before they can be considered as a successful method to remove As(III). Most importantly, the RHBC and SUBC hydrogels can be used for simultaneous removal of As(III) and As(V) as the optimum pH range is the same for both. Moreover, the two arsenic species do not compete for adsorptive sites as their binding sites are different from each another.

CHAPTER 8: DISCUSSION AND CONCLUSION

This chapter represents a comprehensive overview of the key findings of this PhD research project and provides recommendations for future research directions.

8.1. Discussion and Conclusions

This PhD research project initially investigated the current knowledge and research gaps in the field of As removal from water. Those research gaps and our new insights have been used to design and implement science-based, cost-effective, practically employable, easily separable, recyclable, re-useable and sustainable materials to remove As from water to meet the demands of the WHO safe water guideline.

As contamination of water has been a serious issue for a long period of time and a number of decontamination methods are available in literature. However, an efficient and reliable de-contamination method has not been found. The adsorption technique can be used as a low-cost method, but significant associated drawbacks remain. Most of the effective adsorbent materials are in powder form or form small particles which can easily disperse into the water. Further, these materials tend to change the colour of water. Although existing materials are efficient in As removal, the most concerning issue raised is after treatment when the adsorbent must be separated from the water. Separating the powder or particles containing materials such as biochar and nanoparticles from water requires high energy, high-tech procedures and expertise knowledge. This adds additional cost to the water treatment system/process. Further, most of these materials are not available for re-use, and after one treatment cycle the adsorbent must be discarded. This creates a huge amount of waste material which, again, increases the cost of the treatment process.

Taking these important and unresolved facts, this PhD study focused on the development of materials to remove As from water while facilitating easy adsorbent-water separation and reusability. The findings of this study provide new insights to the contaminant removal processes from aqueous media. The study focused on two types of hydrogel materials with BC and Fe₃O₄ nanoparticles. Regarding BC, two types of hydrogels were developed with different BC types: RHBC and SUBC. The BC hydrogels were developed as acrylamide hydrogels. Considering three different pyrolysis temperatures and three different sizes fractions, nine different BCs were developed from the RHBC and SUBC. Finally, nine hydrogels were synthesised from each BC type. Both RHBC and SUBC hydrogels were successfully developed and assessed for As(V) and As(III) removal from water.

Regarding As(V) removal, the best hydrogel types were 700 °C and 0.06 mm size BC containing RHBC and SUBC hydrogels. Both RHBC and SUBC hydrogels showed the pH dependent nature of As(V) removal where the best pH for As(V) removal was the 6-7 range. In both the RHBC and SUBC hydrogels in the 6-7 pH range, the -NH₂ and -CO groups in the polymeric chain tended to protonate and the surface of the hydrogels became positively charged. This positively charged surface facilitated adsorption of the As(V) oxyanions, H₂AsO₄⁻ and HAsO₄²⁻.

Both isotherm and kinetic modeling data for the RHBC and SUBC hydrogel composites suggests that As(V) adsorption is associated with physisorption and chemisorption mechanisms. Physical adsorption is mainly caused by the forces of molar interactions including $\Pi^+\Pi$ electron donor-acceptor interactions, porous diffusion and H-bonding via H-donor-acceptor interactions. The porous diffusion can be identified as the major mechanism as the hydrogel surface contains a porous structure and hydrogels make three-dimensional structures as they swell in aqueous media. The molecules that diffused through porous diffusion later undergo further chemisorption and physisorption mechanisms as the swollen hydrogel opens more functional groups and more porous structures within the RHBC and SUBC particles.

The best pH range for adsorption was found to be 6-7.5 where only the neutral As(III) species (HAsO₂) can be found. The kinetic and isotherm experiments proved the chemisorption and physisorption mechanisms for As(III) adsorption into RHBC and SUBC hydrogels. The porous structure facilitates the porous diffusion of As(III) into RHBC and SUBC hydrogels. Regarding the chemisorption mechanism, the only possible mechanism is the monodentate complexation of the -OH groups of the hydrogels with HAsO₂. With pH levels less than 9, the only As(III) species exists as neutral HAsO₂, and it only attaches with -OH groups which limit As(III) adsorption into RHBC and SUBC hydrogels.

When compared to As(V) adsorption, As(III) adsorption was low into both the RHBC and SUBC hydrogels. However, adsorption can be enhanced if a self-oxidisation process is implanted into the RHBC and SUBC hydrogels. Hence, further research opportunities are available to consider the enhancement of RHBC and SUBC hydrogels' As(III) removal capacity. Most importantly, RHBC and SUBC hydrogels can be used for simultaneous removal of both As(III) and As(V) as the optimum pH range is the same for both As(III) and As(V). Moreover, the two arsenic species do not compete for adsorptive sites as their binding sites are different from each other's.

RHBC and SUBC hydrogel composites can be considered a revolutionary solution for removing As(V) and As(III) from water because of their availability for regeneration and re-use. 0.1 M NaOH is a successful solution for the desorption of As(V) and As(III) from the RHBC hydrogel composite, and it further increases the adsorption capacity of the RHBC hydrogel for As(V). The RHBC and SUBC hydrogels do not dissociate in water and, after the adsorption process, the hydrogels can be removed from water without any particles or colour remaining. After use in the adsorption process, the hydrogels shrink again in the dry conditions. Furthermore, as a result of their re-usable and easy separation characteristics, RHBC and SUBC hydrogels can also be used in large-scale water purification processes.

Regarding Fe₃O₄ nanoparticles-based hydrogel, it was synthesised modifying a chitosan hydrogel. The ChFe hydrogel also showed pH dependent characteristics on As(V) removal and the best pH range for As(V) removal was pH 4-5. Within the pH 3-6.6 range, the hydrogel surface became positively charged due to protonation of the -NH₂ and -OH groups in the chitosan and PVA, and the positive surface attracted H₂AsO₄⁻ and HAsO₄²⁻ oxyanions. Further, within pH 3-6.6, the Fe₃O₄ nanoparticles formed inner and outer surface complexes with H₂AsO₄⁻ and HAsO₄²⁻ oxyanions and so adsorbed As(V).

Chemisorption adsorption mechanisms have been proposed for the adsorption of As(V) into the ChFe hydrogel composite based on kinetic and isotherm data. The ChFe hydrogel was further modified with Cu(II) ions to create more adsorption sites for the As(V). The modification did not change the best pH range for As(V) adsorption. Both isotherm and kinetic modeling data suggest that the As(V) adsorption into the ChFe-Cu hydrogel composite is associated with the chemisorption mechanism. The chemical and physical characterisation data on the ChFe-Cu hydrogel composite further support the chemisorption mechanism proposal showing that there are several kinds of functional groups that attract As(V) oxyanions. These possible mechanisms are electrostatic interactions, Lewis-acid-base interactions, inner-sphere ligand exchange complex formation, bidentate corner-sharing (²C) and bidentate edge-sharing (²E) trimetric surface complex formation. 0.1 M CH₃COOH provided a successful solution for the regeneration of the ChFe and ChFe-Cu hydrogel composites and it further increased the adsorption capacity for As(V). Further, the ChFe and ChFe-Cu hydrogel composite can be considered as a solution to overcome classic drawbacks of adsorbents such as adsorbent-water separation which prevents upscaling to a large industrial scale.

8.2. Recommendations

This PhD research project successfully investigated easily separable and re-usable hydrogel materials for As removal from water. The following research recommendations are made:

1. Conduct field level studies before applying the materials in treatment plants
2. Conduct adsorption studies for other potential contaminants to determine their suitability for use as adsorbent materials for a mix of contaminants
3. Conduct fixed-bed column experiments to determine the effect of flowrate of water on adsorption rate and capacity
4. Conduct an economic feasibility analysis to evaluate the applicability of the studied materials into commercial level and/or large-scale application.

REFERENCES

- Ahmad, K., Shah, H.-U.-R., Nasim, H.A., Ayub, A., Ashfaq, M., Rauf, A., Shah, S.S.A., Ahmad, M.M., Nawaz, H. and Hussain, E., 2022. Synthesis and characterization of water stable polymeric metallo organic composite (PMOC) for the removal of arsenic and lead from brackish water. *Toxin Reviews* 41(2), 577-587.
- Ahmed, E.M., 2015. Hydrogel: Preparation, characterization, and applications: A review. *Journal of Advanced Research* 6(2), 105-121.
- Alburaih, H., Ahmad, N., Ijaz, S., Al-Buriah, M., Farid, H.M.T., Arif, M., Husain, G., Ullah, H. and Alrowaili, Z., 2022. Synthesis of magnesium aluminates nanoparticles for the removal of arsenic from drinking water. <https://doi.org/10.21203/rs.3.rs-1575600/v1>
- Altowayti, W., Othman, N., Shahir, S., Alshalif, A., Al-Gheethi, A., Al-Towayti, F., Saleh, Z. and Haris, S., 2021. Removal of arsenic from wastewater by using different technologies and adsorbents: a review. *International Journal of Environmental Science and Technology*, 1-24.
- Argos, M., Ahsan, H. and Graziano, J.H., 2012. Arsenic and human health: epidemiologic progress and public health implications. *Reviews on Environmental Health* 27(4), 191-195.
- Baig, S.A., Sheng, T., Hu, Y., Xu, J. and Xu, X., 2015. Arsenic removal from natural water using low cost granulated adsorbents: a review. *CLEAN–Soil, Air, Water* 43(1), 13-26.
- Carneiro, M.A., Pintor, A.M., Boaventura, R.A. and Botelho, C.M., 2022. Efficient removal of arsenic from aqueous solution by continuous adsorption onto iron-coated cork granulates. *Journal of Hazardous Materials* 432, 128657.
- Choong, T.S., Chuah, T., Robiah, Y., Koay, F.G. and Azni, I., 2007. Arsenic toxicity, health hazards and removal techniques from water: an overview. *Desalination* 217(1-3), 139-166.
- Das, D., Prakash, P., Rout, P.K. and Bhaladhare, S., 2021. Synthesis and Characterization of Superabsorbent Cellulose-Based Hydrogel for Agriculture Application. *Starch-Stärke* 73(1-2), 1900284.
- de Araujo, C.M.B., Wernke, G., Ghislandi, M.G., Diório, A., Vieira, M.F., Bergamasco, R., da Motta Sobrinho, M.A. and Rodrigues, A.E., 2023. Continuous removal of pharmaceutical drug chloroquine and Safranin-O dye from water using agar-graphene oxide hydrogel: Selective adsorption in batch and fixed-bed experiments. *Environmental Research* 216, 114425.

- Dutta, D., Borah, J. and Puzari, A., 2021. Iron oxide coated hollow poly (methylmethacrylate) as an efficient adsorption media for removal of arsenic from water. *RSC advances* 11(22), 13376-13385.
- Dutta, P.K., Pehkonen, S., Sharma, V.K. and Ray, A.K., 2005. Photocatalytic oxidation of arsenic (III): evidence of hydroxyl radicals. *Environmental Science & Technology* 39(6), 1827-1834.
- Gupta, A.K., Deva, D., Sharma, A. and Verma, N., 2010. Fe-grown carbon nanofibers for removal of arsenic (V) in wastewater. *Industrial & Engineering Chemistry Research* 49(15), 7074-7084.
- Hamza, M.F., Alotaibi, S.H., Wei, Y. and Mashaal, N.M., 2022. High-Performance Hydrogel Based on Modified Chitosan for Removal of Heavy Metal Ions in Borehole: A Case Study from the Bahariya Oasis, Egypt. *Catalysts* 12(7), 721.
- He, J. and Charlet, L., 2013. A review of arsenic presence in China drinking water. *Journal of Hydrology* 492, 79-88.
- Hoffman, A.S., 2012. Hydrogels for biomedical applications. *Advanced Drug Delivery Reviews* 64, 18-23.
- Kobyas, M., Gebologlu, U., Ulu, F., Oncel, S. and Demirbas, E., 2011. Removal of arsenic from drinking water by the electrocoagulation using Fe and Al electrodes. *Electrochimica Acta* 56(14), 5060-5070.
- Kumarathilaka, P., Seneweera, S., Meharg, A. and Bundschuh, J., 2018a. Arsenic accumulation in rice (*Oryza sativa* L.) is influenced by environment and genetic factors. *Science of the Total Environment* 642, 485-496.
- Kumarathilaka, P., Seneweera, S., Meharg, A. and Bundschuh, J., 2018b. Arsenic speciation dynamics in paddy rice soil-water environment: sources, physico-chemical, and biological factors-a review. *Water Research* 140, 403-414.
- Leist, M., Casey, R. and Caridi, D., 2000. The management of arsenic wastes: problems and prospects. *Journal of Hazardous Materials* 76(1), 125-138.
- Li, J., Jia, X. and Yin, L., 2021a. Hydrogel: Diversity of structures and applications in food science. *Food Reviews International* 37(3), 313-372.
- Li, Y., Yang, H.Y. and Lee, D.S., 2021b. Advances in biodegradable and injectable hydrogels for biomedical applications. *Journal of Controlled Release* 330, 151-160.
- Liu, Y., Wang, J., Chen, H. and Cheng, D., 2022. Environmentally friendly hydrogel: A review of classification, preparation and application in agriculture. *Science of The Total Environment*, 157303.

- Lopez-Cueto, G. and Ubide, C., 1990. Promoting effect of iodide on the hexacyanomanganate (IV)—arsenic (III) redox reaction, for kinetic determination of iodide. *Talanta* 37(8), 849-854.
- Marescotti, P., Olivari, E., Vecchio, A. and Pirani, G., 2011. Mineralogical and chemical investigations for the evaluation of arsenic background values in natural and anthropogenic soils: A case Study from the Colleferro industrial site (Valle del Sacco, Italy). *Proceedings of the ICOBTE*.
- Ozturk, M., Metin, M., Altay, V., Bhat, R.A., Ejaz, M., Gul, A., Unal, B.T., Hasanuzzaman, M., Nibir, L. and Nahar, K., 2021. Arsenic and human health: Genotoxicity, epigenomic effects, and cancer signaling. *Biological Trace Element Research*, 1-14.
- Parhi, R., 2017. Cross-linked hydrogel for pharmaceutical applications: a review. *Advanced Pharmaceutical Bulletin* 7(4), 515-530.
- Qazi, U.Y., Javaid, R., Ikhlaq, A., Al-Sodani, K.A.A., Rizvi, O.S., Alazmi, A., Asiri, A.M. and Ibn Shamsah, S.M., 2022. Synergistically Improved Catalytic Ozonation Process Using Iron-Loaded Activated Carbons for the Removal of Arsenic in Drinking Water. *Water* 14(15), 2406.
- Rahman, M.A., Rahman, A., Khan, M.Z.K. and Renzaho, A.M., 2018. Human health risks and socio-economic perspectives of arsenic exposure in Bangladesh: a scoping review. *Ecotoxicology and Environmental Safety* 150, 335-343.
- Sanyang, M., Ghani, W.A.W.A.K., Idris, A. and Ahmad, M.B., 2016. Hydrogel biochar composite for arsenic removal from wastewater. *Desalination and Water Treatment* 57(8), 3674-3688.
- Singh, A.L. and Sarma, P., 2010. Removal of arsenic (III) from waste water using *Lactobacillus acidophilus*. *Bioremediation Journal* 14(2), 92-97.
- Tomiyasu, T., Nakagawa, M., Kodamatani, H. and Kanzaki, R., 2021. The influence of submarine volcano on seasonal changes in arsenic in the waters of Kagoshima Bay, southwestern Japan. *Environmental Earth Sciences* 80(8), 1-12.
- Villaescusa, I. and Bollinger, J.-C., 2008. Arsenic in drinking water: sources, occurrence and health effects (a review). *Reviews in Environmental Science and Bio/Technology* 7(4), 307-323.
- Xiao, C., 2013. Current advances of chemical and physical starch-based hydrogels. *Starch-Stärke* 65(1-2), 82-88.

- Xiao, Y., Gu, Y., Qin, L., Chen, L., Chen, X., Cui, W., Li, F., Xiang, N. and He, X., 2021. Injectable thermosensitive hydrogel-based drug delivery system for local cancer therapy. *Colloids and Surfaces B: Biointerfaces* 200, 111581.
- Yadav, M.K., Saidulu, D., Gupta, A.K., Ghosal, P.S. and Mukherjee, A., 2021. Status and management of arsenic pollution in groundwater: A comprehensive appraisal of recent global scenario, human health impacts, sustainable field-scale treatment technologies. *Journal of Environmental Chemical Engineering* 9(3), 105203.
- Zacharias, J., Fryda, J., Paterová, B. and Mihaljevic, M., 2004. Arsenopyrite and As-bearing pyrite from the Roudny deposit, Bohemian Massif. *Mineralogical Magazine* 68(1), 31-46.
- Zhang, K., Feng, Q., Fang, Z., Gu, L. and Bian, L., 2021. Structurally dynamic hydrogels for biomedical applications: pursuing a fine balance between macroscopic stability and microscopic dynamics. *Chemical Reviews* 121(18), 11149-11193.
- Zhang, Y., Xu, B., Guo, Z., Han, J., Li, H., Jin, L., Chen, F. and Xiong, Y., 2019. Human health risk assessment of groundwater arsenic contamination in Jinghui irrigation district, China. *Journal of Environmental Management* 237, 163-169.
- Zhao, Z., Wang, Z., Li, G., Cai, Z., Wu, J., Wang, L., Deng, L., Cai, M. and Cui, W., 2021. Injectable microfluidic hydrogel microspheres for cell and drug delivery. *Advanced Functional Materials* 31(31), 2103339.

APPENDIX A

Graphical abstracts of published articles

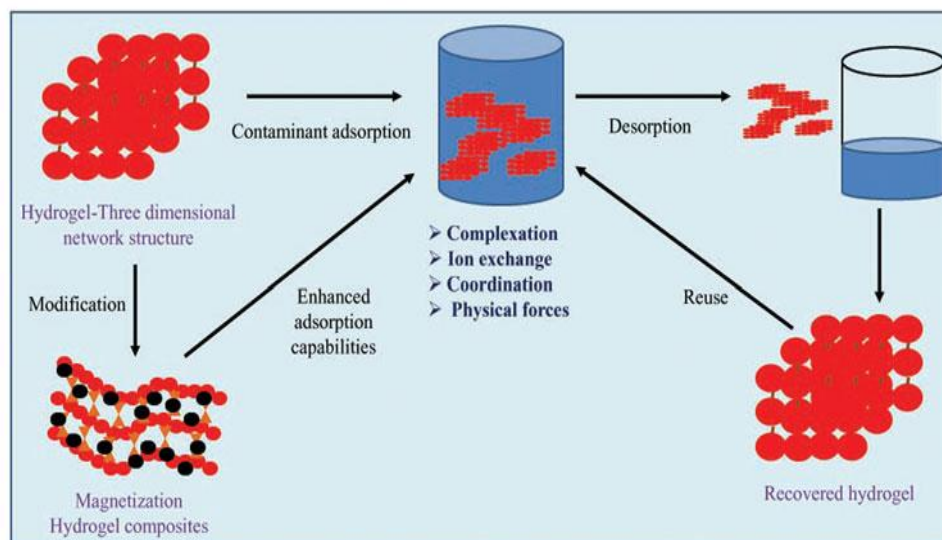


Figure A1 *The graphical abstract of article I: Hydrogels: Novel materials for contaminant removal in water – A review.*

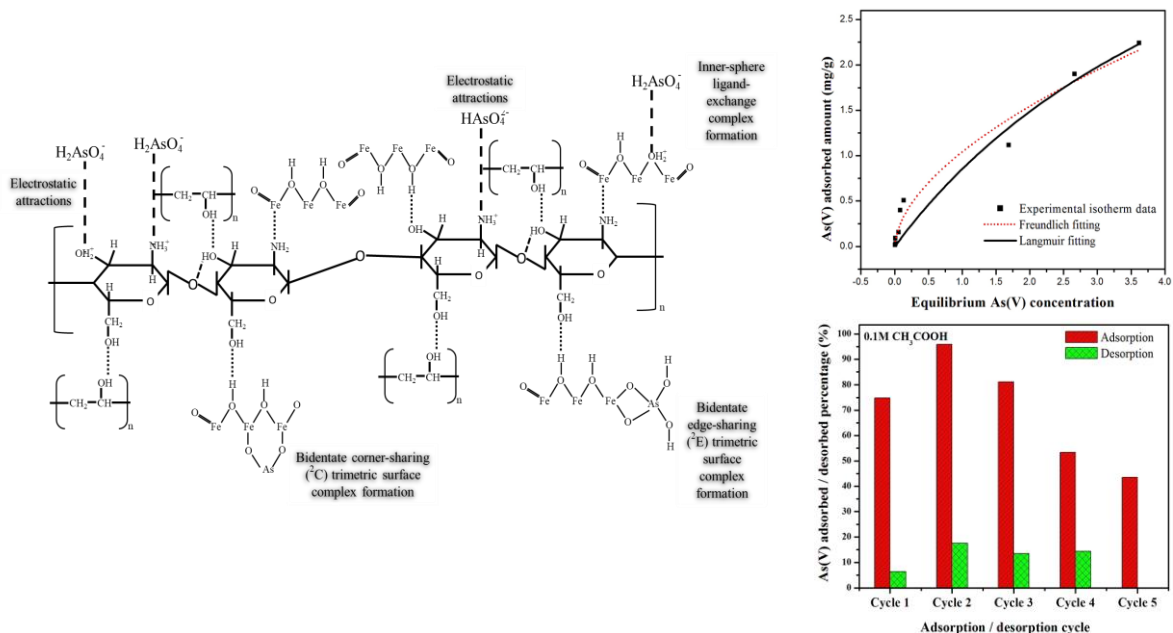


Figure A2 *The graphical abstract of article V: Assessment and optimisation of As(V) adsorption on hydrogel composite integrating chitosan-polyvinyl alcohol and Fe₃O₄ nanoparticles and evaluation of their regeneration and reusable capabilities in aqueous media*

APPENDIX B

Recognition of the review contributed to journals

